Capítulo 9

Aplicación de Herramientas Gráficas al Análisis de la Máquina Síncrona

9.1 Introducción

La máquina síncrona opera como un generador de corriente alterna impulsado por una turbina y convierte la energía mecánica en eléctrica. Esta máquina es la principal fuente de generación de potencia eléctrica en el mundo y representa el elemento básico en el comportamiento dinámico de un sistema eléctrico. Por lo anterior, es muy importante conocer el comportamiento de la máquina síncrona en el análisis de estado estacionario, estado transitorio y de estabilidad [53].

En el presente capítulo, se aplican las herramientas presentadas del capítulo 3 al 7 son aplicadas a un sistema físico, indicándose las ventajas de trabajar en el dominio físico. Primeramente, se obtiene una grafo lineal de la máquina síncrona, a partir del modelo representado en Bond Graph en el capítulo 8. Después, se obtiene la representación en espacio de estado aplicando los procedimientos presentados en el capítulo 3. Posteriormente, se determinan las condiciones de estabilidad de este modelo de la máquina, utilizando los resultados del capítulo 4. Los valores de estado estacionario de la máquina se obtienen aplicando los resultados del capítulo 6. También, se realiza un control por retroalimentación de estados estimados en el dominio físico utilizando los resultados presentados en el capítulo 5 y finalmente se aplican los resultados del capítulo 7 para encontrar el modelo linealizado de la máquina síncrona.

9.2 Obtención Directa de una Representación en Espacio de Estado

Se considera la máquina síncrona descrita en el capítulo 8, a la velocidad constante y despreciando los devanados de amortiguamiento. El Bond Graph se obtiene a partir del Bond Graph de la figura 8.6, eliminando sus bonds 4, 8, 9 y 10, cómo se muestra en la figura 9.1.

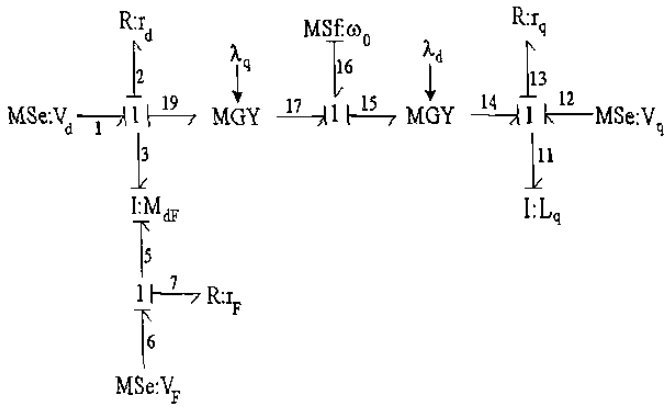

Figura 9.1 Modelo de la máquina síncrona a velocidad constante y sin devanados de amortiguamiento.

Los vectores clave del Bond Graph de la figura 9.1 son:

$$x(t) = \begin{bmatrix} p_3(t) \\ p_5(t) \\ p_{11}(t) \end{bmatrix};\ \dot{x}(t) = \begin{bmatrix} e_3(t) \\ e_5(t) \\ e_{11}(t) \end{bmatrix};\ z(t) = \begin{bmatrix} f_3(t) \\ f_5(t) \\ f_{11}(t) \end{bmatrix}$$

$$D_{in}(t) = \begin{bmatrix} f_2(t) \\ f_7(t) \\ f_{13}(t) \end{bmatrix};\ D_{out}(t) = \begin{bmatrix} e_2(t) \\ e_7(t) \\ e_{13}(t) \end{bmatrix};\ y(t) = \begin{bmatrix} f_3(t) \\ f_{11}(t) \end{bmatrix};\ u(t) = \begin{bmatrix} e_1(t) \\ e_6(t) \\ e_{12}(t) \\ f_{16}(t) \end{bmatrix}$$

con relaciones constitutivas:

$$L = diag\{r_d,\ r_F,\ r_q\} \tag{9.1}$$

$$F^{-1} = diag\{L_{dF},\ L_q\} \tag{9.2}$$

La matriz de Estructura de Unión está dada por (2.25) donde:

$$S_{13} = \begin{bmatrix} I_{3\times 3} & T \end{bmatrix};\ S_{31} = \begin{bmatrix} 1 & 0 & 0 \\ 0 & 0 & 1 \end{bmatrix};\ S_{12} = -I_{3\times 3} \tag{9.3}$$

$$S_{11} = S_{22} = S_{23} = S_{32} = S_{33} = 0;\ T \triangleq \begin{bmatrix} -\lambda_q(t) & 0 & \lambda_d(t) \end{bmatrix}^T$$

Considerando $f_{16} = \omega_0$ como una constante que multiplica a los estados correspondientes y no como una entrada, el vector nuevo de entrada ahora es: $u_n(t) = \left[\begin{array}{ccc} e_1(t) & e_6(t) & e_{12}(t) \end{array} \right]^T$. Así mismo, sustituyendo $\lambda_d(t) = L_d i_d(t) + M_{dF} i_F(t)$ y $\lambda_q(t) = L_q i_q(t)$ en T, tenemos:

$$S_{11}^n = \left[\begin{array}{ccc} 0 & 0 & -L_q\omega_0 \\ 0 & 0 & 0 \\ L_d\omega_0 & M_{dF}\omega_0 & 0 \end{array} \right]; \; S_{13}^n = I_{3\times 3} \tag{9.4}$$

En sistemas eléctricos de potencia y en especial en máquinas eléctricas es común y más práctico utilizar la representación de espacio de estado en términos de co-energía [53]. Así, de (3.9) $E^{-1} = I$ dado que $S_{14} = 0$. Entonces de (2.22), (2.24) y (2.25), se tiene:

$$\left[\begin{array}{c} \dot{z}(t) \\ D_{in}(t) \\ y(t) \end{array} \right] = \left[\begin{array}{ccc} \breve{S}_{11} & \breve{S}_{12} & \breve{S}_{13} \\ S_{21} & S'_{22} & S_{23} \\ S_{31} & S'_{32} & S_{33} \end{array} \right] \left[\begin{array}{c} z(t) \\ D_{in}(t) \\ u_n(t) \end{array} \right] \tag{9.5}$$

donde

$$\breve{S}_{11} \triangleq F S_{11}^n; \quad \breve{S}_{12} \triangleq F S_{12} L; \quad \breve{S}_{13} \triangleq F S_{13}^n \tag{9.6}$$

Para el Bond Graph de la figura 9.1, se tiene:

$$\begin{aligned} \breve{S}_{11} &= \left[\begin{array}{ccc} & 0_{2\times 2} & -L_q\omega_0 L'_d \\ & & -L_q\omega_0 M'_{dF} \\ L_d\omega_0 L_q^{-1} & M_{dF}\omega_0 L_q^{-1} & 0 \end{array} \right] \\ \breve{S}_{12} &= \left[\begin{array}{ccc} -r_d L'_d & -r_F M'_{dF} & \\ -r_d M'_{dF} & -r_F L'_F & 0_{2\times 1} \\ 0_{1\times 2} & & -r_q L_q^{-1} \end{array} \right]; \quad \breve{S}_{13} = F \\ & \qquad\qquad \breve{S}_{22} = \breve{S}_{32} = 0 \end{aligned} \tag{9.7}$$

donde

$$F = diag\left\{ L'_{dF}, L_q^{-1} \right\} \tag{9.4}$$

siendo $L'_{dF} = L_{dF}^{-1} \triangleq \left[\begin{array}{cc} L'_d & M'_{dF} \\ M'_{dF} & L'_F \end{array} \right]$.

Obteniendo la grafo lineal de la figura 9.1, en términos de co-energía, de acuerdo a (8.46) se tiene la figura 9.2.

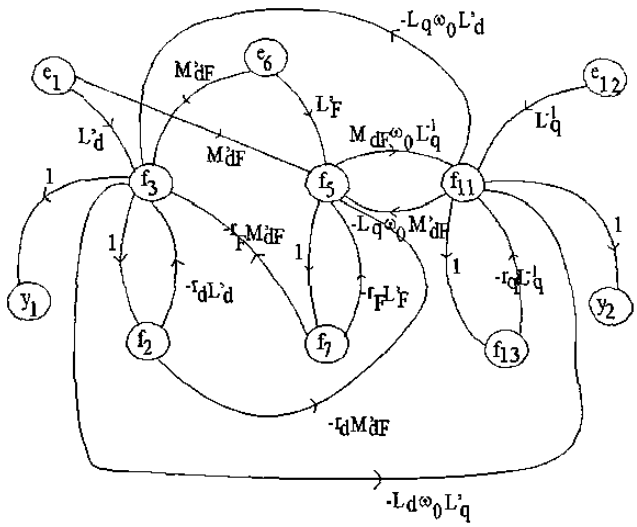

Figura 9.2 Grafo lineal de la máquina síncrona de la figura 9.1.

Los procedimientos presentados en el capítulo 3, pueden ser aplicados a la formulación de co-energía en espacio de estado dada por (8.44), con una estructura de unión dada por (9.6), sin requerir modificación alguna, excepto la notación. Esto se debe a que dichos procedimientos parten de una grafo lineal, la cual refleja los cambios en la interconexión de las ramas y los valores de las transmitancias de las ramas.

Así, utilizando el procedimiento del capítulo 3, sección 3.5, en términos de co-energía y notando que de (9.8) $S'_{22} = 0$, dando $P = I$ de (3.13), por lo tanto se tiene, de (3.15):

$$\check{A}_{px} = \begin{bmatrix} & & -L_q\omega_0 L'_d \\ & 0_{2\times 2} & \\ & & -L_q\omega_0 M'_{dF} \\ L_d\omega_0 L_q^{-1} & M_{dF}\omega_0 L_q^{-1} & 0 \end{bmatrix} \tag{9.9}$$

de (3.16) tenemos:

$$\check{A}_{pd} = \begin{bmatrix} (\check{A}_d)_{11} & (\check{A}_d)_{12} & 0_{2\times 1} \\ (\check{A}_d)_{21} & (\check{A}_d)_{22} & \\ 0_{1\times 2} & & (\check{A}_d)_{33} \end{bmatrix} \tag{9.10}$$

En este caso, $S'_{22} = 0$ entonces $\delta_2 = 1$, de ésta manera, para $(\check{A}_{pd})_{11}$,

$$\delta_1 = -r_d L'_d; \quad \delta_3 = 1 \tag{9.11}$$

Sustituyendo (9.11) en (3.17),

$$(\check{A}_{pd})_{11} = -r_d L'_d \tag{9.12}$$

Para $(\check{A}_{pd})_{22}$,

$$\delta_1 = -r_F L_F^{-1}; \quad \delta_3 = 1 \tag{9.13}$$

Sustituyendo (9.13) en (3.17)

$$(\check{A}_{pd})_{22} = -r_F L'_F \tag{9.14}$$

Para $(\check{A}_{pd})_{33}$,

$$\delta_1 = -r_q L_q^{-1} \quad \delta_3 = 1 \tag{9.15}$$

Sustituyendo (9.15) en (3.17) se tiene:

$$(\check{A}_{pd})_{33} = -r_q L_q^{-1} \tag{9.16}$$

y para $(\check{A}_{pd})_{12}$,

$$\delta_1 = -r_F M'_{dF} \quad \delta_3 = 1 \tag{9.17}$$

sustituyendo (9.17) en (3.17)

$$(\check{A}_{pd})_{12} = -r_F M'_{dF} \tag{9.18}$$

y para $(\check{A}_{pd})_{21}$,

$$\delta_1 = -r_d M'_{dF} \quad \delta_3 = 1 \tag{9.19}$$

sustituyendo (9.19) en (3.17) da:

$$(\check{A}_{pd})_{21} = -r_d M'_{dF} \tag{9.20}$$

Sustituyendo (9.12), (9.14), (9.16), (9.18) y (9.20) en (9.10) y (9.9) y (9.10) en (3.14), la matriz $\check{A}_p$ queda determinada por:

$$\check{A}_p = F \begin{bmatrix} -r_d & 0 & -L_q\omega_0 \\ 0 & -r_F & 0 \\ L_d\omega_0 & M_{dF}\omega_0 & -r_q \end{bmatrix} \tag{9.21}$$

De una manera similar, tenemos para $\check{B}_p$, en éste caso, de (3.22) $\check{B}_{pd} = 0$ y de (3.20) $\check{B}_p = \check{B}_{px}$, la cual está dada por:

$$\check{B}_p = F I_{3\times 3} \tag{9.22}$$

La salida del sistema se obtiene de (3.28), considerando la máquina síncrona como generador, $\check{C}_{pd} = 0$, por lo tanto, de (3.26)

$$\check{C}_p = \check{C}_{px} = \begin{bmatrix} 1 & 0 & 0 \\ 0 & 0 & 1 \end{bmatrix} \tag{9.23}$$

y de (3.32) $\check{D}_p = 0$.

El modelo dinámico de la máquina síncrona a velocidad constante y despreciando los devanados de amortiguamiento, se obtiene de (9.21) y (9.22), el cuál está dado por:

$$\begin{bmatrix} r_d & 0 & L_q\omega_0 \\ 0 & r_F & 0 \\ -L_d\omega_0 & -M_{dF}\omega_0 & r_q \end{bmatrix} \begin{bmatrix} f_3(t) \\ f_5(t) \\ f_{11}(t) \end{bmatrix} + \begin{bmatrix} L_d & M_{DF} & 0 \\ M_{DF} & L_F & 0 \\ 0 & 0 & L_q \end{bmatrix} \frac{d}{dt} \begin{bmatrix} f_3(t) \\ f_5(t) \\ f_{11}(t) \end{bmatrix} = \begin{bmatrix} e_1(t) \\ e_6(t) \\ e_{12}(t) \end{bmatrix} \tag{9.24}$$

En la siguiente sección, se determinan las condiciones de estabilidad para la máquina síncrona considerada en ésta sección, aplicando los resultados del capítulo 4.

9.3 Obtención de las Condiciones de Estabilidad Utilizando una Gráfica Lineal

Se considera la máquina sincrona operando a velocidad constante y sin considerar los devanados de amortiguamiento, tal como se muestra en la figura 9.1.

La determinación de las condiciones de estabilidad de la máquina síncrona, se realiza aplicando los resultados obtenidos del capítulo 4, de ésta manera se obtiene la gráfica lineal para ánalisis de estabilidad a partir de la gráfica lineal de la figura 9.2 sin considerar los nodos de entrada y de salida, ni las ramas asociadas a ellos. La gráfica resultante se muestra en la figura 9.3.

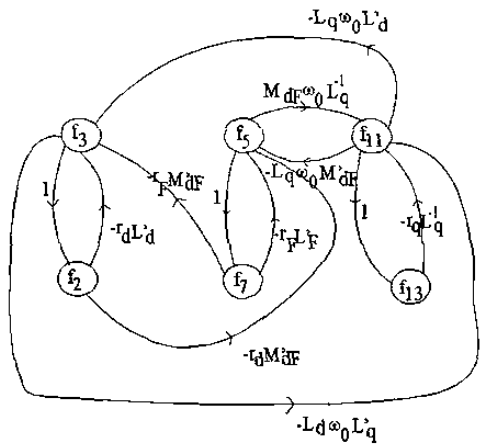

Figura 9.3 Gráfica lineal de la máquina síncrona para ánalisis de estabilidad.

De (4.3) el polinomio característico de la gráfica lineal de la figura 9.3 está dado por:

$$\det(\lambda I - A_c) = \lambda^3 + a_1\lambda^2 + a_2\lambda + a_3 \tag{9.25}$$

A continuación, se obtienen de (4.3) los coeficentes de (9.25) , utilizando la gráfica lineal de la figura 9.3.

La figura 9.4 muestra los factores-1 para a_1.

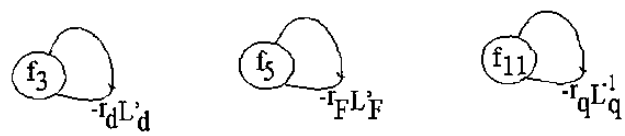

Figura 9.4 Factores-1 para a_1.

$$a_1 = \frac{T_d + T_F}{\Lambda} + T_q \tag{9.26}$$

donde

$$T_d \triangleq \frac{r_d}{L_d} \tag{9.27}$$

$$T_F \triangleq \frac{r_F}{L_F} \tag{9.28}$$

$$T_q \triangleq \frac{r_q}{L_q} \tag{9.29}$$

$$\Lambda \triangleq 1 - \frac{M_{dF}^2}{L_d L_F} \tag{9.30}$$

El coeficiente a_2, se obtiene de la figura 9.5,

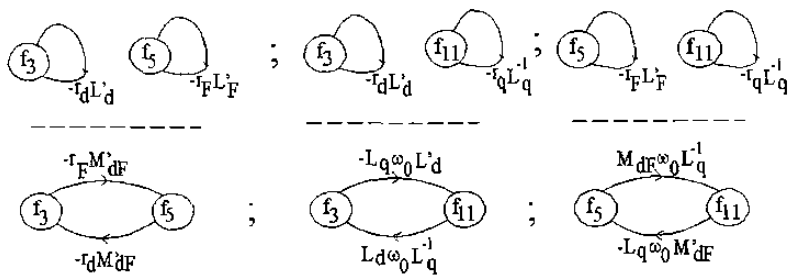

Figura 9.5 Factores-1 para a_2.

$$a_2 = \frac{1}{\Lambda}\left[T_d T_F + \omega_0^2 + T_q\left(T_F + T_d\right)\right] + M_{dF}\left(\frac{\omega_0 M_{dF}}{L_d L_F}\right)^2 \tag{9.31}$$

Finalmente, a_3, se obtiene de la figura 9.6,

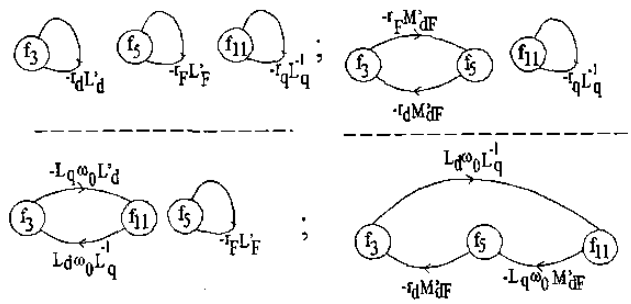

Figura 9.6 Factores-1 para a_3.

$$a_3 = \frac{T_d T_F T_q}{\Lambda} + \frac{T_F}{L_q^2}\Gamma \tag{9.32}$$

Utilizando el Procedimiento 4.1, se obtiene la gráfica de Coates de estabilidad, que se ilustra en la figura 9.7.

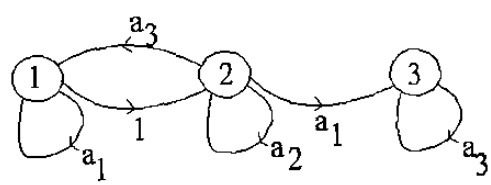

Figura 9.7 Gráfica de estabilidad de Coates.

Los determinantes de Hurwitz se encuentran por medio del Procedimiento 4.2, así, utilizando la figura 9.8, se encuentra D_3,

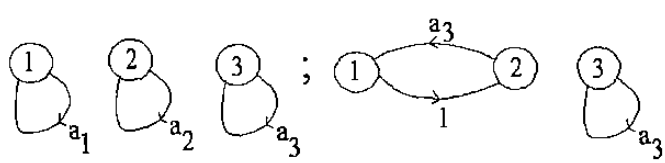

Figura 9.8 Determinante de Hurwitz D_3.

$$D_3 = a_3^2 - a_1 a_2 a_3 \tag{9.33}$$

así mismo, para D_2, de la figura 9.9 se tiene:

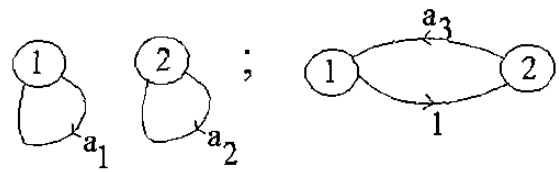

Figura 9.9 Determinante de Hurwitz D_2.

$$D_2 = a_1 a_2 - a_3 \tag{9.34}$$

Finalmente, para D_1 de la figura 9.10 se obtiene:

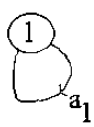

Figura 9.10 Determinante de Hurwitz D_1.

$$D_1 = a_1 \tag{9.35}$$

Las *condiciones* de estabilidad de la máquina síncrona considerada son:

$$\frac{T_d + T_F}{\Lambda} + T_q > 0 \tag{9.36}$$

$$\frac{(T_d + T_F)}{\Lambda}\left[T_d T_F + \omega_0^2 + T_q\left(T_d + T_F\right) + M_{dF}\left(\frac{\omega_0 M_{dF}}{L_d L_F}\right)\right] > T_F\left[T_d T_Q\left(L_d L_F + \frac{M_{dF}^2}{\Lambda}\right) + \omega_0^2\right] \tag{9.37}$$

$$\begin{aligned} T_F\left[T_d T_q\left(L_d L_F + \frac{M_{dF}^2}{\Lambda}\right) + \omega_0^2\right]^2 \;>\; & \left[T_d T_q\left(L_d L_F + \frac{M_{dF}^2}{\Lambda}\right) + \omega_0^2\right]\left(\frac{T_d + T_F}{\Lambda} + T_q\right) \\ & + \left[T_d T_F + \omega_0^2 + T_q\left(T_d + T_F\right) + M_{dF}\left(\frac{\omega_0 M_{dF}}{L_d L_F}\right)^2\right] \end{aligned} \tag{9.38}$$

En la siguiente sección se obtienen los valores de estado estacionario de las variables de estado de *co-energía* de la máquina síncrona aplicando los resultados del capítulo 6.

9.4 Obtención del Estado Estacionario de la Máquina Síncrona utilizando Bond Graph

Como se estudió en el capítulo 6, un modelo representado en Bond Graph permite la obtención de la respuesta de estado estacionario de las variables de estado de un sistema utilizando el Bond Graph en causalidad derivativa.

El Bond Graph en causalidad derivativa de la máquina síncrona a velocidad constante se obtiene de la figura 8.4, y se muestra en la figura 9.11.

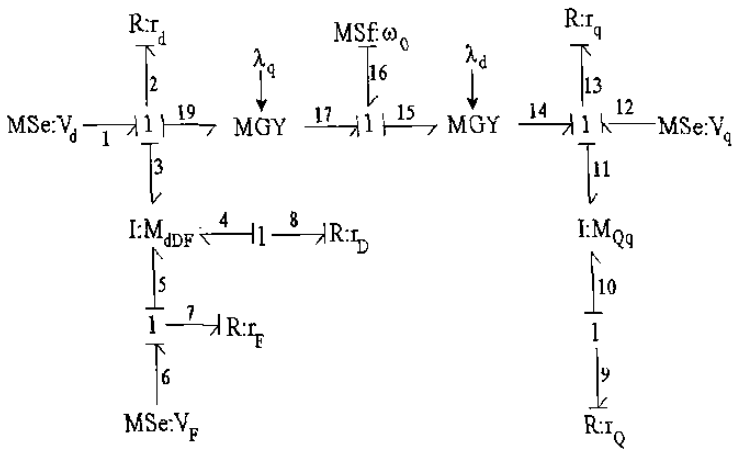

Figura 9.11 Bond Graph de la máquina síncrona en causalidad derivativa y a velocidad constante.

Los vectores clave que cambian, respecto a (8.40), dicionales para el Bond Graph en causalidad derivativa de la figura 9.11 son:

$$D_{ind}(t) = \left[\begin{array}{ccccc} e_2(t) & e_7(t) & e_8(t) & e_9(t) & e_{13}(t) \end{array}\right]^T \tag{9.39}$$

$$D_{outd}(t) = \left[\begin{array}{ccccc} f_2(t) & f_7(t) & f_8(t) & f_9(t) & f_{13}(t) \end{array}\right]^T \tag{9.40}$$

$$L_d = diag\left\{\frac{1}{r_d}, \frac{1}{r_F}, \frac{1}{r_D}, \frac{1}{r_Q}, \frac{1}{r_q}\right\} \tag{9.41}$$

La matriz de estructura de unión es:

$$J_{12} = \left[\begin{array}{ccccc} 1 & 0 & 0 & 0 & 0 \\ 0 & 0 & 1 & 0 & 0 \\ 0 & 1 & 0 & 0 & 0 \\ 0 & 0 & 0 & 1 & 0 \\ 0 & 0 & 0 & 0 & 1 \end{array}\right]; J_{23} = \left[\begin{array}{cccc} 1 & 0 & 0 & \lambda_q(t) \\ 0 & 1 & 0 & 0 \\ 0 & 0 & 0 & 0 \\ 0 & 0 & 0 & 0 \\ 0 & 0 & 1 & -\lambda_d(t) \end{array}\right]$$

$$J_{11} = 0; \quad J_{13} = 0; \quad J_{22} = 0 \tag{9.42}$$

Sustituyendo las ecuaciones de (9.39) a (9.42) en (6.14), (6.17) y (6.22) obtenemos los valores de estado-estacionario de la variables de estado de co-energía:

$$\begin{bmatrix} f_{3ss} \\ f_{4ss} \\ f_{5ss} \\ f_{10ss} \\ f_{11ss} \end{bmatrix} = \begin{bmatrix} \frac{1}{r_d} e_{1ss} + \frac{1}{r_d} \lambda_{qss} \omega_0 \\ 0 \\ \frac{1}{r_F} e_{6ss} \\ 0 \\ \frac{1}{r_q} e_{12ss} - \frac{1}{r_q} \lambda_{dss} \omega_0 \end{bmatrix} \tag{9.43}$$

Resolviendo el sistema anterior (9.43) de ecuaciones algebraicas para f_{3ss} y f_{11ss}, con las relaciones constitutivas para $\lambda_{dss} = L_d f_{3ss} + M_{dF} f_{5ss}$ y $\lambda_{qss} = L_q f_{11ss}$ de (8.26) a (8.29) se tiene el estado ostacionario:

$$z_{ss} = \begin{bmatrix} \frac{e_{1ss} r_F + L_q \omega_0 \left[e_{12ss} - \omega_0 M_{dF} f_{5ss} \right]}{r_d r_q + L_d L_q \omega_0^2} \\ 0 \\ \frac{1}{r_F} e_{6ss} \\ 0 \\ \frac{e_{12ss}}{r_q} - \frac{\omega_0 L_d}{r_q} f_{3ss} - \frac{\omega_0 M_{dF}}{r_q} f_{5ss} \end{bmatrix} \tag{9.44}$$

En la siguiente sección, se obtiene un control por retroalimentación de estados estimados aplicando los resultados del capítulo 5.

9.5 Control de una Máquina Síncrona por Retroalimentación de Estados Estimados

El observador de estados y la retroalimentación de estados estimados de una máquina síncrona, despreciando los devanados de amortiguamiento a velocidad constante, se obtienen aplicando los Procedimientos 5.1 y 5.2, respectivamente, a partir del Bond Graph de la figura 9.1, resultando el Bond Graph de la figura 9.12.

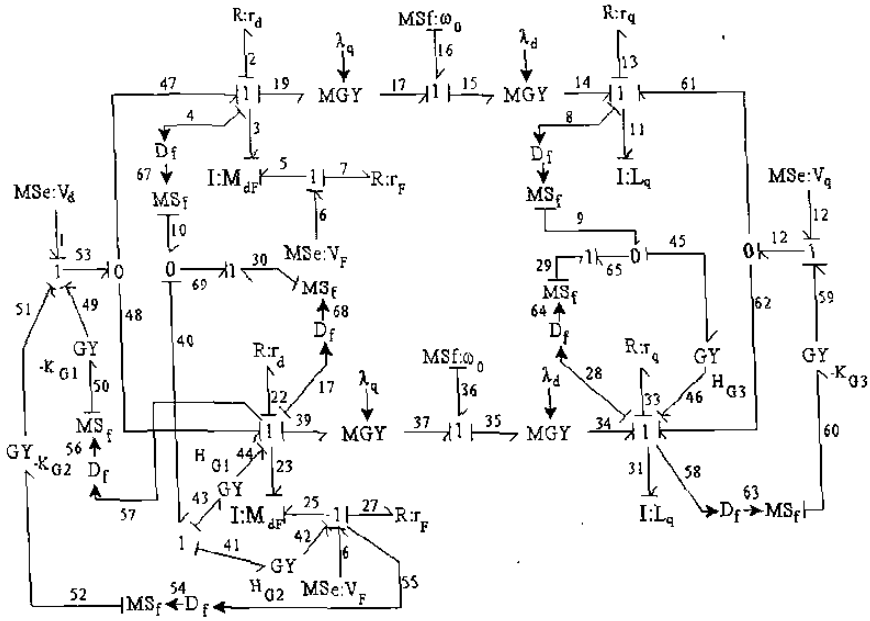

Figura 9.12 Observador de Estados de una Máquina Síncrona.

La estructura de unión para el sistema en lazo cerrado se obtiene de acuerdo al Lema 5.1 y está dada por:

$$\begin{aligned} S_{11} &= \begin{bmatrix} 0 & 0 & -L_q\omega_0 \\ 0 & 0 & 0 \\ L_d\omega_0 & M_{dF}\omega_0 & 0 \end{bmatrix};\ S_{31} = \begin{bmatrix} 1 & 0 & 0 \\ 0 & 0 & 1 \end{bmatrix} \\ S_{12} &= -I_{3\times 3} = -S_{13};\ S_{22} = S_{23} = S_{32} = S_{33} = 0 \end{aligned} \tag{9.45}$$

La estructura de unión del observador reflejada al sistema es:

$$\widehat{S_{11}} = \begin{bmatrix} K_{G1} & K_{G2} & 0 \\ 0 & 0 & 0 \\ 0 & 0 & K_{G3} \end{bmatrix};\ \widehat{S_{21}} = \widehat{S_{31}} = 0 \tag{9.46}$$

Obteniendo una representación en espacio de estado más conveniente para máquinas eléctricas, en términos de co-energía, se tiene de (2.22) y (5.6):

$$\begin{aligned} \dot{z}(t) &= \check{A}_p z(t) - \widehat{A_{pz}}\widehat{z}(t) + \check{B}_p w(t) \\ y(t) &= \check{C}_p z(t) - \widehat{C_{pz}}\widehat{z}(t) + D_p w(t) \end{aligned} \tag{9.47}$$

donde

$$\check{A}_p = FA_pF^{-1} \tag{9.48}$$
$$\check{B}_p = FB_p \tag{9.49}$$
$$\widetilde{A_{pz}} = F\widetilde{A_p}F^{-1} \tag{9.50}$$
$$\check{C}_p = C_pF^{-1} \tag{9.51}$$
$$\widetilde{C_{pz}} = \widetilde{C_p}F^{-1} \tag{9.52}$$

una representación alterna y muy utilizada en sistemas eléctricos de potencia se obtiene a partir de (9.47), se tiene:

$$F^{-1}\dot{z}(t) = F^{-1}\check{A}_pz(t) - F^{-1}\widetilde{A_{pz}}\widehat{z}(t) + F^{-1}\check{B}_pw(t) \tag{9.53}$$

El término $F^{-1}\widetilde{A_{pz}}$ se obtiene del caso 1 del Lema 5.1, donde $E = I$, entonces de (5.18) $\widetilde{A_p} = \widehat{S_{11}}F$ y (9.50) se obtiene:

$$\widetilde{A_{pz}} = F\widehat{S_{11}} \tag{9.54}$$

así mismo, $\check{A}_p$ y $\check{B}_p$ están dadas en (9.21) y (9.22) respectivamente, por otro lado del caso 1 del Lema 5.1 $\widehat{C_{pz}} = 0$, ya que $\widehat{S_{31}} = 0$, y de (9.23) se tiene $\check{C}_p$, con $D_p = 0$. Por lo tanto el modelo de la máquina síncrona en lazo cerrado está dado por:

$$\begin{bmatrix} L_d & M_{dF} & 0 \\ M_{dF} & L_F & 0 \\ 0 & 0 & L_q \end{bmatrix} \frac{d}{dt} \begin{bmatrix} f_3(t) \\ f_5(t) \\ f_{11}(t) \end{bmatrix} = \begin{bmatrix} -r_d & 0 & -L_q\omega_0 \\ 0 & -r_F & 0 \\ L_d\omega_0 & M_{dF}\omega_0 & -r_q \end{bmatrix} \begin{bmatrix} f_3(t) \\ f_5(t) \\ f_{11}(t) \end{bmatrix} - \tag{9.55}$$
$$\begin{bmatrix} K_{G1} & K_{G2} & 0 \\ 0 & 0 & 0 \\ 0 & 0 & K_{G3} \end{bmatrix} \begin{bmatrix} \hat{f}_3(t) \\ \hat{f}_5(t) \\ \hat{f}_{11}(t) \end{bmatrix} + \begin{bmatrix} e_1(t) \\ e_6(t) \\ e_{12}(t) \end{bmatrix}$$
$$y(t) = \begin{bmatrix} 1 & 0 & 0 \\ 0 & 0 & 1 \end{bmatrix} \begin{bmatrix} f_3(t) \\ f_5(t) \\ f_{11}(t) \end{bmatrix}$$

La estructura de unión en lazo cerrado del observador se obtiene del Lema 5.2 y está dada por:

$$\widehat{S_{11}}' = \begin{bmatrix} -K_{G1} - H_{G1} & -K_{G2} & -L_q\omega_0 \\ -H_{G2} & 0 & 0 \\ L_d\omega_0 & M_{dF}\omega_0 & -K_{G3} - H_{G3} \end{bmatrix}; \; S'_{11} = \begin{bmatrix} H_{G1} & 0 & 0 \\ H_{G2} & 0 & 0 \\ 0 & 0 & H_{G3} \end{bmatrix}$$
$$\widehat{S_{12}}' = -\widehat{S_{13}}' = -I_{3\times3}; \; \widehat{S_{22}}' = \widehat{S_{23}}' = \widehat{S_{32}}' = \widehat{S_{33}}' = S'_{12} = 0; \; \widehat{S_{31}}' = S_{31} \tag{9.56}$$

Obteniendo la representación de espacio de estado en términos de co-energía, de (2.22) y (5.9) se tiene:

$$\begin{aligned} \dot{\widehat{z}}(t) &= \widehat{A_{pz}}\widehat{z}(t) + \widehat{B_{pz}}w(t) + \overline{A_{pz}}z(t) \\ \widehat{y}(t) &= \widehat{C_{pz}}\widehat{z}(t) + \widehat{D_p}w(t) \end{aligned} \tag{9.57}$$

donde

$$\widehat{A_{pz}} = F\widehat{A_p}F^{-1} \tag{9.58}$$

$$\widehat{B_{pz}} = F\widehat{B_p} \tag{9.59}$$

$$\overline{A_{pz}} = F\overline{A_p}F^{-1} \tag{9.60}$$

$$\widehat{C_{pz}} = \widehat{C_p}F^{-1} \tag{9.61}$$

Utilizando el Lema 5.2, de (9.45), (9.46) y (9.56) a (9.61), se obtiene el modelo del observador en lazo cerrado de la máquina síncrona:

$$\begin{bmatrix} L_d & M_{dF} & 0 \\ M_{dF} & L_F & 0 \\ 0 & 0 & L_q \end{bmatrix} \begin{bmatrix} \widehat{f_3}(t) \\ \widehat{f_5}(t) \\ \widehat{f_{11}}(t) \end{bmatrix} = \begin{bmatrix} -r_d - K_{G_1} - H_{G_1} & -K_{G_2} & -L_q\omega_0 \\ -H_{G_2} & -r_F & 0 \\ L_d\omega_0 & M_{dF}\omega_0 & -r_q - K_{G_3} - H_{G_3} \end{bmatrix} \begin{bmatrix} \widehat{f_3}(t) \\ \widehat{f_5}(t) \\ \widehat{f_{11}}(t) \end{bmatrix}$$
$$- \begin{bmatrix} H_{G_1} & & \\ H_{G_2} & 0_{2\times 2} & \\ 0 & 0 & H_{G_3} \end{bmatrix} \begin{bmatrix} f_3(t) \\ f_5(t) \\ f_{11}(t) \end{bmatrix} + \begin{bmatrix} e_1(t) \\ e_6(t) \\ e_{12}(t) \end{bmatrix}$$

$$\widehat{y}(t) = \begin{bmatrix} 1 & 0 & 0 \\ 0 & 0 & 1 \end{bmatrix} \begin{bmatrix} \widehat{f_3}(t) \\ \widehat{f_5}(t) \\ \widehat{f_{11}}(t) \end{bmatrix} \tag{9.62}$$

En la próxima sección, se aplican los resultados del capítulo 7 para encontrar el modelo linealizado de la máquina síncrona en el dominio físico.

9.6 Modelo Lineal de la Máquina Síncrona utilizando Bond Graph

Cuando un sistema de potencia está sujeto a un "pequño" cambio de pequeña carga, tiende a adquirir un nuevo estado de operación. Durante la transición entre el estado inicial y el nuevo estado, el comportamiento del sistema es oscilatorio. Si los dos estados son tales que todas las variables de estado cambian suavemente, el sistema está operando cerca del estado inicial. El estado inicial puede ser considerado como una condición de operación *cuasi-estacionaria* para el sistema [53].

Para examinar el comportamiento del sistema, cuando es perturbado tal que el estado de equilibrio nuevo y viejo son cercanamente iguales, las ecuaciones del sistema son linealizadas sobre la condición de operación cuasi-estacionaria.

Considerar el modelo de Bond Graph *d-q* de la máquina síncrona de la figura 8.4, despreciando el coeficiente de amortiguamiento D y de acuerdo al Procedimiento 7.1, se obtiene el Bond Graph linealizado de la máquina que se muestra en la figura 9.13.

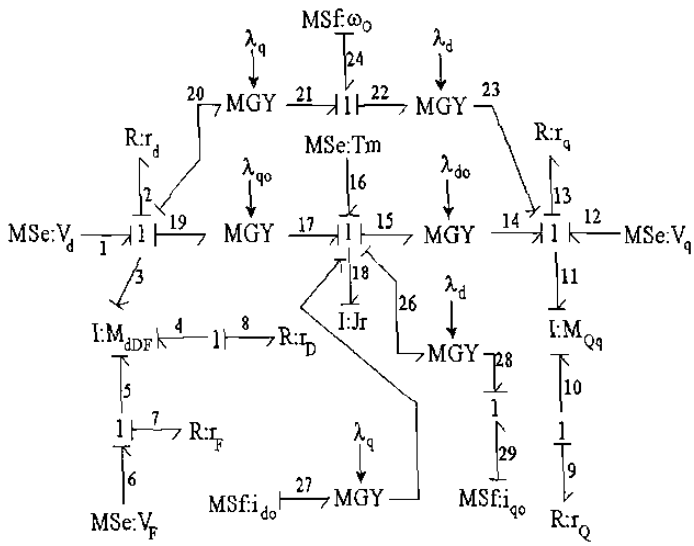

Figura 9.13 Bond Graph linealizado de la máquina sincrona.

Utilizando el Lema 7.1, la estructura de unión para el sistema está dado por (7.17) y (7.18). El modelo de la máquina síncrona está formado por seis ecuaciones diferenciales de las cuales tres ecuaciones son lineales ($f_4(t)$, $f_5(t)$ y $f_{10}(t)$) y sólo tres ($f_3(t)$, $f_{11}(t)$ y $f_{18}(t)$)se linealizan por las siguientes trayectorias:

$$\begin{aligned} \text{Para } I &: M_{dDF}\{3-19-17-18 \\ \text{Para } I &: M_{Qq}\{11-14-15-18 \\ \text{Para } I &: J_r \begin{cases} 18-17-19-3 \\ 18-15-14-11 \end{cases} \end{aligned}$$

donde:

$$S_{11}^x = S_{22} = S_{23} = 0;\ P = \begin{bmatrix} \lambda_{q_0} & 0 & 0 & 0 & -\lambda_{d_0} \end{bmatrix} \tag{9.63}$$

$$S_{11}^0 = \begin{bmatrix} 0_{5x5} & -P^T \\ P & 0 \end{bmatrix} \quad S_{13}^x = \begin{bmatrix} Q & 0_{2x3} \\ 0_{3x1} & I_{3x3} \end{bmatrix};\ Q = \begin{bmatrix} 1 \\ 0 \end{bmatrix} \tag{9.64}$$

$$S_{12} = \begin{bmatrix} -1 & 0 & 0 & 0 & 0 \\ 0 & 0 & -1 & 0 & 0 \\ 0 & -1 & 0 & 0 & 0 \\ 0 & 0 & 0 & -1 & 0 \\ 0 & 0 & 0 & 0 & -1 \\ 0 & 0 & 0 & 0 & 0 \end{bmatrix}; \; S_{13}^{0} = \begin{bmatrix} -\lambda_q(t) & 0 & 0 \\ 0 & 0 & 0 \\ 0 & 0 & 0 \\ 0 & 0 & 0 \\ \lambda_d(t) & 0 & 0 \\ 0 & \lambda_q(t) & -\lambda_d(t) \end{bmatrix} \tag{9.65}$$

Es muy común en sistemas eléctricos de potencia usar la corriente eléctrica como variable de estado y de manera especial para máquinas eléctricas la representación siguiente

$$B_{p\delta} u_{\delta}(t) = -A_{p\delta} F^{-1} z_{\delta}(t) + F^{-1} \dot{z}_{\delta}(t) \tag{9.66}$$

De (7.24) y (9.65) se tiene,

$$S_{13}^{1} = \begin{bmatrix} 0 & 0 & 0 & 0 & -\omega_0 & 0 \\ 0 & 0 & 0 & 0 & 0 & 0 \\ 0 & 0 & 0 & 0 & 0 & 0 \\ 0 & 0 & 0 & 0 & 0 & 0 \\ \omega_0 & 0 & 0 & 0 & 0 & 0 \\ -i_{q_0} & 0 & 0 & 0 & i_{d_0} & 0 \end{bmatrix} \tag{9.67}$$

De (7.19), (8.42), (9.63), (9.64), (9.65) y (9.67) tenemos:

$$A_{p\delta} F^{-1} = \begin{bmatrix} -R_{rDF} & \omega_0 N_{12} & N_{13} \\ -\omega_0 N_{21} & -R_{Qq} & -N_{23} \\ N_{31} & N_{32} & 0 \end{bmatrix} \tag{9.68}$$

donde

$$N_{12} = \begin{bmatrix} H_2 \\ 0_{2x2} \end{bmatrix}; \; N_{21} = \begin{bmatrix} 0_{1x3} \\ H_1 \end{bmatrix}; \; N_{13} = \begin{bmatrix} \lambda_{q_0} \\ 0_{2x1} \end{bmatrix}; \; N_{23} = \begin{bmatrix} 0 \\ \lambda_{d_0} \end{bmatrix} \tag{9.69}$$

$$R_{dDF} = diag\{r_d, r_D, r_F\}; \quad R_{Qq} = diag\{r_Q, r_q\} \tag{9.70}$$

$$\begin{array}{ll} H_1 = \begin{bmatrix} L_d & M_{dD} & M_{dF} \end{bmatrix} & H_2 = \begin{bmatrix} M_{qQ} & L_q \end{bmatrix} \\ N_{31} = i_{q0} H_1 - N_{13}^T & N_{32} = N_{23}^T - i_{d0} H_2 \end{array} \tag{9.71}$$

y finalmente, de (7.20), (9.63) a (9.65) se obtiene:

$$B_{p\delta} = \begin{bmatrix} 1 & 0 & 0 & 0 \\ 0 & 0 & 0 & 0 \\ 0 & 1 & 0 & 0 \\ 0 & 0 & 0 & 0 \\ 0 & 0 & 0 & 0 \\ 0 & 0 & 0 & 1 \end{bmatrix} \tag{9.72}$$

Notar que, de (9.68) y (9.72) el modelo lineal de la máquina síncrona obtenido por Bond Graph es el mismo que en [57], siendo una metodología sencilla para este tipo de sistemas.

En el siguiente capítulo se dan las conclusiones generales de este trabajo de investigación.

9.7 Conclusiones

En este capítulo se aplicaron las herramientas gráficas presentadas en los capítulos 3 al 7 se aplican al modelo de una máquina síncrona en el dominio físico.

Se obtiene una realización en espacio de estado de una máquina síncrona modelada en Bond Graph a partir de su gráfica lineal.

Se presentan condiciones de estabilidad de una máquina síncrona en términos de los parámetros de la máquina.

Se obtienen las condiciones de estado estacionario de una máquina síncrona en el dominio físico.

Se presenta un control por retroalimentación de estado estimado de una máquina síncrona en Bond Graph.

Se propone un modelo linealizado de una máquina síncrona en Bond Graph.

Capítulo 10

Conclusiones y Trabajos Futuros

10.1 Conclusiones

Las conclusiones generales de este trabajo de investigación son las siguientes:

- Todos lo resultados de la presente tesis permiten considerar diferentes tipos de energía, no requieren conocer la función de transferencia o su realización (A_p, B_p, C_p, D_p) y las expresiones obtenidas son simbólicas, no numéricas.

- Se presenta un grafo de Coates modificado que representa un Bond Graph, lo cual permite la aplicación de herramientas de Teoría de Grafos, tales como cálculo de determinante, polinomio característico, inversa de matrices y reducción de grafos. Basado en este grafo se presenta un procedimiento gráfico para la determinación de las matrices (A_p, B_p, C_p, D_p) de un sistema LTI MIMO. Además, se propone la representación del Criterio de Hurwitz mediante un grafo. Basado en este grafo se propone un procedimiento gráfico para determinar las condiciones de estabilidad de un sistema físico LTI MIMO modelado en Bond Graph. Estos resultados pueden ser aplicados a sistemas físicos en lazo abierto o lazo cerrado. La realización (A_p, B_p, C_p, D_p) mediante un grafo del sistema físico, permite conocer la influencia de cada elemento del sistema en la realización obtenida y/o utilizar esta información para diseño del sistema. Finalmente, las condiciones de estabilidad mediante el procedimiento gráfico utiliza el mínimo número de términos para su cálculo.

- Se presenta un control por retroalimentación de estado estimado para sistemas LTI MIMO, es decir, se propone una metodología para obtener el sistema completo en lazo cerrado incluyendo el observador y retroalimentación directamente a partir del Bond Graph en lazo abierto y de estructuras propuestas, garantizando que el control y el observador sean físicamente realizables.

- Se presenta un procedimiento gráfico directo para obtener los valores de estado estacionario de las señales del error, del estado y de la salida de un sistema físico LTI MIMO, en lazo abierto o con retroalimentación de salida en Bond Graph.
- Se presenta un procedimiento gráfico utilizando Bond Graph para la linealización de sistemas nolineales de producto de estados. El sistema y linealización son determinados en el dominio físico. Esta metodología no requiere conocer las ecuaciones diferenciales ordinarias nolineales.
- Un modelo en Bond Graph de la máquina síncrona dado por [23] se analiza y modifica para obtener el mismo modelo matemático dado por [53]. Así, se obtienen de una manera sistemática y directa los modelos simplificados de la máquina síncrona en Bond Graph, lográndose presentar la determinación de las constantes de tiempo de la máquina por medio de modelos simplificados en Bond Graph.
- Las herramientas gráficas anteriores se aplican al modelo de la máquina síncrona en el dominio físico, es decir, se obtiene una realización en espacio de estado de una máquina síncrona modelada en Bond Graph a partir de su gráfica lineal. Se presentan condiciones de estabilidad de una máquina síncrona en términos de los párametros de la máquina. Se obtienen las condiciones de estado estacionario de una máquina síncrona en el dominio físico. Se presenta un control por retroalimentación de estado estimado de una máquina síncrona en Bond Graph y se propone un modelo linealizado de una máquina síncrona en Bond Graph.

10.2 Trabajos Futuros

La herramienta de Bond Graph en el modelado de sistemas físicos tiene un amplio potencial en el desarrollo del entorno científico de modelado y control. Así, se considera que la metodología de Bond Graph puede aplicarse al modelado y control de: Equipo Eléctrico de Generadores, Líneas de Transmisión, Interruptores y Cargas Eléctricas, Modelado de Elementos de Electrónica de Potencia, Sistemas Eléctricos de Potencia, Sistemas Singularmente Perturbados, Sistemas Nolineales, Sistemas con Incertidumbres, Robots y Sistemas Subactuados.

Los problemas inmediatos a resolver son:

- Determinación de los Valores de Estado Estacionario de las Variables de Estado mediante Trayectorias Causales en un Bond Graph.
- Componentes Simétricas en Bond Graph.

- Modelado de Fallas en un Sistema Eléctrico de Potencia utilizando Bond Graph.
- Determinación de los Valores de Estado Estacionario con Elementos Almacenadores de Energía en Causalidad Derivativa en un Bond Graph.
- Determinación de Propiedades de Energía de la Estructura de Unión de un Bond Graph con Bonds Activos.
- Determinación del Error de Estado Estacionario para sistemas con un Control PID, en Cascada o por Retroalimentación de Estados en Bond Graph.
- Flujos de Carga de un sistema eléctrico de potencia en gráfos y/o Bond Graph.
- Transformaciones de similaridad en un Bond Graph.
- Técnicas de reducción de circuitos utilizando Bond Graph.
- Cambios de estructuras del modelo de un sistema físico en Bond Graph.
- Obtención de propiedades de sistemas lineales variantes en el tiempo en el dominio físico.
- Determinación de Funciones de Sensibilidad.

Bibliografía

[1] A. Fakri, F. Rocaries y A. Carriere, "A Simple Method for the Conversion of Bond Graphs Models in Representation by Block Diagrams", *Proceedings of ICBGM'97*, 3rd International Conference on Bond Graph Modeling and Simulation, pp. 15-19, 1997.

[2] Ahmed A. Omara y Ronald C. Rosenberg, "Analysis of a Class of Two-Time-Scale Bond Graph Models", *Proceedings of ICBGM'01*, 5th International Conference on Bond Graph Modeling and Simulation, pp. 55-61, 2001.

[3] Andre Sharon, Neville Hogan and David E. Hardt, "Controller Design in the Physical Domain", *Journal of the Franklin Institute*, Vol. 328, No. 5/6, pp. 697-721, 1991.

[4] Benjamin C. Kuo,"Automatic Control Systems", *Prentice-Hall*, 1991.

[5] C. Sueur y G. Dauphin-Tanguy, "Bond-graph Approach for Structural Analysis of MIMO Linear Systems", *Journal of the Franklin Institute*, Vol.328, No. 1, pp. 55-70, 1991.

[6] C. Sueur y G. Dauphin- Tanguy, "Bond Graph Approach to Multi- Time Scale Systems Analysis", *Journal of the Franklin Institute*, Vol. 328, No. 5/6, pp. 1005-1026, 1991.

[7] C. Pichardo, A. Rahmani, G. Dauphin-Tanguy, M. Delgado, "Bond Graph approaches to build order observers in linear time invariant systems", *4th Mathmod International Conference*, Vienne, Austriche, Febrero 2003.

[8] C. Pichardo-Almarza, A. Rahmani, G. Dauphin- Tanguy, M. Delgado, "Luenberger Observers for Linear Time Invariant Systems Modelled by Bond Graph", para aparecer en *Journal of Mathematical and Computer Modelling of Dynamical System, 2004*.

[9] Carlos Vera , José Manuel Mera, "Frequency Domain Analysis with Bond Graph", *Proceedings of ICBGM'99*, 4th International Conference on Bond Graph Modeling and Simulation, pp. 65-70, 1999.

[10] Charles E. Rohrs, James L. Melsa y Donal G. Shultz, "Linear Control Systems", *Mc.Graw Hill*, 1993.

[11] Chee-Mun Ong, "Dynamic Simulation of Electric Machinery", *Prentice-Hall*, 1998.

[12] Chi-Tsong Cheng, "Linear System Theory and Design", *Hdt, Rinehart and Winston, Inc.*, 1970.

[13] Daniel Gaude, Hervé Morel, Bruno Allard, Hamed Yahoui y Jean-Pierre Masson, "Bond Graph Model of the Induction Motor", *Proceedings of ICBGM'99*, 4th International Conference on Bond Graph Modeling and Simulation, pp. 317-322, 1999.

[14] David G. Luenberger, "An Introduction to Observers", *IEEE Transactions on Automatic Control*, Vol. AC-16, No. 6, pp. 596-602, Diciembre 1971.

[15] David G. Luenberger, "Observers for Multivariable Systems", *IEEE Transactions on Automatic Control*, Vol. AC-11, No. 2, pp. 190-197, Abril 1996.

[16] David G. Luenberger, "Observing the State of a Linear System", *IEEE Transactions on Military Electronics*, Vol. 8, pp. 74-80, Abril 1963.

[17] Dean Karnopp, "State Fuctions and Bond Graph Dynamic Models for Rotary Multi-Winding Electrical Machines", *Journal of the Franklin Institute*, Vol. 328, No. 1, pp.45-54, 1991.

[18] Dean C. Karnopp, Ronald C. Rosenberg, "System Dynamics: A Unified Approach", *Wiley John and Sons*, Abril 1975.

[19] Dean C. Karnopp, Ronald C. Rosenberg, "Introduction to Physical Systems Dynamics", *Mc.Graw Hill*, 1983.

[20] Dean Karnopp, "Bond Graphs in Control: Physical State Variables and Observers", *Journal of the Franklin Institute*, Vol. 308, no. 3, pp. 219-234, 1979.

[21] Karnopp D., "Power and Energy in Linearized Physical Systems", Jounarl of the Flanklin Institute, Vol. 303, No.1, pp.85-97, 1977.

[22] Dean Karnopp, "State Fuctions and Bond Graph Dynamic Model for Rotary, Multi-winding Electrical Machines", Journal of the Flanklin Institute, Vol. 328, No. 1, pp. 45-54, 1991.

[23] Dietrich Sahm, "A Two-Axis, Bond Graph Model of the Dynamics of Sichronous Electrical Machine", *Journal of the Franklin Institute*, Vol.308, No. 3, Septiembre 1979.

[24] Dragan Antic, Biljana Vidojkovic y Miljana Mladenovic, "An Introduction to Bond Graph Modelling of Dynamic Systems", *4th international Conference on Telecommunications in Modern Satellite, Cable and Broadcasting Services*, Vol.2, Octubre 1999.

[25] F. Lorenz y J. Wolper, "Assigning Causality in the Case of Algebraic Loops", *Journal of the Franklin Institute*, Vol. 319, No. 1/2, pp.237-241, Enero/Febrero 1985.

[26] F. R. Gantmacher, "The Theory of Matrices", *Chelsea Publishing Company*, 1974.

[27] Forbes T. Brown, "Engineering System Dynamics", *Marcel Dekker Inc.*, 2001.

[28] Francisco J. Rodriguez Ramírez, "Dinámica de Sistemas", *Editorial Trillas*, 1994.

[29] G. Dauphin- Tanguy, A. Rahmani, C. Sueur, "Bond graph aided design of controlled systems", *Simulation Parctice and Theory, International Journal of the Federation of European Simulation Societies*, Vol. 7, pp. 493-513, 1999.

[30] G. Duaphin- Tanguy y P. Borne, "Order Reduction of Multi-time Scale Systems Using Bond Graphs, the Reciprocal System and Sigular Perturbation Method", *Journal of the Franklin Institute*, Vol. 319, No. 1/2, pp. 157-171. Enero/Febrero 1985.

[31] G. Dauphin-Tanguy, "Modelling of Physical Dynamical Systems by Bond Graph", Linear Systems, Editions Masson, París, Vol. 1, Capítulo 2, pp. 35-112.

[32] G. Dauphin-Tanguy, Pierre Borne, Jean-Pierre Richard, Frédéric Rotella "Modélisation des Systémes Physiques par bond Graph", *Editions Tecnip,* París, Vol.2, Capítulo 5, pp. 25-80.

[33] Gene F. Franklin, J. David Powell y Abbas Emani-Naeini, "Feedback Control of Dynamic Systems", *Addison Wesley Publishing Company*, 1987.

[34] González-A. Gilberto, R. Galindo, "Direct Control in Bond Graph by State Estimated Feedback for MIMO LTI Systems", *Proceedings of the 2002 IEEE International Conference on Control Applications*, September 18-20, 2002, Glasgow, Scotland, U.K.

[35] González-A. Gilberto, R. Galindo, J. de Leon, "A Direct Graph Procedure from Bond Graph for MIMO LTI Systems", *Seventh International Conference on Control, Automation, Robotics and Vision (ICARCV'02)*, Dec. 2002, Singapore.

[36] González-A. Gilberto, R. Galindo, J. de Leon, "Hurwitz Stability Conditions for a LTI System: A Bond Graph Approach", *9th IEEE International Conference on Methods and Models in Automation and Robotics (MMAR 2003)*, 25-28 August, Miedzyzdroje, Poland.

[37] González-A. Gilberto, R. Galindo, "Steady-State Values for a Physical System with Bond Graph Approach", *9th IEEE International Conference on Methods and Models in Automation and Robotics (MMAR 2003)*, 25-28 August, Miedzyzdroje, Poland.

[38] González-A. Gilberto, J. de Leon, "Linearization in Bond Graph", *Sometido a 43rd IEEE Conference on Decision and Control (CDC04)*, December 14-17, Atlantis, Paradise Island, Bahamas, 2004.

[39] González-A. Gilberto, R. Galindo, J. de Leon, "Steady-State Error for a Physical System with Bond Graph Approach", *Sometido a Complex Systems, Intelligence and Modern Technology Applications (CSIMTA)*, September 19-22, Cherbourg, France, 2004.

[40] H. Morel, Ph. Lautier, B. Allard, J. P. Masson y H. Fraisse, "A Bond Graph Model of the Synchronous Motor", *Proceedings of ICBGM'97*, 3rd International Conference on Bond Graph Modeling and Simulation, pp. 227-232, 1997.

[41] Hervé Morel, Bruno Allard, Anis Ammous y S. Ghedira, "Formal Causality Analysis", *Proceedings of ICBGM'99*, 4th International Conference on Bond Graph Modeling and Simulation, pp. 65-70, 1999.

[42] J. D. Lamb, D. R. Woodall y G. M. Asher, "Bond Graphs I: Acausal equivalence", *Dicrete Applied Mathematics*, Vol. 72, No. 3, pp. 261-293, Febrero 1997.

[43] J. D. Lamb, D. R. Woodall y G. M. Asher, "Bond Graphs II: Causality and Sigularity", *Discrete Applied Mathematics*, Vol. 73, No. 2, pp. 143-173, Marzo 1997.

[44] J. D. Lamb, D. R. Woodall y G. M. Asher, "Bond Graphs III: Bond graphs and electrical networks", *Dicrete Applied Mathematics*, Vol. 73, No. 3, pp. 211-250, Marzo 1997.

[45] J. E. Colgate and N. Hogan, "Robust Control of Dynamically interacting Systems", *Journal of the Franklin Institute*, Vol. 1 No.48, pp. 65-88, 1988.

[46] Jannette Garcá-Goméz, Stéphane Rimaux y Marisol Delgado, "Design of an Adaptive Passivity-Based Controller for a Three Phase Induction Motor using Bond Graphs", *Proceedings of ICBGM'99*, 4th International Conference on Bond Graph Modeling and Simulation, pp. 311-316, 1999.

[47] John S. Bay, "Fundamentals of Linear State Space Systems", *Mc.Graw Hill*, 1999.

[48] John J. Grainger y William D. Stevenson Jr, "Análisis de Sistemas de Potencia", *Mc Graw-Hill*, 1988.

[49] K. Sirivadha, E. F. Richards, M. D. Anderson, "The Application of Bond Graphs to Electrical Machinery and Power Engineering", *IEEE Transactions on Power Apparataus and Systems*, Vol. PAS-102, No. 5, Mayo 1985.

[50] Katsuhiko Ogata, "Dinámica de Sistemas", *Prentice-Hall*, 1987.

[51] Katsuhiko Ogata, "Ingeniería de Control Moderna", *Prentice-Hall*, 1980.

[52] P. Kundur, "Power System Stability and Control", *McGraw-Hill*, 1994.

[53] P. M. Anderson, "Power System Control and Stability", *The IOWA State University Press*, 1977.

[54] P. Kubiak, A. Azmani, G. Duaphin-Tanguy, "Determination of State Equation for Bond Graph Model with A Multiport Element", *Proceedings of ICBGM'99*, 4th International Conference on Bond Graph Modeling and Simulation, pp. 111-115, 1999.

[55] P. E. Wellstead, "Physical System Modelling", *Academic Press*, London, 1986.

[56] Paynter, H. M., "Analysis and Design of engineering systems", MIT Press, Cambridge, Mass, 1961.

[57] Peter J, Gawthrop, "Physical Model-based Control: A Bond Graph Approach", *Journal of the Franklin Institute*, Vol. 332B, No. 3, pp. 285-305, 1995.

[58] Peter Gawthrop, Lorcan Smith, "Metamodelling", *Prentice-Hall*, 1996.

[59] Peter C. Breedveld, " Physical Systems Theory in Terms or Bond Graph", *Ph. D. Dissertation*, Twente University, Enshede, Holanda.

[60] Riccardo Marino y Patrizio Tomei, "Nonlinear Control Design", *Prentice-Hall*, 1995.

[61] S. H. Birkett y P. H. Roe, "The Mathematical Foundations of Bond Graphs- I. Algebraic Theory", *Journal of the Franklin Institute*, Vol. 326, No. 3, pp. 329-350, 1989.

[62] S. H. Birkett y P. H. Roe, "The Mathematical Foundations of Bond Graphs- II. Duality", *Journal of the Franklin Institute*, Vol. 326, No. 5, pp. 691-708, 1989.

[63] S. H. Birkett y P. H. Roe, "The Mathematical Foudations of Bond Graphs- III. Matroid Theory", *Journal of the Franklin Institute*, Vol. 327, No. 1, pp. 87-108, 1990.

[64] S. H. Birkett, "On the special properties of graphic and co-graphic bond graphs", *Journal of the Franklin Institute*, Vol. 330, No. 4, pp. 735-761, 1993.

[65] S. Rimaux, C. Suer, G. Dauphin-Tanguy, "Linearization of nonlinear systems modelled by bond graph", Second Eorld Automation Congress WAC 96, Montpellier, France, pp 611-616, Mayo 1996.

[66] Sergio Junco, "Real and Complex-Power Bond Graph Modelling of the Induction Motor", *Proceedings of ICBGM'99*, 4th International Conference on Bond Graph Modeling and Simulation, pp. 323-328, 1999.

[67] Sergio Junco, "Lyapunov Second Method and Feedback Stabilization Directly on Bond Graphs", *Proceedings of ICBGM'01*, 5th International Conference on Bond Graph Modeling and Simulation, pp. 137-142, 2001.

[68] Thomas Kailath, "Linear Systems", *Prentice-Hall*, 1980.

[69] Wai-Kai Chen, "Applied Graph Theory", *North-Holland Publishing Company*, 1976.

[70] Wilson J. Rugh, "Linear System Theory", *Prentice-Hall*, 1996.

[71] X. Xia y S. Scavarda, "Adjoint System by Using the Representation of Bond Graph", *Proceedings of ICBGM'01*, 5th International Conference on Bond Graph Modeling and Simulation, pp. 15-20, 2001.

[72] Y. K. Wong y A. B. Rad, "Bond Graph Simulations of Electrical Systems", *International Conference on Energy Management and Power Delivery*, Vol. 1, Marzo 1998.

[73] Yong Ye, Kamal Youcef-Toumi, "Model Reduction with Physical Interpretation: A Phasor Analysis Approach", *Proceedings of ICBGM'99*, 4th International Conference on Bond Graph Modeling and Simulation, pp. 143-148, 1999.

Apéndice A

Análisis de las Propiedades Estructurales del Modelado en Bond Graph

A.1 Introducción [29]

Uno de los pasos más difíciles del modelado es la identificación de los parámetros. Las propiedades estructurales son algunas propiedades que solamente dependen de la arquitectura del modelo y del tipo de fenómeno físico, tan importante en la fase del modelado, y no en los valores numéricos de los parámetros involucrados en sus leyes características. Por un ejemplo, el polinomio $p(s) = s^2 [s + (a_1 - a_0)]$ tiene dos zeros nulos estructuralmente y un zero no-nulo estructuralmente (excepto para el valor numérico $a_1 = a_0$).

La Estructura de Unión de un Bond Graph contiene información energética en los tipos de elementos, que constituyen al sistema, y en como ellos están interconectados, para cualquier valor numérico de los parámetros.

A.2 Presentación de Herramientas Algebráicas y Gráficas [29]

A.2.1 Definición de la Estructura de $\sum$

Considerar el sistema continuo Lineal Invariante en el Tiempo (*LIT*) de dimensión finita $\sum$:

$$\sum \begin{cases} \dot{x}(t) = Ax(t) + Bu(t) + Ed(t) \\ y(t) = Cx(t) + Du(t) \end{cases} \tag{A.1}$$

donde: $A \in \Re^{n\times n}$; $B \in \Re^{n\times p}$; $C \in \Re^{q\times n}$; $D \in \Re^{q\times p}$; $E \in \Re^{n\times m}$

Definición A.1. Dos sistemas $\sum_o = (A_0, B_0, C_0, D_0)$ y $\sum_1 = (A_1, B_1, C_1, D_1)$ son *estructuralmente equivalentes* o tienen la misma estructura si:

1. Las matrices (A, B, C, D) de ambos sistemas tienen la misma dimensión.
2. Existe una matriz P con $A_2 = PA_1P^T$, $B_2 = PB_1$, $C_2 = C_1P^T$ y $D_2 = D_1$, tal que todos los valores cero de A_2, B_2, C_2 y D_2 son mapeados en los valores cero de A_0, B_0, C_0 y D_0 y viceversa.

La estructura de $\sum$ está definida por la clase de equivalencia $[\sum]$ de sistemas estructuralmente equivalentes. Resultados estructurales son obviamente siempre verdaderos para los sistemas que pertenecen a la clase de equivalencia $[\sum]$, *i.e.*,que tienen la misma estructura.

A.2.2 Controlabilidad/Observabilidad Estructural

Un sistema LTI es *completamente controlable en el estado* si y sólo si

$$Rango\ P = Rango\left[B, AB, ..., A^{n-1}B\right] = n \tag{A.2}$$

Definición A.2. El sistema $[A, B]$ es llamado *estructuralmente controlable en el estado* si existe un sistema completamente controlable en el estado de la misma estructura.

Definición A.3. El sistema $[A, C]$ es llamado *estructuralmente observable en el estado* si existe un sistema completamente observable en el estado de la misma estructura.

Las definiciones dadas anteriormente están en un sentido clásico de sistemas lineales [69], sin embargo, a continuación se describen propiedades fundamentales de éste tipo de sistemas en un enfoque de Bond Graph.

A.3 Rango Estructural [29]

Una definición de rango precisa y su determinación directa a partir de un Bond Graph es la siguiente:

Propiedad A.1

El orden n de un modelo es igual al número de elementos I y C en causalidad integral cuando una causalidad integral predefinida es asignada al modelo de Bond Graph.

Propiedad A.2

- El *rango-Bond Graph* (Rango-BG) q de la matriz A de espacio de estado deducida a partir del Bond Graph es igual al número de elementos I y C en causalidad derivativa cuando una causalidad derivativa predefinida es asignada al modelo de Bond Graph.
- El número $k = n-q$ de *modos nulos estructuralmente* es igual al número de elementos I y C los cuales permanecen en causalidad integral cuando una causalidad derivativa predefinida es asignada al modelo de Bond Graph.
- El rango-Bond Graph de la matriz A es igual al rango de la matriz $[S_{11},\ S_{12}]$ definida en (2.25).

La primer parte de la Propiedad $A.2$ significa que, el modelo matemático asociado con el Bond Graph está dado por:

$$\begin{aligned} x &= A^{-1}\dot{x} - A^{-1}Bu - A^{-1}Ed \\ y &= CA^{-1}\dot{x} - CA^{-1}Bu - CA^{-1}Ed + Du \end{aligned} \tag{A.3}$$

Si alguno de los elementos I y C no aceptan una asignación de causalidad derivativa sin crear un *conflicto* de causalidad en las uniones, significa que la matriz A no es invertible, *i.e.*, no es de rango pleno.

El rango q es llamado Rango-BG debido a que es un rango estructural en el sentido de Teoría de Grafos [29], sin embargo, corresponde al rango numérico a causa de que toma en cuenta la dependencia del parámetro a través de la causalidad.

La segunda parte de la Propiedad $A.2$ se obtiene del polinomio característico de la matriz A:

$$P(s) = \det(sI_n - A) = s^k\left(s^q + a_{q-1}s^{q-1} + ... + a_1 s + a_0\right) \tag{A.4}$$

El punto de vista es estructural debido a que nosotros detectamos k estructuralmente modos nulos pero no en los casos donde a_0 sea nulo.

A.4 Diseño de la Arquitectura para Medición y Control [29]

La determinación del número, el tipo y la localización de sensores y actuadores en un modelo de Bond Graph está directamente relacionado al análisis de las propiedades de controlabilidad y observabilidad.

El camino clásico numérico consiste en calcular el rango numérico de la matriz de controlabilidad $C_o = [B\ AB\ ...\ A^{n-1}B]$ y la matriz de observabilidad $O_b = \left[C^T\ (CA)^T\ ...\ \left(CA^{n-1}\right)^T\right]^T$, donde la matricez C reagrupa la parte de la matriz asociada con lo medible para ser variables controladas y la matriz asociada a salidas de interés no medibles. El rango de estas matrices no depende de los valores numéricos de los parámetros y es consecuentemente robusto.

Propiedad A.3

Para que un modelo de Bond Graph sea *estructuralmente controlable (o observable)* dos condiciones tienen que ser satisfechas:

1. Existe al menos una trayectoria causal enlazando cada elemento I y C en causalidad integral con una fuente de control MS_e o MS_f (con un sensor D_e o D_f) en el Bond Graph en causalidad integral predefinida.

2. Todos los elementos I y C en causalidad integral en el Bond Graph en causalidad integral predefinida aceptan una causalidad derivativa cuando una causalidad derivativa predefinida es asignada en el modelo de Bond Graph. Si no es satisfecha directamente, una dualización de algunas fuentes MS_e o MS_f (de algunos sensores D_e o D_f) tiene que hacerse para transformar las causalidades integrales remanentes.

La Propiedad A.3, parte 1, es la condición de posibilidad de realización de la Teoría de Grafos [29].

La Propiedad A.3, parte 2 corresponde a la determinación del rango estructural de la matriz $[AB]$ compuesta de la matriz A concatenada con la matriz B.

Si el rango-BG $[A] = n$, entonces el rango-BG $[AB] = n$ para cualquier B. Significa que el modelo es controlable con un actuador sencillo, la selección y localización depende solamente de la posibilidad de realización y consideraciones tecnológicas.

Si el rango-BG $[A] = n - k$, entonces el rango-BG $[AB] = n$ si B es seleccionada de tal forma que sus columnas sean linealmente independientes de las columnas de A. Significa que para el modelo a ser controlado, k actuadores son necesarios y ellos tienen que estar bien localizados, lo cual es probado por dualización.

A.5 Trayectoria Causal-Lazo Causal [31, 32]

Un Bond Graph no solamente muestra la estructura topológica de un sistema sino también su organización causal, pues indica las relaciones de causa y efecto, esta estructura causal da la noción de *Trayectoria Causal*, *Lazo Causal* y *Lazo Mason* que a continuación se explican:

- Una *Trayectoria Causal* de una estructura de unión es una secuencia alternante de bonds y nodos tal que:
  1. Para una gráfica acausal, es decir, una gráfica que no tiene la causalidad aplicada a sus elementos o bonds, la secuencia forma una cadena sencilla.
  2. Todos los nodos en la secuencia tienen una completa y correcta causalidad, es decir, se cumplen las condiciones del Procedimiento 2.1.
  3. Dos nodos de una trayectoria causal tienen en el mismo nodo orientaciones causales opuestas.
- Un *Lazo Causal* es una trayectoria causal sencilla cerrada.
- Un *Lazo Mason* es un lazo causal de la salida de un puerto a la entrada del mismo puerto sin trazar el mismo bond en la misma dirección más de una vez.

El polinomio característico está dado por:

$$D(s) = 1 - \sum_{j} L_{1j}(s) + \sum_{k} L_{2k}(s) - \sum_{l} L_{3l}(s) + ... \tag{4.14}$$

donde $L_{rk}(s)$ es el producto de las ganancias de lazo del k^{th} conjunto del r^{th} lazo de Mason, los cuales no se tocan unos con otros.

La $L_{ij}(s)$ ganancia del j^{th} lazo de Mason está definida por:

$$L_{ij}(s) \triangleq (-1)^{n_0+n_1} \prod_{j,k} \left(m_j \text{ o } \frac{1}{m_j}\right)^2 \left(r_k \text{ o } \frac{1}{r_k}\right)^2 \prod_{h} G_h \tag{4.15}$$

donde n_0 y n_1 representan el número total de cambios de orientación de los bonds, respectivamente en las uniones-0, al seguir a la variable de flujo; y en las uniones-1 al seguir a la variable de esfuerzo; $\prod_{j,k}$ denota el producto de m_j ó $\frac{1}{m_j}$ y r_k ó $\frac{1}{r_k}$ que son los módulos de los elementos de TF y de GY, los cuales son incluídos en la trayectoria causal, dependiendo de sus causalidades y $\prod_{h}$ designa el producto de ganancias de los elementos que componen el lazo.

Apéndice B

Estabilidad de Sistemas LTI MIMO

B.1 Introducción

Si la respuesta impulsional de un sistema es absolutamente integrable, entonces el sistema es estable BIBO. La condición de estabilidad en términos de funciones de transferencia es también dada en esta sección. Se estudian los conceptos de *equilibrio de estado, estabilidad en el sentido de Lyapunov* y *estabilidad asintótica [68, 12].*

B.2 Estabilidad Externa (Estabilidad BIBO) [12]

Considerar un sistema LTI MIMO con la siguiente descripción entrada/salida:

$$y(t) = \int_0^t G(t-\tau)\, u(\tau)\, d\tau = \int_0^t G(\tau)\, u(t-\tau)\, d\tau \tag{B.1}$$

donde $g(t)$ es la respuesta impulsional del sistema. En una descripción de la forma $(B.1)$, el par entrada/salida del sistema satisface linealidad, causalidad y propiedades de invariancia en el tiempo. Además, se asume que el sistema está relajado en $t = 0$.

Teorema B.1 [12]

Un sistema LTI MIMO relajado en $t = 0$ y *descrito por*:

$$y(t) = \int_0^t G(t-\tau)\, u(\tau)\, d\tau \tag{B.2}$$

es estable Entrada Acotada/Salida Acotada (BIBO) si y sólo si,

$$\int_0^\infty |G(t)|\, dt \leq k < \infty \tag{B.3}$$

para cualquier k.

La prueba de este Teorema se da en [12].

Teorema B.2 [12]

Considerar un LTI MIMO, relajado en $t = 0$ *cuya entrada* $u(t)$, *y salida* $y(t)$ *están relacionadas por*:

$$y(t) = \int_0^t G(t-\tau)\, u(\tau)\, d\tau$$

si $\int_0^t \|G(t)\|dt \leq k < \infty$ *para cualquier constante* k, *entonces se tiene lo siguiente*

1. *Si* $u(t)$ *es una función periódica con periodo* T, *entonces* $y(t)$ *tiende a una función periódica con el mismo periodo.*
2. *Si* $u(t)$ *es acotada y tiende a una constante, entonces* $y(t)$ *tiende a una constante.*
3. *Si* $u(t)$ *es de energía finita, entonces* $y(t)$ *también es de energía finita.*

La prueba de este Teorema se da en [12].

B.3 Estabilidad en el Sentido de Lyapunov o Estabilidad Interna o Criterio de Estabilidad de Lyapunov [68]

Estabilidad interna se refiere a la estabilidad de una realización de un sistema. La realización del sistema,

$$\dot{x} = Ax(t) + Bu(t) \quad y(t) = Cx(t) \tag{B.4}$$

donde $A \in \Re^{n\times n}$, $B \in \Re^{n\times p}$ y $C \in \Re^{q\times n}$, es *internamente estable* o estable en el *sentido de Lyapunov* si la solución de

$$\dot{x} = Ax(t) \quad x(t_0) = x_0 \quad t \geq t_0 \tag{B.5}$$

tiende hacia cero cuando $t \to \infty$ para cualquier x_0.

Examinando la solución en el dominio de la transformada de Laplace,

$$X(s) = (sI - A)^{-1} x_0 \tag{B.6}$$

y notando que

$$t^k e^{-at} \leftrightarrow (s+a)^{-k} \tag{B.7}$$

donde $\longleftrightarrow$ denota la *Transformada de Laplace* y su inversa; podemos ver que la realización es estable si y sólo si,

$$\mathrm{Re}\{\lambda_i(A)\} < 0 \tag{B.8}$$

donde $\{\lambda_i(A)\}$ son los eigenvalores de A.

Las ecuaciones $(B.6)$ y $(B.8)$ indican que una realización estable internamente siempre tiene una respuesta impulsional que satisface la condición (4.3); en otras palabras; también es externamente estable. Sin embargo, lo contrario no es cierto.

Teorema B.3 (Lyapunov) [68]

Una matriz A es una matriz de estabilidad, *es decir,* $\mathrm{Re}\{\lambda_i(A)\} < 0$ *para todos los eigenvalores de A, si y sólo si para cualquier matriz (simétrica) definida positiva Q existe una matriz P definida positiva (simétrica) que satisface*

$$A'P + PA = -Q \tag{B.9}$$

La prueba de este Teorema se da en [68].

Este teorema es raramente utilizado para verificación numérica directa de estabilidad. En lugar de esto, se tienen los siguientes corolarios.

Corolario 4.1 (Kalman) [68]

En el Teorema anterior, podemos tomar Q semidefinida positiva, teniendose que $x'(t)Qx(t)$ no es identicamente cero a lo largo de cualquier solución de $\dot{x}(t) = Ax(t)$.

Las bases físicas de estos resultados son las siguientes. La cantidad:

$$V[x(t)] = x'(t)Px(t) \tag{B.10}$$

puede ser considerada como energía generalizada asociada con la realización. En un sistema estable la energía debe decaer con el tiempo, ésto es, de $(B.5)$, $(B.9)$ y $(B.10)$,

$$\begin{aligned} \frac{d}{dt}V[x(t)] &= \dot{x}'(t)Px(t) + x'(t)P\dot{x}(t) \\ &= x'(t)\left[A'P + PA\right]x(t) \\ &= -x'(t)Qx(t) \end{aligned} \tag{B.11}$$

concluimos que $x(t) \to 0$ cuando $t \to \infty$.

Corolario 4.2 [68]

Si A es una matriz de estabilidad, entonces la ecuación de Lyapunov

$$A'P + PA + Q = 0$$

tiene una solución P única para toda Q.

Apéndice C

Publicaciones

C.1 A Direct Graph Procedure from Bond Graph for MIMO LTI Systems

Gonzalez-A. Gilberto, R. Galindo, J. de Leon

Seventh International Conference on Control, Automation, Robotics and Vision (ICARCV'02), Dec. 2002, Singapore.

Seventh International Conference on Control, Automation,
Robotics And Vision (ICARCV'02), Dec 2002, Singapore

A Direct Graph Procedure from Bond Graph for MIMO LTI Systems

Gonzalez-A. Gilberto[1,2], R. Galindo[1], J. de Leon[1]

[1]University of Nuevo Leon, Department of Electrical Engineering
66451 San Nicolas de los Garza, N.L. Mexico (+52)8183294020 Ext.5773
[2]University of Michoacan, Faculty of Electrical Engineering
58030, Morelia, Michoacan, Mexico (+52)4433265776

Abstract

A physical Multi-Input-Multi-Output (MIMO) Linear Time Invariant (LTI) system formed by a variety of energy types and modelled graphically in Bond Graph is considered. A single direct graphical form to represent this physical system is presented. This modified Coates graph is based on its Bond Graph. It allows to propose a direct graphical procedure getting a state space model. Also, the characteristic polynomial is obtained from the proposed Coates Graph. An electromechanical example is given.

Keywords.-Bond Graph, Coates Graph, Physical Control, Modelling Tools

1 Introduction

A Bond Graph is a model of a dynamic system where a collection of components interact with each other through energy ports. A Bond Graph consists of subsystems linked by lines to show the energetic connections. It can represent a variety of energy types and can describe how the power flows through the system [2, 7]. Bond graph was established by [1]. The idea was developed how a powerful tool of modelling [2, 3].

On the other hand, a linear graph is a set of connected lines. The lines represent symbolically the elements of the system. The line segments are conventionally called edges and the end of a set of edges is termed a *node*. The Graph Theory [7] has been used to find the Coates Matrix, its determinant, characteristic polynomial, etc.

Our main motivation, is to apply some of the Graph Theory technics in a physical MIMO LTI system modelled on Bond Graph, with the objetive to reach a linear graph representation. Also, a graph methodology from its Bond Graph toward this linear graph to obtain a representation in state variables is presented. In [8] a work to obtain a linear graph from its Bond Graph has developed, but it is not represented on its key vectors [4] and therefore it does not allow to apply it to solve other problems like the tackled on this paper.

Section 2 gives the modelling by Bond Graph of a physical system. A procedure to obtain a graph from its Bond Graph which represents a modified Coates matrix is presented in section 3. In section 4 a graphical representation of a MIMO system is found. Section 5 presents a graph procedure to find the A, B, C and D matrices, to get a state space model. Section 6 applies a result of [7] to get a characteristic polynomial of the system found in section 5. An example is given in section 7. Finally, section 8 gives our conclusions.

2 Bond Graph Model [3, 4]

Consider a multiport LTI system which has the key vectors of figure 1.

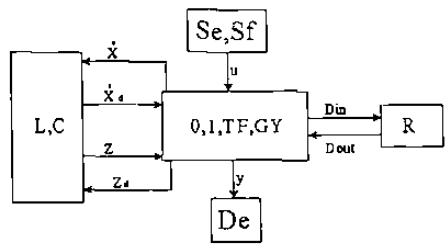

Fig. 1. Key vectors of a Bond Graph

Here, (Se, Sf), (L,C) and (R) denote the source, the storage and the dissipation fields, (De) the detector and (0, 1, TF, GY) the junction structure with transformers, TF, and gyrators, GY. The state $x \in R^n$ is composed of energy variables of effort, e, and flow, f, with integral causality, $x_d \in R^m$ denotes the vector for elements with derivative causality, $u \in R^p$ the plant input, $y \in R^q$ the plant output, $z \in R^n$ the co-energy, $z_d \in R^m$ the derivative co-energy and $D_{in} \in R^r$ and $D_{out} \in R^r$ are a mixture of e and f showing the energy exchanges between the dissipation field and the junction structure. The relations of the storage and dissipation fields are:

$$z = Fx \quad (1)$$

$$D_{out} = LD_{in} \quad (2)$$

$$z_d = F_d x_d \quad (3)$$

where L is a diagonal matrix composed of R and $1/R$ coefficients, and F and F_d are composed of $1/L$ and $1/C$ coefficients. The relations of the junction struc-

ture are:

$$\begin{bmatrix} \dot{x} \\ D_{in} \\ y \end{bmatrix} = S \begin{bmatrix} z \\ D_{out} \\ u \\ \dot{x}_d \end{bmatrix} \quad (4)$$

$$z_d = -S_{14}^T z \quad (5)$$

where the junction structure of the system is given by:

$$S = \begin{bmatrix} S_{11} & S_{12} & S_{13} & S_{14} \\ S_{21} & S_{22} & S_{23} & 0 \\ S_{31} & S_{32} & S_{33} & 0 \end{bmatrix} \quad (6)$$

The entries of S take the values inside the set $\{0, \pm 1, \pm m, \pm n\}$ where m and n are transformer and gyrator modules; S_{11} and S_{22} are square skew-symmetric submatrices and S_{12} and S_{21} are submatrices each other negative transpose. The state equation is [5]:

$$\begin{aligned} \dot{x} &= Ax + Bu \quad (7) \\ y &= Cx + Du \end{aligned}$$

where

$$A = E^{-1}(S_{11} + S_{12}MS_{21})F \quad (8)$$

$$B = E^{-1}(S_{13} + S_{12}MS_{23}) \quad (9)$$

$$C = (S_{31} + S_{32}MS_{21})F \quad (10)$$

$$D = S_{33} + S_{32}MS_{23} \quad (11)$$

being

$$E = I + S_{14}F_d^{-1}S_{14}^T F \quad (12)$$

$$M = (I - LS_{22})^{-1}L \quad (13)$$

Next section presents a linear graph for the system of figure 1.

3 Getting a Graph from a Bond Graph

A procedure to obtain a graphical respresentation of a Bond Graph, which represents a physical system is presented.

For a LTI system, from (1)-(6), a junction structure equation is obtained:

$$\begin{bmatrix} \dot{x} \\ D_{in} \\ y \end{bmatrix} = S' \begin{bmatrix} x \\ D_{in} \\ u \\ \dot{x}_d \end{bmatrix} \quad (14)$$

$$S' = \begin{bmatrix} S'_{11} & S'_{12} & S_{13} & S_{14} \\ S'_{21} & S'_{22} & S_{23} & 0 \\ S'_{31} & S'_{32} & S_{33} & 0 \end{bmatrix} \quad (15)$$

$$x_d = -S'_{14}x \quad (16)$$

where

$$\begin{aligned} S'_{11} &= S_{11}F;\ S'_{21} = S_{21}F;\ S'_{31} = S_{31}F; \quad (17) \\ S'_{12} &= S_{12}L;\ S'_{22} = S_{22}L; \\ S'_{32} &= S_{32}L;\ S'_{14} = F_d^{-1}S_{14}^T F \end{aligned}$$

Let suppose that (15) is a Coates Matrix . Then, it is shown in figure 2. Also, from (12) and (17) we obtain:

$$E^{-1} = (I + S_{14}S'_{14})^{-1} \quad (18)$$

Now, replacing (18) on the graph of figure 2, we get to the graph shown in figure 3.

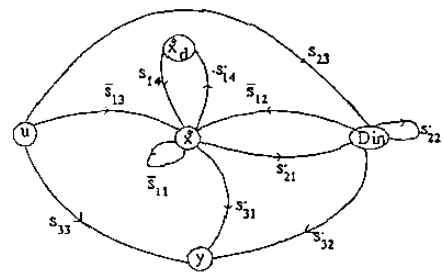

Fig. 2. Linear Planar System Graph

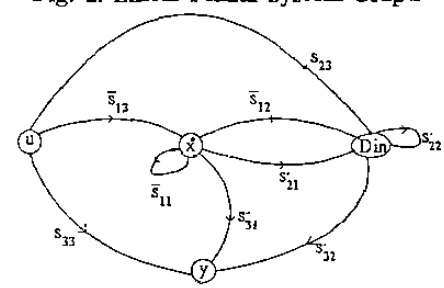

Figura 3. Modified Coates Graph.

The representation of the graph of the figure 3 is given by:

$$\begin{bmatrix} \dot{x} \\ D_{in} \\ y \end{bmatrix} = \begin{bmatrix} \bar{S}_{11} & \bar{S}_{12} & \bar{S}_{13} \\ S'_{21} & S'_{22} & S_{23} \\ S'_{31} & S'_{32} & S_{33} \end{bmatrix} \begin{bmatrix} x \\ D_{in} \\ u \end{bmatrix} \quad (19)$$

where

$$\bar{S}_{11} = E^{-1}S'_{11}\ ;\ \bar{S}_{12} = E^{-1}S'_{12}\ ;\ \bar{S}_{13} = E^{-1}S'_{13} \quad (20)$$

The representation (19)-(20) includes the effect of the elements with derivative causality in the elements with integral causality, having a structure more compact of the physical system.

We can rewrite (19) giving:

$$\begin{bmatrix} \dot{x}^T & D_{in}^T & u^T & y^T \end{bmatrix}^T = \hat{S} \begin{bmatrix} x^T & D_{in}^T & u^T & y^T \end{bmatrix}^T \quad (21)$$

where $\hat{S}$ represents a modified Coates Matrix [7].

If $\dot{x}$ is used instead of x in (19) or (21), the elements of the first column are the diferent by a factor $\frac{1}{s}$ where s is the Laplace operator. In what follows, we omit this factor because for LTI systems does not afect the elements interconnection and for getting directly A and C of (7) as shown in the following section.

4 Representation of a MIMO System

An analysis of the graphical representation of a multivariable system is presented. In figure 3, we have a

representation of a physical system on a graph, from its bond graph and junction structure matrix. Next, we introduce a general form of the physical system representation in Bond Graph to study the interconnection properties as shown in figure 4.

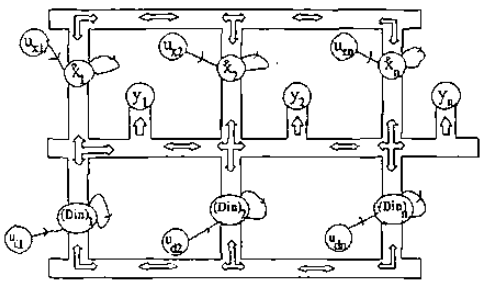

Fig. 4. Representation of a MIMO system.

Consider the scheme of figure 3, note that the node $\dot{x}$ is a set of nodes $\dot{x}_1$, $\dot{x}_2$, $\dot{x}_3$, ..., $\dot{x}_n$; the same is true for u, y and D_{in} as shown the matrix representation of figure 4. The interconnection of the nodes in figure 4, is represented by $\Leftrightarrow$ indicating a set of edges that can have double sense.

Figure 5, represents the interconnection between two nodes 1 and i of figure 4 with all possible combinations. In figure 5, α_{11} , α_{1i} α_{i1}, α_{ii}, β_{11}, β_{1i}, β_{i1}, β_{ii}, γ_{11}, γ_{1i}, γ_{i1}, γ_{ii}, P_{11}, P_{1i}, P_{i1} and P_{ii} denote the edges transmittances. From (13), figure 3 and 5, we have:

$$P = (I - S'_{22})^{-1} := \varkappa^{-1} \tag{22}$$

The submatrix P has two cases: $S'_{22} = 0$ or $S'_{22} \neq 0$

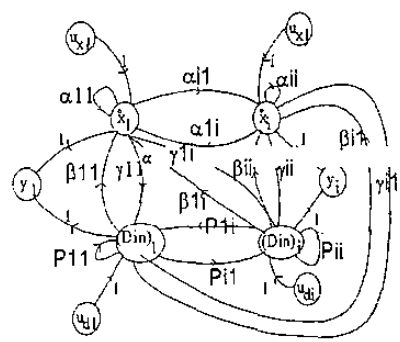

Fig. 5 MIMO System of two nodes.

5 Getting the Matrices A, B, C and D

Consider that figure 3 corresponds to a physical system of n states, r dissipative elements, with p inputs and q outputs. In the following, a procedure for the direct calculation of the matrices A, B, C and D that represents a MIMO LTI system of (7) is presented.

This method is obtained from the reduced graph of figure 5, whose generalization is the scheme of figure 4 and the matrix representation of figure 3.

5.1 Getting a Graph of the Matrix A

To find A the arriving and leaving edges from the nodes of $\dot{x}$ and their directed closed paths (directed circuits) are considered, as shown in,

Procedure 1

1. Descompose A in the sum of two components:

$$A = A_x + A_d \tag{23}$$

where the first component A_x is formed by the edges transmittances between nodes of the different states derivatives giving their elements out of the diagonal and transmittances of the self-loops of these nodes, forming their diagonal elements of this matrix, *i.e.*, for figure 5

$$A_x = \begin{bmatrix} \alpha_{11} & \alpha_{1i} \\ \alpha_{i1} & \alpha_{ii} \end{bmatrix} \tag{24}$$

The second component A_d is formed by the edges transmittances between nodes of $\dot{x}$ and nodes of D_{in}

$$A_d = \begin{bmatrix} (A_d)_{11} & (A_d)_{1i} \\ (A_d)_{i1} & (A_d)_{ii} \end{bmatrix} \tag{25}$$

2. Find the diagonal elements of A_d, by means of:

- Begin in the nodes $\dot{x}_1$ and $(D_{in})_1$. Fix the edge that arrives to $\dot{x}_1$ respective to $(D_{in})_1$. Construct all possible combinations of directed circuits through by the hinge edge, beginning and finishing in $\dot{x}_1$ and satisfying:

· A circuit must have only one edge of D_{in}. If the circuit is formed by an output and input edge of the same node of D_{in}, it will have the self-loop of D_{in}.

- Continue with the following edge that arrives to node $\dot{x}_1$ respective to D_{in}, and so on, until consider the last edge that arrives to $\dot{x}_1$ respective to D_{in}.

- Use the previous procedure for the next nodes of $\dot{x}$ but the input and output edges must be the actual node.

- Each term of each element of A_d, is given by:

$$\begin{aligned} \text{Term of the element } (A_d)_{hk} &= (\delta_1)(\delta_2)(\delta_3) \qquad (26) \\ h &= 1, 2, .., n;\ k = 1, 2, .., r \end{aligned}$$

δ_1 = Transmittance of the edge h which arrives to $\dot{x}_h$

δ_2 = Transmittance of the self-loop of $(D_{in})_k$ or transmittance of the edge $(D_{in})_k$ which conects $(D_{in})_k$ with $(D_{in})_{k+1}$

δ_3 = Transmittance of the edge k which leaves of $\dot{x}_k$

1. For figure 5, we have: $(A_d)_{11} = \beta_{11}P_{11}\gamma_{11} + \beta_{11}P_{1i}\gamma_{1i} + \beta_{i1}P_{i1}\gamma_{11} + \beta_{1i}P_{ii}\gamma_{1i}$; $(A_d)_{ii} = \beta_{i1}P_{11}\gamma_{i1} + \beta_{i1}P_{1i}\gamma_{ii} + \beta_{ii}P_{i1}\gamma_{i1} + \beta_{ii}P_{ii}\gamma_{ii}$

3. Find the elements out of the diagonal of the matrix A_d, using the procedure giving in step 2, but the terms of the elements $(A_d)_{hk}$ $(h \neq k)$, must be formed by directed paths from node h to node k.

   For the figure 5, $(A_d)_{1i} = \beta_{11}P_{11}\gamma_{i1} + \beta_{11}P_{1i}\gamma_{ii} + \beta_{1i}P_{i1}\gamma_{i1} + \beta_{1i}P_{ii}\gamma_{ii}$; $(A_d)_{i1} = \beta_{i1}P_{11}\gamma_{11} + \beta_{i1}P_{1i}\gamma_{1i} + \beta_{ii}P_{i1}\gamma_{11} + \beta_{ii}P_{ii}\gamma_{1i}$

Note that if the submatrix $S'_{22} = 0$, then $P = I$ and thus $\delta_2 = 1$

5.2 Getting a Graph of the Matrix B

The edges transmittances of the nodes of the u are considered in B. The procedure to find B is:

Procedure 2

1. Descompose B in two components:

$$B = \begin{bmatrix} B_x & B_d \end{bmatrix} \tag{27}$$

   The first component B_x is formed by the edge transmittance which connects an input node with the state derivative node directly. For the example, in figure 5: $B_x = \begin{bmatrix} 1 & 0 \\ 0 & 1 \end{bmatrix}$

   The second component B_d is formed by the edges transmittances which connect an input node with a node of $\dot{x}$ through the node of the D_{in}. For figure 5, we have:

$$B_d = \begin{bmatrix} (B_d)_{11} & (B_d)_{1i} \\ (B_d)_{i1} & (B_d)_{ii} \end{bmatrix} \tag{28}$$

2. Get the terms of the diagonal elements of B_d, by:

   - Begin in the node, u_{d1}. Constuct all directed path of the possible combinations of the edges transmittances that connect u_{d1} with $\dot{x}_1$, through by $(D_{in})_1$, satisfying:

   · A path must have only one edge of D_{in} and if only has an edge between $\dot{x}_1$ and $(D_{in})_1$, it has the self-loop of $(D_{in})_1$, so each term is given by

$$\begin{aligned} \text{Term of the element } (B_d)_{hk} &= (\eta_1)(\eta_2)(\eta_3) \qquad (29) \\ h &= 1,2,..,r;\ k = 1,2,..,p \end{aligned}$$

η_1 = Transmittance of the edge h which arrives to $\dot{x}_h$

η_2 = Transmittance of the self-loop of $(D_{in})_k$ or transmittance of the edge which connects $(D_{in})_k$ to $(D_{in})_{k+1}$

η_3 = Transmittance of the edge k that goes out of u_{Dk}

1. For example in figure 5, we have $(B_d)_{11} = \beta_{11}P_{11} + \beta_{1i}P_{i1}$; $(B_d)_{ii} = \beta_{i1}P_{1i} + \beta_{ii}P_{ii}$

2. Obtain the terms of the elements that are out of the diagonal of B_d, in a similar way that for their diagonal elements, but for the terms of element $(B_d)_{hk}$, take the arrival node $\dot{x}_k$ and the output node u_{dk} and for the term of element $(B_d)_{kh}$ is the opposite, the previous is resumed using (29) for $h \neq k$.

   For example in figure 5: $(B_d)_{1i} = \beta_{11}P_{1i} + \beta_{1i}P_{ii}$; $(B_d)_{i1} = \beta_{i1}P_{11} + \beta_{ii}P_{i1}$

5.3 Getting a Graph of the Matrix C

To find C, edges transmittances which arrives to nodes of y and goes out of nodes of $\dot{x}$ are considered, as shown in,

Procedure 3

1. Descompose C in two components:

$$C = C_x + C_d \tag{30}$$

   The first component C_x, is formed by the edges transmittances which connects an output node with node of $\dot{x}$ directly. For example in figure 5: $C_x = \begin{bmatrix} 1 & 0 \\ 0 & 1 \end{bmatrix}$

   The second component, C_d, is formed by the edges transmittances which connect an output node with a node of $\dot{x}$ through the node of D_{in}.

2. Get terms of the diagonal elements of C_d:

   - Begin by the first output node y_1. Construct all directed paths of the possible combinations of the edges transmittances that connects y_1 with $\dot{x}_1$ through $(D_{in})_1$, satisfying:

   · A path must have only one edge of D_{in} and if only exists a edge between $\dot{x}_1$ and $(D_{in})_1$, it take the self-loop of $(D_{in})_1$ and so on, with the rest of outputs. Thus, each term is given by:

$$\begin{aligned} \text{Term of the element } (C_d)_{hk} &= (\rho_1)(\rho_2)(\rho_3) \qquad (31) \\ h &= 1,2,...,q;\ k = 1,2,...,r \end{aligned}$$

ρ_1 = Transmittance of the edge h which arrives to y_h

ρ_2 = Transmittance of the self-loop of $(D_{in})_k$ or transmittance which connects edge $(D_{in})_k$ to edge $(D_{in})_{k+1}$

ρ_3 = Transmittance of the edge k that leaves of $\dot{x}_h$

1. For example in figure 5: $(C_d)_{11} = P_{11}\gamma_{11} + P_{i1}\gamma_{1i}$; $(C_d)_{ii} = P_{ii}\gamma_{ii} + P_{i1}\gamma_{i1}$

The system representation is obtained from (19):

$$\bar{S}_{11} = \begin{bmatrix} 0 & -\frac{1}{m} & 0 & 0 \\ k_1 & 0 & -k_2 & 0 \\ 0 & \frac{1}{m} & 0 & -\frac{1}{M} \\ 0 & 0 & k_2 & 0 \end{bmatrix} \quad \bar{S}_{12} = \begin{bmatrix} 0 \\ -b \\ 0 \\ b \end{bmatrix}$$
$$S'_{21} = \begin{bmatrix} 0 & \frac{1}{m} & 0 & -\frac{1}{M} \end{bmatrix} \quad S'_{22} = 0$$
$$S'_{31} = \begin{bmatrix} 0 & \frac{1}{m} & 0 & -\frac{1}{M} \end{bmatrix} \quad S'_{32} = 0 \tag{37}$$

The graph respective to the equation (37) is shown in figure 8.

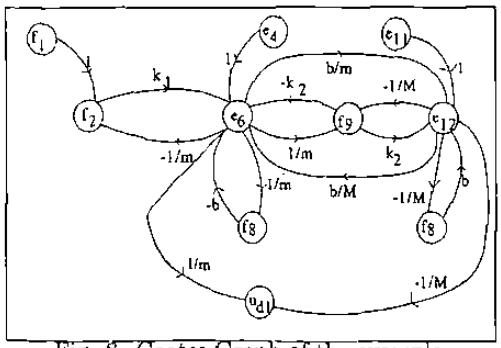

Fig. 8. Coates Graph of the example.

The dynamic model in state variables is given by (7), we use section V, noting that from (37), $S'_{22} = 0$, giving $P = I$. Now, from (24), we have:

$$A_x = \begin{bmatrix} 0 & -\frac{1}{m} & 0 & 0 \\ k_1 & 0 & -k_2 & \frac{b}{M} \\ 0 & \frac{1}{m} & 0 & -\frac{1}{M} \\ 0 & \frac{b}{m} & k_2 & 0 \end{bmatrix} \tag{38}$$

From (25) we have:

$$A_d = \begin{bmatrix} 0 & 0 & 0 & 0 \\ 0 & (A_d)_{22} & 0 & 0 \\ 0 & 0 & 0 & 0 \\ 0 & 0 & 0 & (A_d)_{44} \end{bmatrix} \tag{39}$$

To get $(A_d)_{22}$ and $(A_d)_{44}$ from (26) we obtain:

$$(\delta_1)_{22} = -b; \ (\delta_2)_{22} = 1; \ (\delta_3)_{22} = \frac{1}{m} \tag{40}$$

sustituting (40) into (26) gives:

$$(A_d)_{22} = -\frac{b}{m} \tag{41}$$

Analogously:

$$(\delta_1)_{44} = b; \ (\delta_2)_{44} = 1; \ (\delta_3)_{44} = -\frac{1}{M} \tag{42}$$

sustituting (42) in (26) gives:

$$(A_d)_{44} = -\frac{b}{M} \tag{43}$$

So, from (23), (38), (39), (41), and (43), A is given by:

$$A = \begin{bmatrix} 0 & -\frac{1}{m} & 0 & 0 \\ k_1 & -\frac{b}{m} & -k_2 & \frac{b}{M} \\ 0 & \frac{1}{m} & 0 & -\frac{1}{M} \\ 0 & \frac{b}{m} & k_2 & -\frac{b}{M} \end{bmatrix} \tag{44}$$

From (27) B is obtained, noting that $B_d = 0$ and $B = B_x$:

$$B = \begin{bmatrix} 1 & 0 & 0 \\ 0 & 1 & 0 \\ 0 & 0 & 0 \\ 0 & 0 & 1 \end{bmatrix} \tag{45}$$

Noting that $C_d = 0$, from (30) C is given by:

$$C = \begin{bmatrix} 0 & \frac{1}{m} & 0 & -\frac{1}{M} \end{bmatrix} \tag{46}$$

Finally,

$$D = 0 \tag{47}$$

Note that with a little of experience and skill A, B, C, and D are obtained directly, easy and quicly from the Coates Graph, as shown in the previous example. The same is true in general if $E = I$ and $S_{22} = 0$.

8 Conclusions

A graph from Bond Graph that represents a physical system on key vectors, is obtained. A graphical procedure to obtain the state space representation of a dynamic MIMO LTI model is presented.

References

[1] H.M. Paynter, *Analysis and design of engineering systems*, MIT press, Cambridge, Mass, 1961.

[2] Dean C. Karnopp and Ronald C. Rosenberg, *System Dynamics: A Unified Approach*, Wiley, John & Sons, 1975.

[3] P.E. Wellstead, *Physical System Modelling*, Academic Press, London, 1979.

[4] C. Suer and G. Dauphin-Tanguy, "Bond graph approach for structural analysis of MIMO linear systems", *J.Flanklin Inst.*, vol. 328, No.1 pp. 55-70, 1991.

[5] Y.K. Wong and A.B. Rad, "Bond Graph Simulations of Electrical Systems", *IEEE Catalogue* No. 98E137, (1998).

[6] Wai-Kai Chen, *Applied Graph Theory: Graphs and Electrical Networks*, 1976, North-Holland Publishing Company.

[7] S.H. Birkett and P.H. Roe, "The Mathematical Foundations of Bond Graphs -I. Algebraic Theory", *J. of the Franklin Institute*, vol. 326, no. 3, pp. 329-350, 1989.

C.2 Hurwitz Stability Conditions For a LTI System: A Bond Graph Approach

Gonzalez-A. Gilberto, R. Galindo, J. de Leon

9th IEEE International Conference On Methods and Models in Automation and Robotics (MMAR 2003), 25-28 August 2003, Miedzyzdroje, Poland.

HURWITZ STABILITY CONDITIONS FOR A LTI SYSTEM: A BOND GRAPH APPROACH

GONZALEZ-A. GILBERTO[1,2], R. GALINDO[1], J. DE LEON[1]

[1]University of Nuevo Leon, Department of Electrical Engineering 66451 San Nicolas de los Garza, N.L. Mexico (+52)8183294020 Ext.5773
[2]University of Michoacan, Faculty of Electrical Engineering 58030, Morelia, Michoacan, Mexico (+52)4433265776

Abstract. A direct graphical procedure to know the stability conditions for a physical Linear Time Invariant (LTI) system is presented. It is based on the Bond Graph model of the physical system and on a linear graph of the characteristic polynomial of the system. The proposed linear graph represents a Coates matrix and a Hurwitz matrix. It is shown, that using the Hurwitz criterion the stability conditions can be obtained directly from this linear graph. This methodology is applied for open and closed loop systems through the examples given.

Key Words. Bond Graph, Coates Graph, Hurwitz Matrix, Physical Control, Modelling Tools, Stability.

1 Introduction

One of the most basic requirements of any control system is stability. A LTI system is stable if all the poles of its transfer function or its realization $(A,\ B,\ C,\ D)$ lie in the left half plane[1]. For these requirement the system model is needed. Thus, Bond Graph methodology is applied to find the model.

Bond Graph deals with a graphical approach to system modelling, the essential feature of the Bond Graph approach is the representation of energetic interactions between systems and/or system components by a single line. It can represent many energy types and describes how the power flows through the system[2, 3].

Moreover, given a Bond Graph model of a system, we can find the coefficients of the characteristic polynomial using causal paths [5] or a Coates matrix[11].

If we have the characteristic polynomial of the system we can apply the Routh-Hurwitz criterion to know the system stability, but this criterion is an algebraic method that for large systems with many parameters become an abstract and difficult task. Also, for control objectives it is desirable a methodology closer to the physical system, i.e., for control in the physical domain.

So, we present an easy and direct graphical procedure to get the stability conditions of the physical system using graph theory. This methodology does not need to know the transfer function or its realization $(A,\ B,\ C,\ D)$.

Section II resumes the Bond Graph modelling of a physical system. A procedure to obtain a graph from its Bond Graph which represents a modified Coates matrix is given in section III. The methodology to obtain the characteristic polynomial using causal paths or a Coates graph is described in section IV. In section V we present a graphical procedure to get a linear graph of the characteristic polynomial. The linear graph represents a Coates matrix of the Hurwitz matrix. Stability conditions for a physical system are presented. Examples are given in section VI. Finally, section VII gives our conclusions.

2 Bond Graph Model [3, 5, 6]

Consider a multiport LTI system which has the key vectors of figure 1.

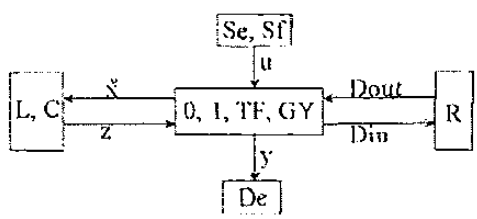

Figure 1. Key vectors of a Bond Graph

Here, (Se, Sf), (L,C) and (R) denote the source, the storage and the dissipation fields, (De) the detector and (0, 1, TF, GY) the junction structure with transformers, TF, and gyrators, GY.

The state $x \in R^n$ is composed of energy variables of effort, e, and flow, f, with integral causality, $u \in R^p$ the plant input, $y \in R^q$ the plant output, $z \in R^n$ the co-energy and $D_{in} \in R^r$ and $D_{out} \in R^r$ are a mixture of e and f showing the energy exchanges between the dissipation field and the junction structure.

The relations of the storage and dissipation fields are:

$$z = Fx \quad (1)$$

$$D_{out} = LD_{in} \quad (2)$$

where L is a diagonal matrix composed of R and $1/R$ coefficients, and F is composed of $1/L$ and $1/C$ coefficients.

The relation of the junction structure is:

$$\begin{bmatrix} \dot{x} \\ D_{in} \\ y \end{bmatrix} = S \begin{bmatrix} z \\ D_{out} \\ u \end{bmatrix} \quad (3)$$

where the junction structure of the system is given by:

$$S = \begin{bmatrix} S_{11} & S_{12} & S_{13} \\ S_{21} & S_{22} & S_{23} \\ S_{31} & S_{32} & S_{33} \end{bmatrix} \quad (4)$$

The entries of S take the values inside the set $\{0, \pm 1, \pm m, \pm r\}$ where m and r are transformer and gyrator modules; S_{11} and S_{22} are square skew-symmetric submatrices and S_{12} and S_{21} are submatrices each other negative transpose.

The linear graph and the Coates Matrix of [11] for the system of figure 1 is summarized in the next section.

3 Getting the Graph from Bond Graph [10]

Consider the scheme of figure 1. The procedure to obtain the graphical representation of a Bond Graph, is summarized for integral causality.

From (1)-(4):

$$\begin{bmatrix} \dot{x} \\ D_{in} \\ y \end{bmatrix} = S' \begin{bmatrix} x \\ D_{in} \\ u \end{bmatrix} \quad (5)$$

$$S' = \begin{bmatrix} S'_{11} & S'_{12} & S_{13} \\ S'_{21} & S'_{22} & S_{23} \\ S'_{31} & S'_{32} & S_{33} \end{bmatrix} \quad (6)$$

where

$$S'_{11} = S_{11}F;\ S'_{21} = S_{21}F;\ S'_{31} = S_{31}F \quad (7)$$
$$S'_{12} = S_{12}L;\ S'_{22} = S_{22}L;\ S'_{32} = S_{32}L$$

Let suppose that S' is a Coates matrix .The graphical representation of (5) is shown in figure 2.

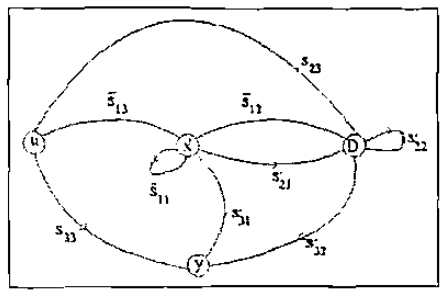

Figure 2. Linear Planar System Graph.

We can rewrite (5) as:

$$\begin{bmatrix} \dot{x} \\ D_{in} \\ u \\ y \end{bmatrix} = \hat{S} \begin{bmatrix} x \\ D_{in} \\ u \\ y \end{bmatrix} \quad (8)$$

The matrix $\hat{S}$ represents a modified Coates matrix [11] . If $\dot{x}$ is used instead of x in (8) the elements of the first column are different by a factor $\frac{1}{s}$, where s is the Laplace operator. We omit this factor because for LTI systems does not affect the elements interconnection.

Next, we show how to get the characteristic polynomial using a linear graph or a Bond Graph of a physical system.

4 Getting the Characteristic Polynomial

The stability of a system can be determined knowing the characteristic polynomial. This polynomial can be found analytically or graphically using Bond Graphs or Coates Graphs.

4.1 Coates Graph [11]

Without loss generality, we obtain a sectional subgraph with Coates matrix A_c of the linear graph of figure 2 neglecting the inputs and outputs. So, we obtain the linear graph and the Coates matrix A_c and the determinant is given by [8]:

$$\det(\lambda I - A_c) = \lambda^n + \sum_{k=1}^{n} \lambda^{n-k} \left[\sum_{A_c[V_k]} \sum_{u} (-1)^{L_h} f(h_{uk}) \right] \quad (9)$$

where h_{uk} are the 1-factors u^{th} in $A_c[V_k]$, $A_c[V_k]$ is a sectional subgraph of k-nodes of A_c and L_h is the number of directed circuits in h_{uk}.

4.2 Causal Path-Causal Loop [5]

A Bond Graph shows not only the topological structure of a system but also its causal organization, by pointing out the cause and effect relations, this causal structure gives the notion of causal path. A junction structure causal path is an alternating sequence

of bonds and nodes such that: a) for the acausal graph, the sequence forms a single chain, b) all nodes in the sequence have complete and correct causality, c) two nodes from a causal path have at the same node opposite causal orientations. A causal loop is a closed single path. A Mason loop is a causal loop from the output of a port back to the input of the same port, without tracing the same bond in the same direction more than once.

The characteristic polynomial is given by:

$$D(s) = 1 - \sum_{j} L_{1j}(s) + \sum_{k} L_{2k}(s) - \sum_{l} L_{3l}(s) + \ldots \tag{10}$$

where $L_{rk}(s)$ is the product of the loop gains of k^{th} set of r Mason loops which does not touch one to another. The $L_{1j}(s)$ loop gain of the j^{th} Mason loop is defined by:

$$L_{ij}(s) = (-1)^{n_0+n_1} \prod_{j,k} \left(m_j \, \acute{o} \, \frac{1}{m_j} \right)^2 \left(r_k \, \acute{o} \, \frac{1}{r_k} \right)^2 \prod_{g} \tag{11}$$

where n_0 and n_1 represent the total number of changes of orientations for the bonds, respectively at the 0-junctions while following the flow variable, and at the 1-junctions while following the effort variable; $\prod_{j,k}$ denotes the product of m_j, $\frac{1}{m_j}$ and r_k, $\frac{1}{r_k}$ that are the modules of the TF and GY elements which are included in the causal path, depending on their causalities and $\prod_{g}$ designs the product of gains of elements composing the loop.

Next section presents a graphical procedure to get the stability conditions of a system.

5 Getting the Stability Conditions

A procedure to get a linear graph which represents the characteristic polynomial is presented. It is used to get the stability conditions using the Hurwitz matrix in a graphical way.

To construct the stability Coates graph $G_c(D)$, we present the following:

Procedure A.

1.- Consider that the characteristic polynomial is given by:

$$a_0\lambda^n + a_1\lambda^{n-1} + a_2\lambda^{n-2} + \ldots + a_n\lambda^0 = 0 \tag{12}$$

where $a_0 = 1$

2.- The number of nodes is equal to the polynomial order. Construction each node a self-loop as shown in figure 3:

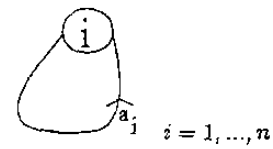

Figure 3. Self loop of a node.

3.- Construct edges between different nodes using the following figures 4 and 5.

A) Edges to the right. Initially $j = 1$ $h = 0$

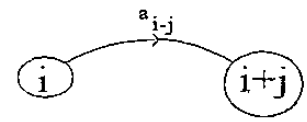

Figure 4. Edges to the right.

For $i = j, \ldots, k$; where $k = n - 2j + h + 1 \; \forall \, i \leq k$
If $i = k$ then $j \leftarrow j + 1$ and $h \leftarrow h + 1$ and we increase i until $j < k$, where $x \leftarrow y$ denotes that the y value is assigned to x.

B) Edges to the left. Initially $j = 1$, $h = 0$.

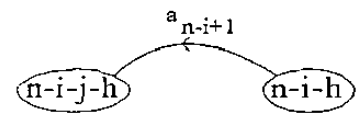

Figure 5. Edges to the left.

For $i = 1, \ldots, k$; where $k = n - j - 1 - h \; \forall \, i \leq k$
If $i = k$ then $j \leftarrow j + 1$ and $h \leftarrow h + 1$ and we increase i until $j < k$. ■

As shown by the following examples the previous procedure generates a linear graph which has a single structure.

The graph $G_c(D)$ represents a Coates graph of the Hurwitz matrix. Therefore, we can give the stability conditions, using Hurwitz Criterion [1] The necessary and sufficient condition that all roots of (12) lie in the left half plane is that the Hurwitz determinants D_k, $k = 1, 2, \ldots, n$, must all be positive.

So, from graph theory[11] the Hurwitz determinant D_n is given by:

$$\det D = D_n = (-1)^n \sum_{h} (-1)^{L_h} f(h) \tag{13}$$

where h is a 1-factor in $G_c(D)$ and L_h denotes the number of directed circuits in h and $f(h)$ represents the product of the weights associated with the edges of h.

In according to Hurwitz criterion, we have to get n determinants, so, we propose the following procedure:

Procedure B.

1.- Calculate D_n from (13).

2.- The determinant D_{n-1} is obtained from the graph $G_c(D)$, removing the n-node and using (13) with $n-1$, then from the graph $G_c(D)$.

3.- Removing the n and $n-1$ nodes, and using (13) we calculate D_{n-2} and son on, to reach D_1. ■

6 Examples

Example 1.

Consider the mechanical system of figure 6.

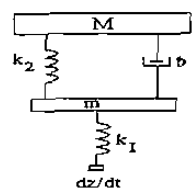

Figure 6. Mechanical system of example 1

In figure 7, we show the Bond Graph of this system.

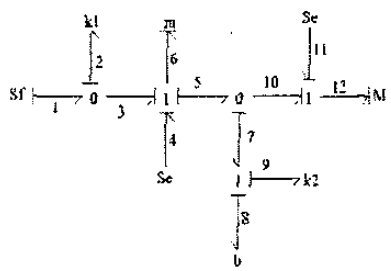

Figure 7. Bond graph of the example 1.

The key vectors are:

$$x = \begin{bmatrix} f_{a_2} \\ e_{a_6} \\ f_{a_9} \\ e_{a_{12}} \end{bmatrix}; \dot{x} = \begin{bmatrix} f_2 \\ e_6 \\ f_9 \\ e_{12} \end{bmatrix}; z = \begin{bmatrix} e_2 \\ f_6 \\ e_9 \\ f_{12} \end{bmatrix}$$

$$u = \begin{bmatrix} f_1 \\ e_4 \\ e_{11} \end{bmatrix}; y = f_8;\ D_{in} = f_8;\ D_{out} = e_8$$

where f is the velocity and e is the force in each element of the mechanical system; f_{a_2} and f_{a_9} are the translational displacements in k_1 and k_2 respectively; e_{a_6} and $e_{a_{12}}$ are the translational momentums m and M respectively ; f_1 is the input velocity and e_4 and e_{11} are the gravity force under m and M respectively.

The constitutive relations for the elements are:

$$\begin{bmatrix} e_2 \\ f_6 \\ e_9 \\ f_{12} \end{bmatrix} = \begin{bmatrix} k_1 & 0 & 0 & 0 \\ 0 & \frac{1}{m} & 0 & 0 \\ 0 & 0 & k_2 & 0 \\ 0 & 0 & 0 & \frac{1}{M} \end{bmatrix} \begin{bmatrix} f_{a_2} \\ e_{a_6} \\ f_{a_9} \\ e_{a_{12}} \end{bmatrix}$$

$$e_8 = bf_8 \qquad (14)$$

The junction structure of the system is given by (4), where

$$S_{11} = \begin{bmatrix} 0 & -1 & 0 & 0 \\ 1 & 0 & -1 & 0 \\ 0 & 1 & 0 & -1 \\ 0 & 0 & 1 & 0 \end{bmatrix}$$

$$S_{12} = -S_{21}^T = \begin{bmatrix} 0 \\ -1 \\ 0 \\ 1 \end{bmatrix}; S_{22} = S_{23} = S_{32} = S_{33} = 0$$

$$S_{13} = \begin{bmatrix} 1 & 0 & 0 \\ 0 & 1 & 0 \\ 0 & 0 & 0 \\ 0 & 0 & 1 \end{bmatrix}; S_{31} = S_{21}$$

The linear graph of the system is shown in figure 8

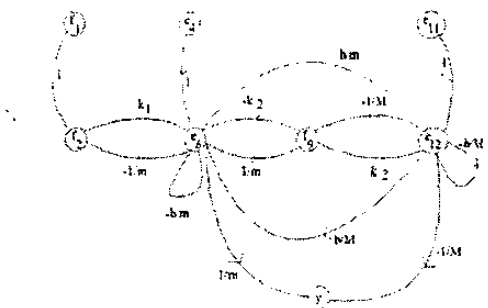

Figure 8. Linear Graph of the example 1.

From (9) the characteristic polynomial is:

$$\det(\lambda I - A_c) = \lambda^4 + a_1\lambda^3 + a_2\lambda^2 + a_3\lambda + a_4 \quad (15)$$

The following coefficients are obtained from (9) using figure 8. For a_1 the 1-factors are shown in figure 9.

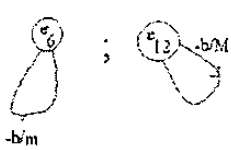

Figure 9. Sectional Subgraph of 1-node.

$$a_1 = \frac{b}{m} + \frac{b}{M} \qquad (16)$$

For a_2 use figure 10

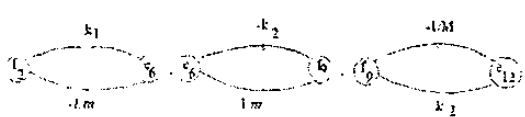

Figure 10. Sectional Subgraph of 2-nodes.

$$a_2 = \frac{k_1}{m} + \frac{k_2}{m} + \frac{k_2}{M} \qquad (17)$$

For a_3 use figure 11

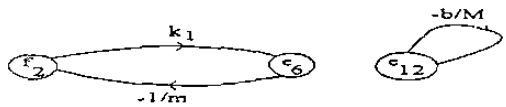

Figure 11. Sectional Subgraph of 3-nodes.

$$a_3 = \frac{k_1 b}{mM} \tag{18}$$

Finally a_4 use figure 12

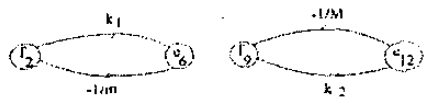

Figure 12. Sectional Subgraph of 4 nodes.

$$a_4 = \frac{k_1 k_2}{mM} \tag{19}$$

Using the procedure A given on section V, we have the stability Coates graph of figure 13.

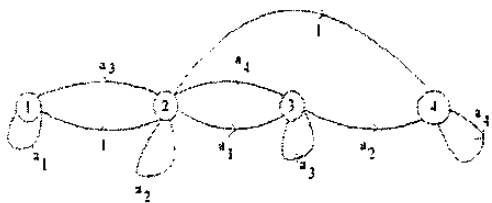

Figure 13. Stability Caotes graph.

We can find the Hurwitz Determinants from Procedure B.

Consider figure 14, D_4 is given by

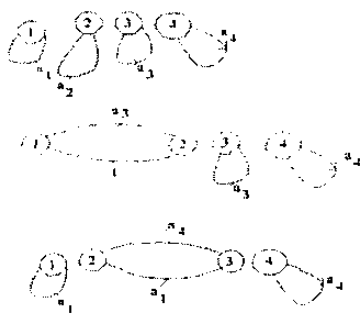

Figure 14 Sectional Subgraph of 4-nodes.

$$D_4 = a_1 a_2 a_3 a_4 - a_3^2 a_4 - a_1^2 a_4^2 \tag{20}$$

From figure 15, D_3 is:

Figure 15. Sectional Subgraph of 3-nodes.

$$D_3 = a_1 a_2 a_3 - a_3^2 - a_1^2 a_4 \tag{21}$$

Figure 16, yields D_2

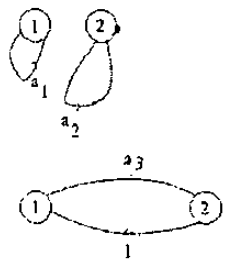

Figure 16. Sectional Subgraph of 2-nodes.

$$D_2 = a_1 a_2 - a_3 \tag{22}$$

Finally, D_1 is obtained from figure 17.

Figure 17. Sectional Subgraph of 1-node.

$$D_1 = a_1 \tag{23}$$

Substituting (16) to (19) in (20) to (23) we have the stability conditions for the physical system:

$$D_4 = \frac{b^2 k_1^3 k_2}{m^4 M^2} > 0 \tag{24}$$

$$D_3 = \frac{b^2 k_1^2}{m^3 M} > 0 \tag{25}$$

$$D_2 = \frac{b(k_1 + k_2)}{m^2} + \frac{2bk_2}{mM} + \frac{bk_2}{M^2} > 0 \tag{26}$$

$$D_1 = \frac{b}{m} + \frac{b}{M} > 0 \tag{27}$$

This graphical procedure, allow us to know the performance of the system in a single form through the acknowledge of the stability conditions and system parameters. Moreover, this procedure show how the system parameters are reflected in the physical system.

Example 2.

Consider an output feedback where k_c is the feedback gain, for the system of example 1. The linear graph of the closed loop is shown in Figure 18.

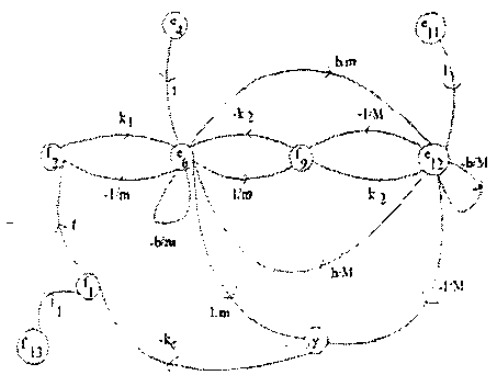

Figure 18. Linear graph of the closed loop system.

Reducing the graph of figure 18, we have figure 19.

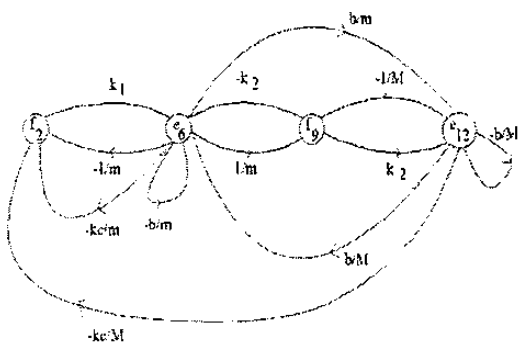

Figure 19. Linear graph reduced of the closed loop system.

The characteristic polynomial for this example is given by (15), and its coefficients are obtained in the same way as for example 1. So, the coefficients are obtained using section IV:

$$\begin{aligned} a_1 &= \frac{b}{m} + \frac{b}{M} \\ a_2 &= \frac{k_1 + k_2 + k_1 k_c}{m} + \frac{k_2}{M} \\ a_3 &= \frac{k_1 b + 2k_1 k_c b}{mM} \\ a_4 &= \frac{k_1 + k_2 + 2k_1 k_2 k_c}{mM} \end{aligned}$$

The stability Coates graph is shown in figure 13 and from (20) to (23) we have the stability conditions:

$$\begin{aligned} D_1 &= b\left(\frac{1}{m} + \frac{1}{M}\right) > 0 \\ D_2 &= b\left(\frac{k_1 + k_2 + k_1 k_c}{m^2} + \frac{k_2}{M^2} + \frac{k_2 - k_1 k_c}{mM}\right) > 0 \\ D_3 &= \frac{k_1^2 b^2}{m^2 M}\left(\frac{1 + 3k_c + 2k_c^2}{m} - \frac{k_c + 2k_c^2}{M}\right) > 0 \\ D_4 &= \frac{b^2 k_1^3 k_2}{m^3 M^2}\left(\frac{1 + 7k_c + 4k_c^3 + 6k_c^2}{m} - \frac{k_c + 4k_c^3 + 6k_c^2}{M}\right) > 0 \end{aligned}$$

This example shows that, the proposed graphical procedure lets to get the conditions for the controller gain, guaranteeing stability in the closed loop system.

7 Conclusions

A graph that represents the Hurwitz matrix of a LTI system is proposed. A graphical procedure to determine the stability conditions in a physical LTI system is presented. This methodology does not require to know the transfer function or its realization (A, B, C, D). The results can be applied to open or closed loop systems.

References

[1] B. C. Kuo "Automatic Control Systems", 6^{th} ed. Englewood Cliffs, N.J., Prentice Hall, (1991).

[2] Dean C. Karnopp, Ronald C. Rosenberg, "System Dynamics: A Unified Approach", Wiley, John & Sons, April (1975).

[3] P.E. Wellstead, "Physical System Modelling", Academic Press, London, (1979).

[4] D.C. Karnopp, "Bond graphs in control: Physical state variables and observers", J. Flanklin Institute, 308(3) pp. 221-234, (1979).

[5] G. Dauphin-Tanguy, Serge Scavarda "Modelisation des Systemes physiques par bond graphs", Systemes Lineaires Ouvrage Collectif. Editions Masson, Paris, Vol 1, Chap 2, pp 35-112, (1993).

[6] C. Suer, G. Dauphin-Tanguy, "Bond graph approach for structural analysis of MIMO linear systems", J.Flanklin Inst., vol. 328, No.1 pp. 55-70, (1991).

[7] Chi-Tsong Chen "Linear System Theory and Design", Third ed., Oxford University Press, (1999).

[8] Gene F. Franklin, J. David Powell, Abbas Emani-Naeini, "Feedback Control of Dynamic Systems" Addison Wesley Publishing Company, (1988).

[9] P.J. Gawthop, "Physical Model-Based Control:A Bond Graph Approach", J. of the Franklin Institute, 332B(3), pp. 285-305, (1995).

[10] Gonzalez-A. Gilberto, R. Galindo, J. de Leon, "A Direct Graph Procedure from Bond Graph for MIMO LTI Systems", ICARCV'02, pp.880-885, Singapore, Dec. (2002).

[11] Wai-Kai Chen,"Applied Graph Theory: Graphs and Electrical Networks", (1976), North-Holland Publishing Company.

C.3 Direct Control in Bond Graph by State Estimated Feedback for MIMO LTI Systems

Gonzalez-A. Gilberto, R. Galindo

IEEE International Conference on Control Applications, September 18-20, Glasgow, Scotland, U.K., 2002.

Proceedings of the 2002 IEEE International
Conference on Control Applications
September 18-20, 2002 • Glasgow, Scotland, U.K.

Direct Control in Bond Graph by State Estimated Feedback for MIMO LTI Systems

González-A. Gilberto[1,2]*; R.Galindo[1] †
[1]University of Nuevo Leon, Department of Electrical Engineering
66451 San Nicolás de los Garza, N.L., Mexico.(+52)83294020 Ext. 5773 Fax (+52)83764514
[2] University of Michoacan, Faculty of Electrical Engineering
58030, Morelia, Michoacan, Mexico (+52)3265776

Abstract. A state estimated feedback based on Bond Graphs for Multivariable Linear Time Invariant (LTI) Systems is proposed. A direct graphical technique (Bond Graph) to obtain the closed loop system in state variables using the open loop graph is presented. Structures for the controller and the observer directly in closed loop are presented. Therefore, the control in the physical or in the Bond Graph domains is realized. The dynamic assignment problem is solved and examples are given.

Keywords.–Bond Graph, State Feedback, Observer, Dynamic Assignment, Direct graph Control

I. Introduction

A Bond Graph is a model of a dynamic system where a collection of components interact with each other through energy ports. These components are placed in the system which exchanges energy. A Bond Graph consists of subsystems linked by lines to show the energetic connections. A Bond Graph can represent a variety of energy types and describes how the power flows through the system [10, 11, 12].

Bond Graph was established by [1]. The idea was developed by [2] and [3] how a powerful tool of modelling. Control applications in Bond Graph specially another approach for state feedback with observer can be found in [4, 5]. Also, in [11] a non based join junction structure approach can be found.

The control objective is to get a realizable controller and to consider the physical characteristics of the system under control. So, the extension of Bond Graph for control techniques, not only for modelling, allows to design the control from the physical model, assuring a realizable controller.

The main key points of the Bond Graph methodology are: a model containing the energetic junction structure, *i.e.*, the system architecture; different energy domains are covered and the coupling of subsystems are allowed; the cause to effect relations of each element are obtained graphically; and the state variables have a physical meaning.

Section II gives the Bond Graph model of a physical system using the junction structure. The state estimated feedback control is described in section III [8]. The closed loop state space and observer models are obtained in Section IV, using the information of the open loop junction structure. These models are obtained directly from open loop Bond Graph model. Also, an equivalence to the traditional state estimated feedback is given which allows to solve the dynamic assignment problem. Section V proposes the direct gains design in the Bond Graph for the controller and the observer. The obtained results are applied in section VI, for an electrical system. Finally, conclusions are given in section VII.

II. Bond Graph Model [3, 6, 7]

Consider the multiport LTI system scheme which has the key vectors of figure 1.

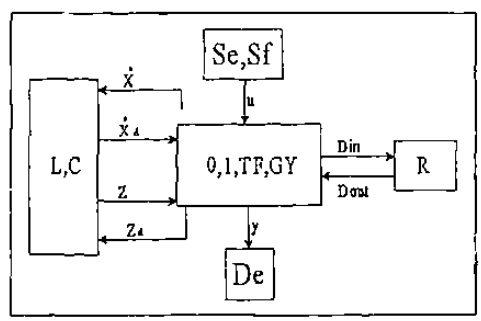

Figure 1. Key vectors of a Bond Graph

In figure 1, (Se, Sf), (L,C) and (R) denote the source the storage and the dissipation fields, (De) the detector and (0, 1, TF, GY) the junction structure with transformers, TF, and gyrators, GY.

The state $x \in \Re^n$ and $x_d \in \Re^m$ are composed of energy variables for effort, e, and flow, f, with integral and

*gilmichga@yahoo.com.mx
†rgalindo@gama.fime.uanl.mx

0-7803-7386-3/02/$17.00 © 2002 IEEE

derivative causality respectively, $u \in \Re^p$ denotes the plant input, $y \in \Re^q$ the plant output, $z \in \Re^n$ the co-energy, $z_d \in \Re^m$ the derivative co-energy and $D_{in} \in \Re^r$ and $D_{out} \in \Re^r$ are a mixture of e and f showing the energy exchanges between the dissipation field and the junction structure.

The relations of the storage and dissipation fields are:

$$z = Fx \quad (1)$$
$$D_{out} = LD_{in} \quad (2)$$
$$z_d = F_d x_d \quad (3)$$

The relations of the junction structure are:

$$\begin{bmatrix} \dot{x} \\ D_{in} \\ y \end{bmatrix} = S \begin{bmatrix} z \\ D_{out} \\ u \\ \dot{x}_d \end{bmatrix} \quad (4)$$

$$z_d = -S_{14}^T z \quad (5)$$

where the junction structure of the system is given by:

$$S = \begin{bmatrix} S_{11} & S_{12} & S_{13} & S_{14} \\ S_{21} & S_{22} & S_{23} & 0 \\ S_{31} & S_{32} & S_{33} & 0 \end{bmatrix} \quad (6)$$

The entries of S take values inside the set $\{0, \pm 1, \pm m, \pm n\}$ where m and n are transformer and gyrator modules; S_{11} and S_{22} are square skew-symmetric matrices and S_{12} and S_{21} are matrices each other negative transpose. The state equation is [8, 9]:

$$\dot{x} = Ax + Bu \quad (7)$$
$$y = Cx + Du$$

where

$$A = E^{-1}(S_{11} + S_{12}MS_{21})F \quad (8)$$
$$B = E^{-1}(S_{13} + S_{12}MS_{23}) \quad (9)$$
$$C = (S_{31} + S_{32}MS_{21})F \quad (10)$$
$$D = S_{33} + S_{32}MS_{23} \quad (11)$$

being

$$E = I + S_{14}F_d^{-1}S_{14}^T F \quad (12)$$
$$M = (I - LS_{22})^{-1}L \quad (13)$$

Next section gives the control by state estimated feedback [8]. This scheme is used in section IV for the Bond Graph approach.

III. Control by State Estimated Feedback

Once the model in state variables is had, the control law by state feedback can be applied. However, often x is not easy to know or to measure. So, a solution is to use an observer as shown in figure 2

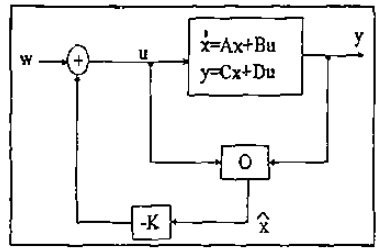

Figure 2. Closed loop estimator

The control law by state estimated feedback is:

$$u = -K\hat{x} + w \quad (14)$$

where $w \in \Re^p$ denotes the input reference, K the feedback gain and $\hat{x} \in \Re^n$ the estimated state.

From (14) and (7), the closed loop system is:

$$\dot{x} = Ax - \tilde{A}\hat{x} + Bw \quad (15)$$
$$y = Cx - \tilde{C}\hat{x} + Dw$$

where

$$\tilde{A} = BK \quad (16)$$
$$\tilde{C} = DK \quad (17)$$

The asymptotic observer of Lurenber is [8]:

$$\dot{\hat{x}} = A\hat{x} + Bu + H(y - \hat{y}) \quad (18)$$
$$\hat{y} = C\hat{x} + Du$$

where H is the observer gain.

Substituting (14) into (18) yields:

$$\dot{\hat{x}} = \hat{A}\hat{x} + \hat{B}w + \tilde{A}x \quad (19)$$
$$\hat{y} = \hat{C}\hat{x} + \hat{D}w$$

where

$$\hat{A} = A - BK - HC \quad (20)$$
$$\tilde{A} = HC \quad (21)$$
$$\hat{C} = C - \tilde{C};\ \hat{B} = B;\ \hat{D} = D \quad (22)$$

In section IV, we get (15) and (19) directly open loop Bond Graph model.

IV. Control by Bond Graph

A direct graphical technique for an open loop model represented by Bond Graph is presented. The closed loop and the observer Bond Graph models are obtained directly from the open loop model. We assume that all the elements have linear constitutive relations.

The control general structure for state estimated feedback in Bond Graph is shown in figure 3.

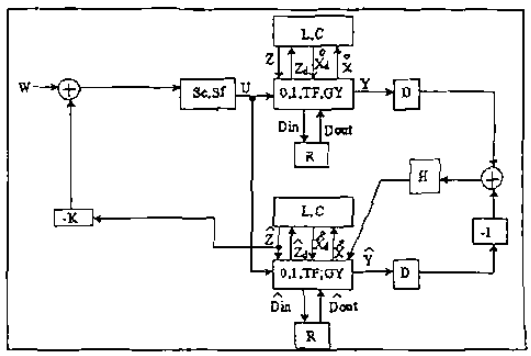

Figure 3. Closed loop with observer in Bond Graph

The objective to represent the model and the observer in block diagrams is to obtain the feedback system model from S in (4). This let us to know, the change of S due to the observer and the state feedback, with the purpose to assign the pole placements of the system in according to the control gain. Next Lemmas 1 and 2 show that $\tilde{A}, \tilde{C}$, $\hat{A}$, $\bar{A}$ and $\hat{C}$ of the closed loop system can be obtained from equations (8) to (11) using S. There are two cases due to the elements place in the Bond Graph. The first case when the dissipation field (R) is located before the storage field (L, C), otherwise is the second case.

Lemma 1

Consider the control scheme of figure 3. The structure of the closed loop system is given by:

$$\begin{bmatrix} \dot{x} \\ D_{in} \\ y \end{bmatrix} = S \begin{bmatrix} z \\ D_{out} \\ w \\ \dot{x}_d \end{bmatrix} - \hat{S} \begin{bmatrix} \hat{z} \\ \hat{D}_{out} \\ w \\ \hat{x}_d \end{bmatrix} \tag{23}$$

where the junction structure of the observer reflected to the system is:

$$\hat{S} = \begin{bmatrix} \hat{S}_{11} & 0 & 0 & 0 \\ \hat{S}_{21} & 0 & 0 & 0 \\ \hat{S}_{31} & 0 & 0 & 0 \end{bmatrix} \tag{24}$$

1) If $\hat{S}_{21} = 0$, $\hat{S}_{11} \neq 0$ and/or $\hat{S}_{31} \neq 0$, then,

$$\tilde{A} = E^{-1}\hat{S}_{11}F \tag{25}$$
$$\tilde{C} = \hat{S}_{31}F \tag{26}$$

2) If $\hat{S}_{11} = \hat{S}_{31} = 0$ and $\hat{S}_{21} \neq 0$, then,

$$\bar{A} = E^{-1}S_{12}M\hat{S}_{21}F \tag{27}$$
$$\bar{C} = S_{32}M\hat{S}_{21}F \tag{28}$$

being

$$E = I + S_{14}F_d^{-1}S_{14}^T F$$
$$M = L\left(I - S_{22}L\right)^{-1} \tag{29}$$

Proof. For LTI systems, substituting (1), (3), (5) into the first line of (23), we have:

$$\dot{x} = E^{-1}\left(S_{11}z + S_{12}D_{out} + S_{13}w - \hat{S}_{11}\hat{z}\right) \tag{30}$$

from (2) and the second line of (23), and from (2) gives:

$$D_{in} = (I - S_{22}L)^{-1}\left(S_{21}z + S_{23}w - \hat{S}_{21}\hat{z}\right) \tag{31}$$

taking (1), (2), (13) and (31) into (30):

$$\begin{aligned} \dot{x} &= E^{-1}\left[\left(S_{11} + S_{12}MS_{21}\right)Fx + \left(S_{13} + S_{12}MS_{23}\right)w\right] \\ &\quad -E^{-1}\left(\hat{S}_{11} + S_{12}M\hat{S}_{21}\right)F\hat{x} \end{aligned} \tag{32}$$

Comparing with (15) with (32)

$$\bar{A} = E^{-1}\left(\hat{S}_{11} + S_{12}M\hat{S}_{21}\right)F \tag{33}$$

Equation (33) proves both cases (25) and (27).

To get (26) and (28), taking (1), (2) ,(29) and (31) into the third line of (23) we have:

$$\begin{aligned} y &= \left(S_{31} + S_{32}MS_{21}\right)Fx + \left(S_{33} + S_{32}MS_{23}\right)w \\ &\quad -\left(\hat{S}_{31} + S_{32}M\hat{S}_{21}\right)F\hat{x} \end{aligned} \tag{34}$$

Comparing (15) with (34):

$$\bar{C} = \left(\hat{S}_{31} + S_{32}M\hat{S}_{21}\right)F \tag{35}$$

Equation (35) proves both cases (26) and (28). ■

Note that (32) and (34) show that $\bar{A}$ of (33) and $\bar{C}$ of (35)are the matrices which maps the observer into the system

Lemma 2

Consider the control scheme of figure 3. The structure of the observer is given by:

$$\begin{bmatrix} \dot{\hat{x}} \\ \hat{D}_{in} \\ \hat{y} \end{bmatrix} = \hat{S}' \begin{bmatrix} \hat{z} \\ \hat{D}_{out} \\ w \\ \hat{x}_d \end{bmatrix} + S' \begin{bmatrix} z \\ D_{out} \\ w \\ \dot{x}_d \end{bmatrix} \tag{36}$$

where the junction structure of the system reflected to the observer is:

$$S' = \begin{bmatrix} S'_{11} & S'_{12} & 0 & 0 \\ 0 & 0 & 0 & 0 \\ 0 & 0 & 0 & 0 \end{bmatrix} \tag{37}$$

The observer model is:

$$\hat{A} = \hat{E}^{-1}\left(\hat{S}'_{11} + \hat{S}'_{12}M'\hat{S}'_{21} - S'_{12}M\hat{S}_{21}\right)F \tag{38}$$
$$\hat{B} = \hat{E}^{-1}\left(\hat{S}'_{13} + \hat{S}'_{12}M'\hat{S}'_{23} + S'_{12}MS_{23}\right) \tag{39}$$
$$\bar{A} = \hat{E}^{-1}\left(S'_{11} + S'_{12}MS_{21}\right)F \tag{40}$$
$$\hat{C} = \left(\hat{S}'_{13} + \hat{S}'_{32}M'\hat{S}'_{21}\right)F \tag{41}$$
$$\hat{D} = \hat{S}'_{33} + \hat{S}'_{32}M'\hat{S}'_{23} \tag{42}$$

where

$$\hat{E} = I + \hat{S}'_{14} F_d^{-1} (\hat{S}'_{14})^T F \quad (43)$$

$$M' = L \left(I - \hat{S}'_{22} L \right)^{-1} \quad (44)$$

Proof. Substituting (1), (3) and (5) into the first line of (36), gives:

$$\hat{\dot{x}} = \hat{E}^{-1} \left(\hat{S}'_{11} \hat{z} + \hat{S}'_{12} \hat{D}_{out} + \hat{S}'_{13} w \right) + \hat{E}^{-1} \left(S'_{11} z + S'_{12} D_{out} + S'_{13} w \right) \quad (45)$$

taking the estimated of (2) into (36), we have:

$$\hat{D}_{in} = (I - \hat{S}'_{22} L)^{-1} (\hat{S}'_{21} F \hat{x} + \hat{S}'_{23} w) \quad (46)$$

substituting the estimated of (1), (2), (30) and (45) into (44):

$$\hat{\dot{x}} = \hat{E} \left({}^{-1}\hat{S}'_{11} + \hat{S}'_{12} M' \hat{S}'_{21} - S'_{12} M \hat{S}_{21} \right) F \hat{x} + \hat{E}^{-1} \left(\hat{S}'_{13} + \hat{S}'_{12} M' \hat{S}'_{23} + S'_{12} M S_{23} \right) w + \hat{E}^{-1} \left(S'_{11} + S'_{12} M' S_{21} \right) F x \quad (47)$$

comparing (19) and (47) we have (38), (39) and (40). To get (41) and (42), substituting (1), (2) and (46) into the third line of (36), we get:

$$\hat{y} = \left(\hat{S}'_{31} + \hat{S}'_{32} M' \hat{S}'_{21} \right) F \hat{x} + \left(\hat{S}'_{32} M' \hat{S}'_{23} + \hat{S}'_{33} \right) w \quad (48)$$

comparing (19) and (48), we get (41) and (42). ■

Note that the matrices $\hat{B}$ and $\hat{D}$ can calculate directly from (22).

V. Gains Design

Next, expressions for the controller and observer gains are presented.

Theorem 1

Let a Multivariable LTI system with linear constitutives relations in the control scheme of the figure 3.

1) If $\hat{S}_{21} = 0$, $\hat{S}_{11} \neq 0$ *and/or* $\hat{S}_{31} \neq 0$, *then, the direct-graph gain for the controller in the Bond graph is given by:*

$$\hat{S}_{11} = EBKF^{-1} \quad (49)$$

2) If $\hat{S}_{11} = \hat{S}_{31} = 0$ and $\hat{S}_{21} \neq 0$, *then, the direct-graph gain for the controller* $\hat{S}_{21}$ *is obtained equating the elements of:*

$$S_{12} M \hat{S}_{21} = EBKF^{-1} \quad (50)$$

Moreover, the direct-graph gain for the observer S'_{11} and/or S'_{12} and/or S'_{13} *is given by:*

$$\hat{E}^{-1} \left(S'_{11} + S'_{12} M S_{21} \right) F = HC \quad (51)$$

being $E = I + S_{14} F_d^{-1} S_{14}^T F$, $\hat{E} = I + \hat{S}'_{14} F_d^{-1} \left(\hat{S}'_{14} \right)^T F$ and $M = L (I - S_{22} L)^{-1}$

Proof. The control and the observer K and H gains can be determined using the separation principle [8, 9], i.e., the state feedback and the state estimator designs can be carried out independently. The characteristic equation [8, 9] of (16) is given by:

$$\det (sI - A - BK) = 0 \quad (52)$$

For the first case, from (25) of Lemma 1 and (52) we get:

$$\det \left(sI - A - E^{-1} \hat{S}_{11} F \right) = 0 \quad (53)$$

Comparing (52) and (53) proves (49). For the second case, from (27) of Lemma 1 and (52), we have:

$$\det \left(sI - A - E^{-1} S_{12} M \hat{S}_{21} F \right) = 0 \quad (54)$$

Comparing (52) and (54) using (49) proves (50). On the other hand, for the observer of (18) we obtain:

$$\det (sI - A + HC) = 0 \quad (55)$$

Therefore, from (21), (40) of Lemma 2 and (55):

$$\det \left[sI - A + \hat{E}^{-1} \left(S'_{11} + S'_{12} M S_{21} \right) F \right] = 0 \quad (56)$$

Comparing (55) and (56) proves (51). ■

We can determine the control and observer gains selecting Hurtwitz polynomials for (53), (54) and (56) respectively.

VI. Example

Consider the DC motor scheme ,and its Bond Graph which are shown in figure 4.

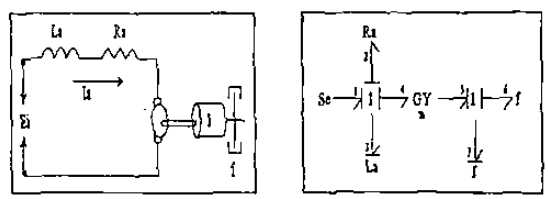

Figure 4. DC motor scheme and its Bond graph.

The key vectors are:

$$x = \begin{bmatrix} e_{a3} \\ e_{a7} \end{bmatrix}; \dot{x} = \begin{bmatrix} e_3 \\ e_7 \end{bmatrix}; z = \begin{bmatrix} f_3 \\ f_7 \end{bmatrix}; y = f_6$$

$$u = e_1; D_{in} = \begin{bmatrix} f_2 \\ f_6 \end{bmatrix}; D_{out} = \begin{bmatrix} e_2 \\ e_6 \end{bmatrix}$$

where e_2 and e_3 denote voltages; f_2 and f_3 currents in L_a and R_a respectively; e_6 and e_7 torques; f_6 and f_7 speeds in J and F respectively; e_{a3} flux linkage in L_a; and e_{a7} rotational momentum in J.

The constitutive relations for the elements are:

$$\begin{bmatrix} f_3 \\ f_7 \end{bmatrix} = \begin{bmatrix} \frac{1}{L_a} & 0 \\ 0 & \frac{1}{J} \end{bmatrix} \begin{bmatrix} e_{a3} \\ e_{a7} \end{bmatrix} \quad (57)$$

$$\begin{bmatrix} e_2 \\ e_6 \end{bmatrix} = \begin{bmatrix} R_a & 0 \\ 0 & f \end{bmatrix} \begin{bmatrix} f_2 \\ f_6 \end{bmatrix} \quad (58)$$

$$F_d = 0 \quad (59)$$

The input-output relation for the gyrator is:

$$\begin{bmatrix} e_4 \\ f_4 \end{bmatrix} = \begin{bmatrix} 0 & n \\ \frac{1}{n} & 0 \end{bmatrix} \begin{bmatrix} e_5 \\ f_5 \end{bmatrix} \quad (60)$$

Consider the system Bond Graph with estimated state feedback of figure 3 which is shown in figure 5 for the DC motor.

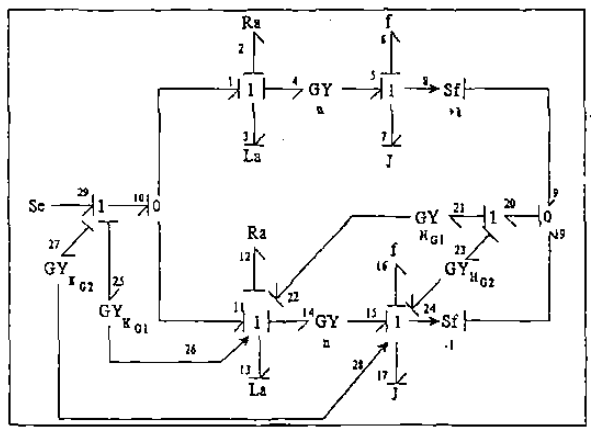

Figure 5. Observer and state feedback for the DC motor

The junction structure for the system is given by (23), where:

$$S_{11} = \begin{bmatrix} 0 & -n \\ n & 0 \end{bmatrix}; S_{12} = -S_{21}^T = \begin{bmatrix} -1 & 0 \\ 0 & -1 \end{bmatrix}$$

$$S_{13} = \begin{bmatrix} 1 \\ 0 \end{bmatrix}; \; S_{31} = \begin{bmatrix} 0 & 1 \end{bmatrix}$$

$$\hat{S}_{11} = \begin{bmatrix} K_{G1} & K_{G2} \\ 0 & 0 \end{bmatrix} \quad (61)$$

being K_{G1} and K_{G2} the direct graph control gains and $S_{22} = S_{23} = S_{32} = S_{33} = \hat{S}_{12} = \hat{S}_{13} = \hat{S}_{21} = \hat{S}_{22} = \hat{S}_{23} = \hat{S}_{31} = \hat{S}_{32} = \hat{S}_{33} = 0$.

The junction structure for the observer is given by (36), where:

$$\hat{S}'_{11} = \begin{bmatrix} -K_{G1} & -K_{G2} - H_{G1} - n \\ n & -H_{G2} \end{bmatrix}; S'_{31} = \begin{bmatrix} 0 & 1 \end{bmatrix}$$

$$\hat{S}'_{13} = \begin{bmatrix} 1 \\ 0 \end{bmatrix}; \; \hat{S}'_{12} = -\hat{S}'^T_{21} = \begin{bmatrix} -1 & 0 \\ 0 & -1 \end{bmatrix}$$

$$S'_{11} = \begin{bmatrix} 0 & H_{G1} \\ 0 & H_{G2} \end{bmatrix} \quad (62)$$

being H_{G1} and H_{G2} the direct graph observer gains and $\hat{S}'_{22} = \hat{S}'_{23} = \hat{S}'_{32} = \hat{S}'_{33} = S'_{12} = S'_{13} = S'_{21} = S'_{22} = S'_{23} = S'_{31} = S'_{32} = S'_{33} = 0$.

Using the first case of Lemma 1, from (25), (26), (57), and (61)

$$\tilde{A} = \begin{bmatrix} \frac{K_{G1}}{L_a} & \frac{K_{G2}}{J} \\ 0 & 0 \end{bmatrix} \quad (63)$$

Also, since $\hat{S}_{31} = 0$ from (26) we have:

$$\tilde{C} = 0 \quad (64)$$

Substituting (57), (58) and (61) in (8) to (13) we obtain:

$$A = \begin{bmatrix} -\frac{R_a}{L_a} & -\frac{n}{J} \\ \frac{n}{L_a} & -\frac{f}{J} \end{bmatrix}; \; B = \begin{bmatrix} 1 \\ 0 \end{bmatrix} \quad (65)$$

$$C = \begin{bmatrix} 0 & \frac{1}{J} \end{bmatrix}; \; D = 0 \quad (66)$$

From (63) to (66) and (15), the closed loop control physical system is obtained:

$$\begin{bmatrix} e_3 \\ e_7 \end{bmatrix} = \begin{bmatrix} -\frac{R_a}{L_a} & -\frac{n}{J} \\ \frac{n}{L_a} & -\frac{f}{J} \end{bmatrix} \begin{bmatrix} e_{a3} \\ e_{a7} \end{bmatrix} + \begin{bmatrix} 1 \\ 0 \end{bmatrix} e_{29} - \begin{bmatrix} \frac{K_{G1}}{L_a} & \frac{K_{G2}}{J} \\ 0 & 0 \end{bmatrix} \begin{bmatrix} \hat{e}_{a3} \\ \hat{e}_{a7} \end{bmatrix}$$

$$y = \begin{bmatrix} 0 & \frac{1}{J} \end{bmatrix} \begin{bmatrix} e_{a3} \\ e_{a7} \end{bmatrix} \quad (67)$$

Using the first case of Lemma 2, from (38), (40), (41) (57), (62) and (65) we get:

$$\hat{A} = \begin{bmatrix} -\frac{R_a}{L_a} - \frac{K_{G1}}{L_a} & -\frac{n}{J} - \frac{K_{G2}}{J} - \frac{H_{G1}}{J} \\ \frac{n}{L_a} & -\frac{f}{J} - \frac{H_{G2}}{J} \end{bmatrix} \quad (68)$$

Substituting $\hat{S}_{11}$ from (57) and (62) into (40) obtains:

$$\bar{A} = \begin{bmatrix} 0 & \frac{H_{G1}}{J} \\ 0 & \frac{H_{G2}}{J} \end{bmatrix} \quad (69)$$

Taking (64) and (66) into (22) gives:

$$\hat{C} = \begin{bmatrix} 0 & \frac{1}{J} \end{bmatrix} \quad (70)$$

From (65), (66), (68), (69) and (18) we obtain the observer model:

$$\begin{bmatrix} \hat{e}_3 \\ \hat{e}_7 \end{bmatrix} = \begin{bmatrix} -\frac{R_a}{L_a} - \frac{K_{G1}}{L_a} & -\frac{n}{J} - \frac{K_{G2}}{J} - \frac{H_{G1}}{J} \\ \frac{n}{L_a} & -\frac{f}{J} - \frac{H_{G2}}{J} \end{bmatrix} \begin{bmatrix} \hat{e}_{a3} \\ \hat{e}_{a7} \end{bmatrix} + \begin{bmatrix} 0 & \frac{H_{G1}}{J} \\ 0 & \frac{H_{G2}}{J} \end{bmatrix} \begin{bmatrix} e_{a3} \\ e_{a7} \end{bmatrix} + \begin{bmatrix} 1 \\ 0 \end{bmatrix} e_{29}$$

$$\hat{y} = \begin{bmatrix} 0 & \frac{1}{J} \end{bmatrix} \begin{bmatrix} \hat{e}_{a3} \\ \hat{e}_{a7} \end{bmatrix} \quad (71)$$

Note that using the methodology proposed in Lemmas 1 and 2, we obtain the closed loop model directly from

the open loop bond graph including control and observer.

The model parameters are $L_a = 0.1$, $f = 0.1$, $R_a = 0.5$, $J = 1.5$, $n = 3$ and $e_1 = 10$. The control gains to have a damping coefficient of 0.5 are $K_1 = 5.94$ and $K_2 = 2$. From Theorem 1 the direct gain for the controller is:

$$\hat{S}_{11} = \begin{bmatrix} 0.594 & 3 \\ 0 & 0 \end{bmatrix} \tag{72}$$

The closed loop poles due to the observer are placed in $p_{1,2} = -9.1683 \pm j5.2549$, from (55) we have $H_1 = 13.33$ and $H_2 = 13.33$. From Theorem the direct gain for the observer is:

$$S'_{11} = \begin{bmatrix} 0 & 13.33 \\ 0 & 13.33 \end{bmatrix} \tag{73}$$

Figures 6 and 7 show the simulation for this example.

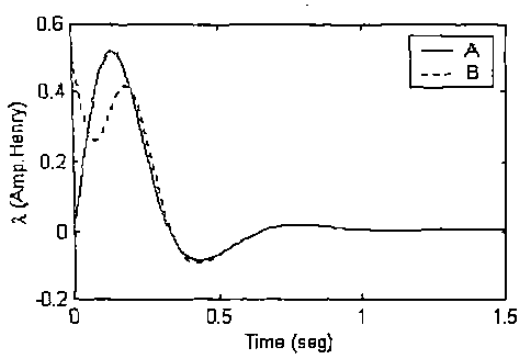

Figure 6. Graph of the flux linkage behavior where A) system state; B) estimated state.

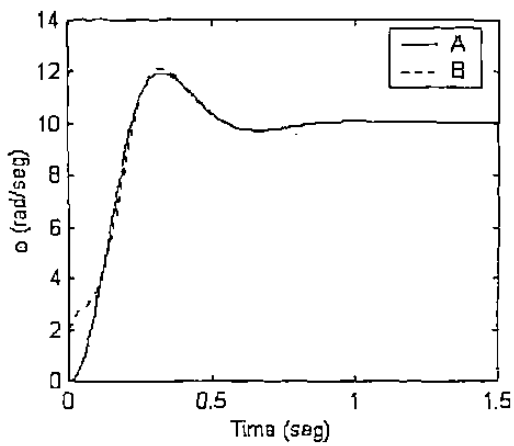

Figure 7. Graph of the output behavior where A) system output; B) estimated output.

We can observe in both figures 6 and 7 that the previous design conditions for the controller and the observer are satisfied.

VII. Conclusions

A state estimated feedback is presented for LTI MIMO systems. The closed loop model of the control and the observer are obtained directly from the open loop Bond graph and the proposed structures. The methodology let consider different kinds of energies. The controller is realizable due to the fact that the physical domain is considered. Also, the dynamic assignment problem is solved guaranteeing stability and assuring regulation.

References

[1] Paynter, H.M. "Analysis and design of engineering systems", MIT press, Cambridge, Mass (1961).

[2] Dean C. Karnopp, Ronald C. Rosenberg, "System Dynamics: A Unified Approach", Wiley, John & Sons, April (1975).

[3] P.E. Wellstead, "Physical System Modelling", Academic Press, London, (1979).

[4] P.J. Gawthrop, " Bond graph based control", Systems, Man and Cybernetics, 1995, Intelligent System for the 21st Century., IEEE International Conference on Published: 1995, Vol. 4, pp. 3011-1016 (1995).

[5] D.C. Karnopp, "Bond graphs in control: Physical state variables and observers", J. Flanklin Institute, 308(3) pp. 221-234, (1979).

[6] G. Dauphin-Tanguy "Modelling of physical Dynamical Systems by Bond Graphs".

[7] C. Suer, G. Dauphin-Tanguy, "Bond graph approach for structural analysis of MIMO linear systems", J.Flanklin Inst., vol. 328, No.1 pp. 55-70, (1991).

[8] Chi-Tsong Chen "Linear System Theory and Design", Third ed., Oxford University Press..

[9] Gene F. Franklin, J. David Powell, Abbas Emami-Naeini, "Feedback Control of Dynamic Systems" Addison Wesley.

[10] Y.K. Wong and A.B. Rad "Bond Graph Simulations of Electrical Systems", IEEE Catalogue No. 98E137, (1998).

[11] P.J. Gawthop, " Physical Model-Based Control:A Bond Graph Approach", J. of the Franklin Institute, 332B(3), pp. 285-305.

[12] Antic, D.Vidojkovic, B. Mladenovic, M. "An Introduction to Bond Graph Modelling of Dynamic Systems", Telecommunications in Modern Satellite, Cable and Broadcasting Services, 1999, 4th Int. Conf. on Published: 1999, vol. 2, pp. 661-664.

C.4 Steady-State Values for a Physical System with Bond Graph Approach

Gonzalez-A. Gilberto, R. Galindo

9th IEEE International Conference On Methods and Models in Automation and Robotics (MMAR 2003), 25-28 August 2003, Miedzyzdroje, Poland.

MMAR 2003 9th IEEE International Conference on Methods and Models in Automation and Robotics
25-28 August 2003, Międzyzdroje, Poland

STEADY-STATE VALUES FOR A PHYSICAL SYSTEM WITH BOND GRAPH APPROACH

GONZALEZ-A. GILBERTO[1,2], R. GALINDO[1]

[1]University of Nuevo Leon, Department of Electrical Engineering 66451 San Nicolas de los Garza, N.L. Mexico (+52)8183294020 Ext.5773
[2]University of Michoacan, Faculty of Electrical Engineering 58030, Morelia, Michoacan, Mexico (+52)4433265776

Abstract. A single and direct graphical procedure to get the steady state value of a physical system represented in Bond Graph is presented. To get this objetive an inverse matrix is requiered. However, we show that using the junction structure of the Bond Graph in derivative causality of the system, this inverse matrix is not required.

Key Words. Bond Graph, Coates Graph, Physical Control, Modelling Tools, Steady State.

1 Introduction

The Bond Graph technique is an energy based modelling approach, unifying symbology for phenomena from different physical domains. Bond Graph is a directed graph whose nodes represent subsystems and its arrows, the transfer of energy between the subsystems. Bond Graph was established by [1]. The idea was developed by [2] and [3] how a powerful tool of modelling.

The use of Bond Graph provides structured approach to system dynamics modelling. The Bond Graph language is used to abstract physical systems into basic elements that represent localized dynamic properties of a small part of the system.

The steady-state performance is an important characteristic of a system when its dynamic period has finished. Actually, some equipments in electrical machines or in power electrical systems requires to know the steady state values for calibration.

Nevertheless, the steady state value of the state variables require to calculate and to invert the matrix A, which is almost allways invertible for a physical system. As shown it is not necessary, if we obtain the Bond Graph in derivative causality of the system. So, we can get the response in steady state directly.

This graph methodology from Bond Graph for a MIMO-LTI physical system can be incorporated to analyze or design control strategies in the physical domain, guaranteeing to get a realizable controller.

Section II gives the modelling by Bond Graph of a physical system; section III presents a procedure to obtain the steady state value of the system. Two examples are given in section IV. Finally, section V gives our conclusions.

2 Bond Graph Model [3, 6, 7]

Consider a multiport linear system which has the key vectors of figure 1.

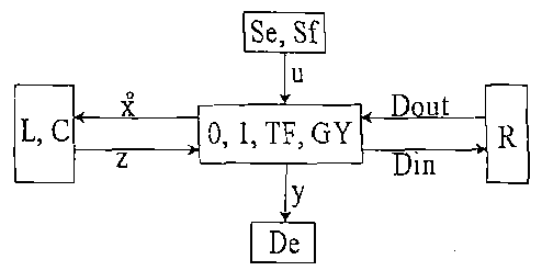

Figure 1. Key vectors of a Bond Graph

Here, (Se, Sf), (L,C) and (R) mean the source, the storage and the dissipation fields, (De) the detector and (0, 1, TF, GY) the junction structure with transformers, TF, and gyrators, GY.

The state $x \in R^n$ is composed of energy variables for effort, e, and flow, f, with integral causality, $u \in R^p$ the plant input, $y \in R^q$ the plant output, $z \in R^n$ the co-energy, and $D_{in} \in R^r$ and $D_{out} \in R^r$ are a mixture of e and f showing the energy exchanges between the dissipation field and the junction structure.

The relations of the storage and dissipation fields are:

$$z = Fx \quad (1)$$

$$D_{out} = LD_{in} \quad (2)$$

where L is a diagonal matrix composed of R and $1/R$ coefficients, and F is composed of $1/L$ and $1/C$ coefficients.

The relation of the junction structure is:

$$\begin{bmatrix} \dot{x} \\ D_{in} \\ y \end{bmatrix} = S \begin{bmatrix} z \\ D_{out} \\ u \end{bmatrix} \tag{3}$$

where the junction structure of the system is given by:

$$S = \begin{bmatrix} S_{11} & S_{12} & S_{13} \\ S_{21} & S_{22} & S_{23} \\ S_{31} & S_{32} & S_{33} \end{bmatrix} \tag{4}$$

The entries of S take the values inside the set $\{0, \pm 1, \pm m, \pm r\}$ where m and r are transformer and gyrator modules; S_{11} and S_{22} are square skew-symmetric submatrices and S_{12} and S_{21} are submatrices each other negative transpose. The state equation is [7]:

$$\begin{aligned} \dot{x} &= Ax + Bu \qquad (5) \\ y &= Cx + Du \end{aligned}$$

where

$$A = (S_{11} + S_{12} M S_{21}) F \tag{6}$$
$$B = (S_{13} + S_{12} M S_{23}) \tag{7}$$
$$C = (S_{31} + S_{32} M S_{21}) F \tag{8}$$
$$D = S_{33} + S_{32} M S_{23} \tag{9}$$

being

$$M = (I - L S_{22})^{-1} L \tag{10}$$

Next, we introduce a new approach to get the steady state of the state variables of the system.

3 Steady-State

The response of the steady state is useful to know the value that reachs each state variable of the physical system when the dynamic period has finished. So, (5) doing $\dot{x} = 0$, we have

$$\begin{aligned} x_{ss} &= -A^{-1} B u \qquad (11) \\ y_{ss} &= \left(D - C A^{-1} B\right) u \end{aligned}$$

So, using (11) we can calculate the steady state, but we need A^{-1} and it is not easy to get for some high order systems.

We can use the Bond Graph in derivative causality to solve directly the problem ot get A^{-1}.

Suppose that (A^{-1} is invertible) and a derivative causality assigment is performed on the Bond Graph model [13]. From (3) the junction structure is given by:

$$\begin{bmatrix} z \\ D_{ind} \\ y_d \end{bmatrix} = \begin{bmatrix} J_{11} & J_{12} & J_{13} \\ J_{21} & J_{22} & J_{23} \\ J_{31} & J_{32} & J_{33} \end{bmatrix} \begin{bmatrix} \dot{x} \\ D_{outd} \\ u \end{bmatrix}$$
$$D_{outd} = L_d D_{ind} \tag{12}$$

where the entries of J have the same properties that S. The storage elements in (12) have a derivative causality. So, D_{ind} and D_{outd} are defined of the same manner that D_{in} and D_{out}, but they depend on the causality assigment for the storage elements and that junctions must have a correct causality assigment.

From (5) to (10) and (12) we obtain

$$\begin{aligned} z &= A^* \dot{x} + B^* u \qquad (13) \\ y_d &= C^* \dot{x} + D^* u \end{aligned}$$

where

$$A^* = J_{11} + J_{12} N J_{21} \tag{14}$$
$$B^* = J_{13} + J_{12} N J_{23} \tag{15}$$
$$C^* = J_{31} + J_{32} N J_{21} \tag{16}$$
$$D^* = J_{33} + J_{32} N J_{23} \tag{17}$$

being

$$N = (I - L_d J_{22})^{-1} L_d \tag{18}$$

The state output equations of this system in integral causality are given by (5). It follows, from (1), (5) and (13) that:

$$A^* = F A^{-1} \tag{19}$$
$$B^* = -F A^{-1} B \tag{20}$$
$$C^* = C A^{-1} \tag{21}$$
$$D^* = D - C A^{-1} B \tag{22}$$

From (20), (22) and (11), we obtain the steady state

$$\begin{aligned} x_{ss} &= F^{-1} B^* u \qquad (23) \\ y_{ss} &= D^* u \end{aligned}$$

4 Examples

Example 1.

Consider the mechanical system of the figure 2.

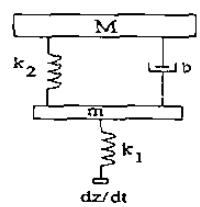

Figure 2. Mechanical system of example 1

In Figure 3, we have the Bond Graph in integral causality.

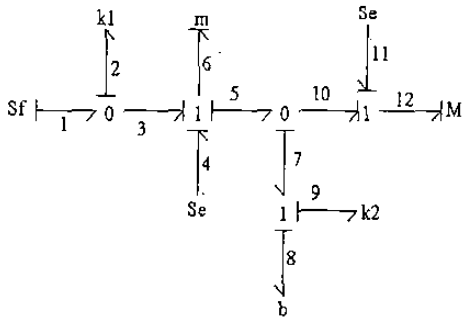

Figure 3. Bond Graph in integral causality.

The key vectors are:

$$x = \begin{bmatrix} f_{a_2} \\ e_{a_6} \\ f_{a_9} \\ e_{a_{12}} \end{bmatrix}; \dot{x} = \begin{bmatrix} f_2 \\ e_6 \\ f_9 \\ e_{12} \end{bmatrix}; z = \begin{bmatrix} e_2 \\ f_6 \\ e_9 \\ f_{12} \end{bmatrix}$$

$$u = \begin{bmatrix} f_1 \\ e_4 \\ e_{11} \end{bmatrix}; y = f_8; D_{in} = f_8; D_{out} = e_8$$

where f is velocity and e is force in each element of the mechanical system; f_{a_2} and f_{a_9} are translational displacement in k_1 and k_2 respectively; e_{a_6} and $e_{a_{12}}$ are translational momentums m and M respectively ; f_1 is the input velocity and e_4 and e_{11} are the gravity forces under m and M respectively.

The constitutives relations (1) , (2) for the elements are:

$$\begin{bmatrix} e_2 \\ f_6 \\ e_9 \\ f_{12} \end{bmatrix} = \begin{bmatrix} k_1 & 0 & 0 & 0 \\ 0 & \frac{1}{m} & 0 & 0 \\ 0 & 0 & k_2 & 0 \\ 0 & 0 & 0 & \frac{1}{M} \end{bmatrix} \begin{bmatrix} f_{a_2} \\ e_{a_6} \\ f_{a_9} \\ e_{a_{12}} \end{bmatrix}$$

$$e_8 = b f_8 \quad (24)$$

The Bond Graph in derivative causality is shown in Figure 4.

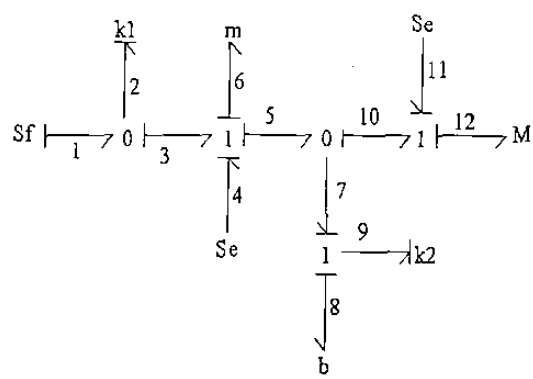

Figure 4. Bond graph in derivative causality.

From (12) the junction structure for the Bond Graph of figure 4 is given by:

$$J_{11} = \begin{bmatrix} 0 & 1 & 0 & 1 \\ -1 & 0 & 0 & 0 \\ 0 & 0 & 0 & 1 \\ -1 & 0 & -1 & 0 \end{bmatrix}$$

$$J_{12} = -J_{21}^T = \begin{bmatrix} 0 \\ 0 \\ -1 \\ 0 \end{bmatrix}$$

$$J_{13} = \begin{bmatrix} 0 & -1 & -1 \\ 1 & 0 & 0 \\ 0 & 0 & -1 \\ 1 & 0 & 0 \end{bmatrix}; J_{22} = J_{23} = 0$$

For this example $D_{ind} = D_{in}$ and $D_{outd} = D_{out}$. So, from (20) B^* is given by:

$$B^* = \begin{bmatrix} 0 & -1 & -1 \\ 1 & 0 & 0 \\ 0 & 0 & -1 \\ 1 & 0 & 0 \end{bmatrix} \quad (25)$$

Finally, the steady state value of the state variables is getting from (23)

$$x_{ss} = \begin{bmatrix} 0 & -\frac{1}{k_1} & -\frac{1}{k_1} \\ m & 0 & 0 \\ 0 & 0 & -\frac{1}{k_2} \\ M & 0 & 0 \end{bmatrix} \begin{bmatrix} f_1 \\ e_4 \\ e_{11} \end{bmatrix} \quad (26)$$

We can observe that, this is a single and direct procedure and it is not necessary to calculate A, A^{-1} and B.

The dynamic model of this example can be obtained from (4)

$$S_{11} = \begin{bmatrix} 0 & -1 & 0 & 0 \\ 1 & 0 & -1 & 0 \\ 0 & 1 & 0 & -1 \\ 0 & 0 & 1 & 0 \end{bmatrix}; \; S_{31} = S_{21}$$

$$S_{12} = -S_{21}^T = \begin{bmatrix} 0 \\ -1 \\ 0 \\ 1 \end{bmatrix}; \; S_{13} = \begin{bmatrix} 1 & 0 & 0 \\ 0 & 1 & 0 \\ 0 & 0 & 0 \\ 0 & 0 & 1 \end{bmatrix}$$

$$S_{22} = S_{23} = S_{32} = S_{33} = 0$$

So, the model is given by (5):

$$\begin{bmatrix} f_2 \\ e_6 \\ f_9 \\ e_{12} \end{bmatrix} = \begin{bmatrix} 0 & -\frac{1}{m} & 0 & 0 \\ k_1 & -\frac{b}{m} & -k_2 & \frac{b}{M} \\ 0 & \frac{1}{m} & 0 & -\frac{1}{M} \\ 0 & \frac{b}{m} & k_2 & -\frac{b}{M} \end{bmatrix} \begin{bmatrix} f_{a_2} \\ e_{a_6} \\ f_{a_9} \\ e_{a_{12}} \end{bmatrix} + \begin{bmatrix} 1 & 0 & 0 \\ 0 & 1 & 0 \\ 0 & 0 & 0 \\ 0 & 0 & 1 \end{bmatrix} \begin{bmatrix} f_1 \\ e_4 \\ e_{11} \end{bmatrix} \quad (27)$$

With the system parameters $k_1 = 5$, $k_2 = 10$, $m = 3$, $M = 6$, $b = 10$, $f_1 = 1$, $e_4 = 1$ and $e_{11} = 1$ the response of the state variables of the system are given by figures 5 to 8.

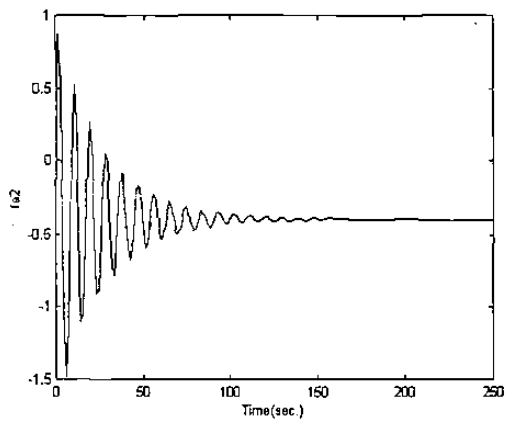

Figure 5. State variable f_{a_2}.

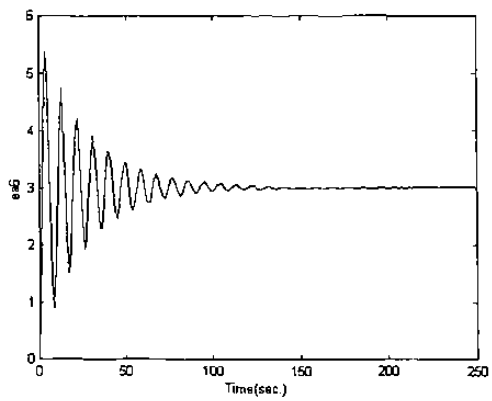

Figure 6. State variable e_{a_6}.

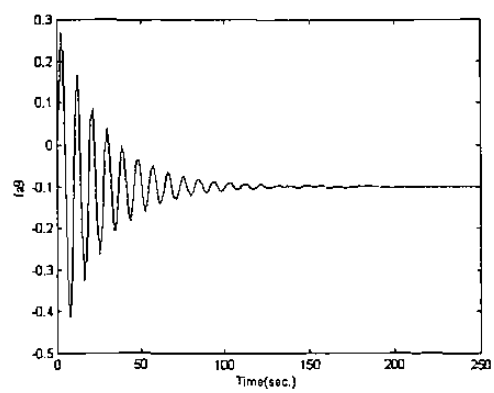

Figure 7. State variable f_{a_9}.

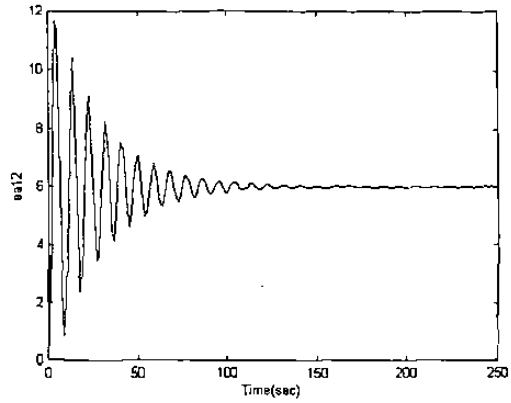

Figure 8. State variable $e_{a_{12}}$.

Note that the steady state values are: $f_{a_2} = -0.5$, $e_{a_6} = 3$, $f_{a_9} = -0.1$ and $e_{a_{12}} = 6$, as expected.

We can observe that, this procedure to get the steady state of the state variables is an easy tool for system analysis.

Example 2.

Consider the electrical system of figure 9.

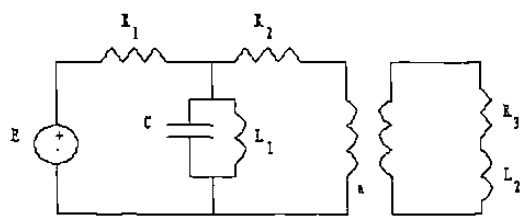

Figure 9. Electrical system of the example 2.

The Bond Graph in integral causality is shown in Figure 10.

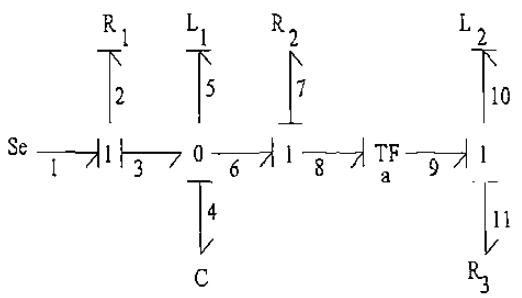

Figure 10. Bond Graph in integral causality.

The key vectors are:

$$x = \begin{bmatrix} f_{a_4} \\ e_{a_5} \\ e_{a_{10}} \end{bmatrix}; \dot{x} = \begin{bmatrix} f_4 \\ e_5 \\ e_{10} \end{bmatrix}; z = \begin{bmatrix} e_4 \\ f_5 \\ f_{10} \end{bmatrix}$$

$u = e_1$; $y = f_{11}$

$$D_{in} = \begin{bmatrix} e_2 \\ f_7 \\ f_{11} \end{bmatrix}; D_{out} = \begin{bmatrix} f_2 \\ e_7 \\ e_{11} \end{bmatrix}$$

where e is voltage and f is current in each element of the electrcial system; f_{a_4} is the capacitor charge in C and e_{a_5} and $e_{a_{10}}$ are the fluxes linkages in L_1 and L_2, respectively.

The constitutive relations for the elements are:

$$\begin{bmatrix} e_4 \\ f_5 \\ f_{10} \end{bmatrix} = \begin{bmatrix} \frac{1}{C} & 0 & 0 \\ 0 & \frac{1}{L_1} & 0 \\ 0 & 0 & \frac{1}{L_2} \end{bmatrix} \begin{bmatrix} f_{a_4} \\ e_{a_5} \\ e_{a_{10}} \end{bmatrix} \quad (28)$$

$$\begin{bmatrix} f_4 \\ e_5 \\ e_{10} \end{bmatrix} = \begin{bmatrix} \frac{1}{R_1} & 0 & 0 \\ 0 & R_2 & 0 \\ 0 & 0 & R_3 \end{bmatrix} \begin{bmatrix} e_2 \\ f_7 \\ f_{11} \end{bmatrix}$$

$$\begin{bmatrix} e_8 \\ f_8 \end{bmatrix} = \begin{bmatrix} a & 0 \\ 0 & \frac{1}{a} \end{bmatrix} \begin{bmatrix} e_9 \\ f_9 \end{bmatrix}$$

The Bond Graph in derivative causality is shown in figure 11.

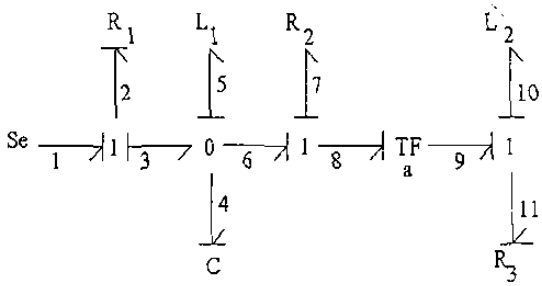

Figure 11. Bond Graph in derivative causality.

The key vectors D_{ind} and D_{outd} in derivative causality are:

$$D_{ind} = \begin{bmatrix} e_2 \\ f_7 \\ e_{11} \end{bmatrix}; \; D_{outd} = \begin{bmatrix} f_2 \\ e_7 \\ f_{11} \end{bmatrix}$$

The junction structure of figure 11 is:

$$J_{11} = \begin{bmatrix} 0 & 1 & 0 \\ -1 & 0 & 0 \\ 0 & 0 & 0 \end{bmatrix}; \; J_{23} = \begin{bmatrix} 1 \\ 0 \\ 0 \end{bmatrix}$$

$$J_{12} = -J_{21}^T = \begin{bmatrix} 0 & 0 & 0 \\ 1 & 0 & -\frac{1}{a} \\ 0 & 0 & 1 \end{bmatrix}; \; J_{13} = 0$$

$$J_{22} = \begin{bmatrix} 0 & 0 & 0 \\ 0 & 0 & \frac{1}{a} \\ 0 & -\frac{1}{a} & 0 \end{bmatrix}$$

The vector B^* is given by:

$$B^* = \begin{bmatrix} 0 \\ \frac{1}{R_1} \\ 0 \end{bmatrix} \quad (29)$$

From (23), the steady state value of the state variables is

$$x_{ss} = \begin{bmatrix} 0 \\ \frac{L_1}{R_1} \\ 0 \end{bmatrix} e_1 \quad (30)$$

From (4) the junction structure in integral causality of this example is obtained. It is used to get the dynamic model:

$$S_{11} = \begin{bmatrix} 0 & -1 & -\frac{1}{a} \\ 1 & 0 & 0 \\ \frac{1}{a} & 0 & 0 \end{bmatrix}; \; S_{13} = S_{32} = S_{33} = S_{22} = 0$$

$$S_{12} = -S_{21}^T = \begin{bmatrix} 1 & 0 & 0 \\ 0 & 0 & 0 \\ 0 & -\frac{1}{a} & -1 \end{bmatrix}; \; S_{23} = \begin{bmatrix} 1 \\ 0 \\ 0 \end{bmatrix}$$

$$S_{31} = \begin{bmatrix} 0 & 0 & 1 \end{bmatrix}$$

The dynamic model is given by:

$$\begin{bmatrix} f_4 \\ e_5 \\ e_{10} \end{bmatrix} = \begin{bmatrix} -\frac{1}{R_1 C} & -\frac{1}{L_1} & -\frac{1}{aL_2} \\ \frac{1}{C} & 0 & 0 \\ \frac{1}{aC} & 0 & -\frac{R_2}{a^2 L_2} - \frac{R_3}{L_2} \end{bmatrix} \begin{bmatrix} f_{a_4} \\ e_{a_5} \\ e_{a_{10}} \end{bmatrix} + \begin{bmatrix} \frac{1}{R_1} \\ 0 \\ 0 \end{bmatrix} e_1 \quad (31)$$

The system parameters are $R_1 = 10$, $R_2 = 5$, $R_3 = 2$, $L_1 = 0.1$, $L_2 = 0.2$, $C = 0.01$, $a = 10$ and $e_1 = 1$, the response of the state variables of the system are shown in figure 12, 13 and 14.

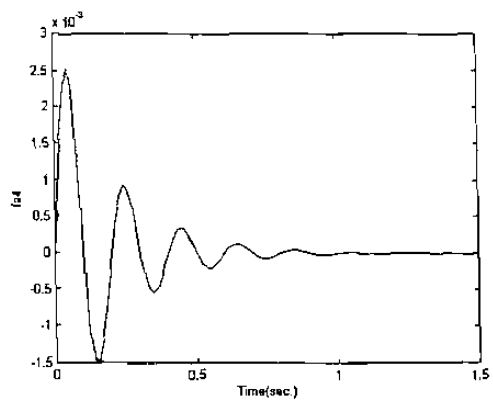

Figure 12. State variable f_{a_4}.

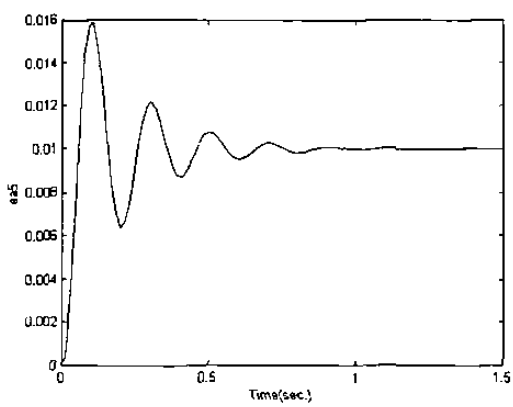

Figure 13. State variable e_{a_5}.

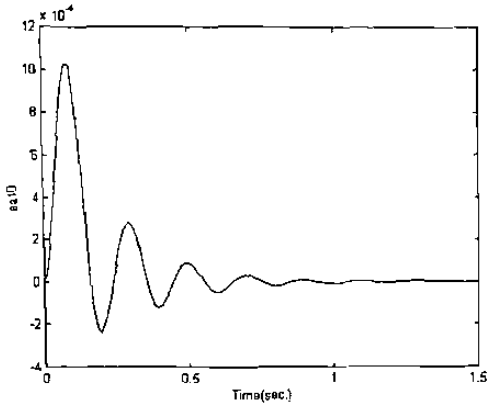

Figure 14. State variable $e_{a_{10}}$.

We can use this procedure to get the steady state of other variables, for instance, output and steady state error to analyse the performance in an open or closed loop control scheme.

5 Conclusions

A direct graphical procedure to obtain the steady state values of a physical system is presented. This methodology lets to consider different kinds of energies.

References

[1] Paynter, H.M. "Analysis and design of engineering systems", MIT press, Cambridge, Mass (1961).

[2] Dean C. Karnopp, Ronald C. Rosenberg, "System Dynamics: A Unified Approach", Wiley, John & Sons, April (1975).

[3] P.E. Wellstead, "Physical System Modelling", Academic Press, London, (1979).

[4] P.J. Gawthrop, " Bond graph based control", Systems, Man and Cybernetics, 1995, Intelligent System for the 21st Century., IEEE International Conference on Published: 1995, Vol. 4, pp. 3011-1016 (1995).

[5] D.C. Karnopp, "Bond graphs in control: Physical state variables and observers", J. Flanklin Institute, 308(3) pp. 221-234, (1979).

[6] C. Sueur, G. Dauphin-Tanguy "Bond-graph Approach for Structural Analysis of MIMO Linear Systems", J. Flanklin Institute, 328(1) pp. 55-70, (1991).

[7] C. Sueur, G. Dauphin-Tanguy, "Bond graph approach for structural analysis of MIMO linear systems", J.Flanklin Inst., vol. 328, No.1 pp. 55-70, (1991).

[8] Chi-Tsong Chen "Linear System Theory and Design", Third ed., Oxford University Press,(1999).

[9] Gene F. Franklin, J. David Powell, Abbas Emani-Naeini, "Feedback Control of Dynamic Systems" Addison Wesley Publishing Company, (1988)

[10] Y.K. Wong and A.B. Rad "Bond Graph Simulations of Electrical Systems", IEEE Catalogue No. 98E137, (1998).

[11] P.J. Gawthop, " Physical Model-Based Control:A Bond Graph Approach", J. of the Franklin Institute, 332B(3), pp. 285-305, (1995).

[12] Antic, D.Vidojkovic, B. Mladenovic, M. "An Introduction to Bond Graph Modelling of Dynamic Systems", Telecommunications in Modern Satellite, Cable and Broadcasting Services, 1999, 4th Int. Conf. on Published: 1999, vol. 2, pp. 661-664.

[13] Wai-Kai Chen,"Applied Graph Theory: Graphs and Electrical Networks", 1976, North-Holland Publishing Company.

[14] C. Sueur and G. Dauphin-Tanguy, "Bond Graph Approach to Multi-time Scale Systems Analysis", J. of the Franklin Institute, 0016-0032/91.

[15] John J. Gainger, William D. Stevenson Jr. "Analisis de Sistemas Electricos de Potencia", Mc. Graw Hill, 1998.

C.5 Linearization in Bond Graph

Linearization in Bond Graph

Gonzalez-A. Gilberto, J. de Leon

Sometido a la 43rd IEEE Conference on Decision and Control (CDC04), December 14-17, 2004, Atlantis, Paradise Island, Bahamas.

Linearization in Bond Graph

González-A. Gilberto[1,2]*, J. De Leon[1]†
[1]University of Nuevo Leon, Department of Electrical Engineering
66451 San Nicolás de los Garza, N.L., Mexico.
[2] University of Michoacan, Faculty of Electrical Engineering
58030, Morelia, Michoacan, Mexico

Abstract. A graphical procedure to obtain the linearization of a class of nonlinear physical system, designed here like nonlinear system of states product, using Bond Graph is proposed. A direct structure for the linearized Bond Graph is presented. Therefore, the system and linearization are determined in the physical domain. Examples of a synchronous machine and a rigid body are given.

Keywords.–Bond Graph, Nonlinear systems, Linearization, Synchronous Machine.

I. Introduction

The Bond Graph is an useful and important tool for physical system modelling. This is based on power representation, it enables the description of the system through energy storage and dissipative elements.

A Bond Graph can represent a variety of energy types, whose junction structure can give a valuable information of the properties of the physical system. [1, 3]

An important property of the Bond Graph theory is the causal path, so, we can determine observability, controlability or the relation between state variables to linearize a class of nonlinear system designed here nonlinear system of states product, that can be represented in Bond Graph.

A linealized system is useful to know the behavior of the system when it is perturbed such that the new and old equilibrium points are nearly equal, the system equations are linearized around the operating points. The new linear equations so derived are assumed to be valid in a region near the equilibriun point. [4]

There are several applications of linearized systems for example small-signal stability [4] that is the ability of the power system to maintain synchronism when subjected to small disturbances. In this context, a disturbance is considered to be small if the equations that describe the response of the system can be linearized for the purpose of analysis [6].

We propose a scheme and procedure to obtain a linearization through Bond Graph for a nonlinear system of states product. It is based on a new Bond Graph which represents the linearization of the system in a physical domain.

Section II gives the Bond Graph model of a physical system. Section III sumarizes the algebraic linearization of nonlinear systems. A scheme of linearized Bond Graph using the junction structure is presented in section IV. A procedure to get the linearization from the a given Bond Graph is proposed in section V. Examples of a synchronous machine and a rigid body ilustrate the procedure in section VI. Finally, section VII gives our conclusions.

II. Bond Graph Model [3, 7]

Consider the scheme of a multiport LTI system which has the key vectors of figure 1.

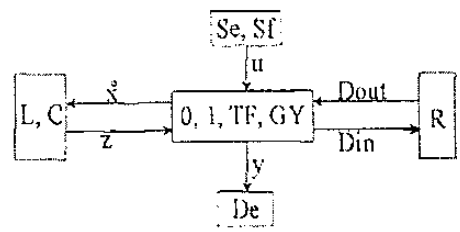

Figure 1. Key vectors of a Bond Graph

In figure 1, (Se, Sf). (L, C) and (R) denote the source the storage and the dissipation fields, (De) the detector and $(0, 1. TF, GY)$ the junction structure with transformers. TF, and gyrators, GY.

*gilmichga@yahoo.com.mx
†drjleon@hotmail.com.mx

The state $x \in \Re^n$ is composed of energy variables for effort, e, and flow, f, with integral causality, $u \in \Re^p$ denotes the plant input, $y \in \Re^q$ the plant output, $z \in \Re^n$ the co-energy, and $D_{in} \in \Re^r$ and $D_{out} \in \Re^r$ are a mixture of e and f showing the energy exchanges between the dissipation field and the junction structure.

The relations of the storage and dissipation fields are:

$$z = Fx \tag{1}$$
$$D_{out} = LD_{in} \tag{2}$$

The relations of the junction structure are:

$$\begin{bmatrix} \dot{x} \\ D_{in} \\ y \end{bmatrix} = S \begin{bmatrix} z \\ D_{out} \\ u \end{bmatrix} \tag{3}$$

where the junction structure of the system is given by:

$$S = \begin{bmatrix} S_{11} & S_{12} & S_{13} \\ S_{21} & S_{22} & S_{23} \\ S_{31} & S_{32} & S_{33} \end{bmatrix} \tag{4}$$

The entries of S take values inside the set $\{0, \pm 1, \pm m, \pm n\}$ where m and n are transformer and gyrator modules; S_{11} and S_{22} are square skew-symmetric matrices and S_{12} and S_{21} are matrices each other negative transpose. The state equation is [8,9]:

$$\begin{aligned} \dot{x} &= Ax + Bu \\ y &= Cx + Du \end{aligned} \tag{5}$$

where

$$A = (S_{11} + S_{12}MS_{21})F \tag{6}$$
$$B = (S_{13} + S_{12}MS_{23}) \tag{7}$$
$$C = (S_{31} + S_{32}MS_{21})F \tag{8}$$
$$D = S_{33} + S_{32}MS_{23} \tag{9}$$

being

$$M = (I - LS_{22})^{-1} L \tag{10}$$

Next section sumarizes the algebraic linearization technique [2]. This analysis is used in section IV for the Bond Graph approach.

III. Linearization [2]

A linear state equation is useful as an approximation of a nonlinear state equation in the following sense. Consider

$$\dot{x} = f(x,u) \qquad x(t_0) = x_0 \tag{11}$$

where the state $x \in \Re^n$ and the input $u \in \Re^p$.

Let (11) be solved for a particular input signal called the nominal input $\tilde{u}$ and a particular initial state called the nominal initial state $\tilde{x}_0$ to obtain a unique nominal solution, often called a nominal trayectory $\tilde{x}$. Consider

$$u = \tilde{u} + u_\delta \tag{12}$$
$$x_0 = \tilde{x}_0 + x_{0_\delta} \tag{13}$$

where $\|x_{0_\delta}\|$ and $\|u_\delta\|$ are appropriately small for $t \geq t_0$.

We assume that the corresponding solution remains close to $\tilde{x}$, at each t, and is given by

$$x = \tilde{x} + x_\delta \tag{14}$$

substituting (12) and (14) in (11) we have

$$\frac{d}{dt}\tilde{x} + \frac{d}{dt}x_\delta = f(\tilde{x} + x_\delta, \tilde{u} + u_\delta), \quad \tilde{x}(t_0) + x_\delta(t_0) = \tilde{x}_0 + x_{0_\delta} \tag{15}$$

Assuming that the derivatives of (11) exist, we can expand the right side using Taylor series around $\tilde{x}$ and $\tilde{u}$, and then retain only the terms through of 1. This is a reasonable approximation since u_δ and x_δ are assumed to be small for all t.

For the i^{th} component retaining the first order terms, and momentarily dropping t-arguments for simplicity, we can write

$$f_i(\tilde{x} + x_\delta, \tilde{u} + u_\delta) \cong f_i(\tilde{x}, \tilde{u}) + \frac{\partial f_i}{\partial x_1}(\tilde{x}, \tilde{u}) x_{\delta_1} + \ldots + \frac{\partial f_i}{\partial x_n}(\tilde{x}, \tilde{u}) x_{\delta_n} + \frac{\partial f_i}{\partial u_1}(\tilde{x}, \tilde{u}) + \ldots + \frac{\partial f_i}{\partial u_m}(\tilde{x}, \tilde{u}) \tag{16}$$

performing in vector matrix form gives

$$\frac{d}{dt}\tilde{x} + \frac{d}{dt}x_\delta \cong f(\tilde{x}, \tilde{u}) + \frac{\partial f}{\partial x}(\tilde{x}, \tilde{u}) x_\delta + \frac{\partial f}{\partial u}(\tilde{x}, \tilde{u}) u_\delta \tag{17}$$

where the notation $\frac{\partial f}{\partial x}$ denotes the Jacobian, a matrix with i, j-entry $\frac{\partial f_i}{\partial x_j}$.

Since

$$\frac{d}{dt}\tilde{x} = f(\tilde{x}, \tilde{u}), \quad \tilde{x}(t_0) = \tilde{x}_0 \tag{18}$$

the relation between x_δ and u_δ is approximately described by a linear time invariant state equation of the form

$$\dot{x}_\delta = A_\delta x_\delta + B_\delta u_\delta \tag{19}$$

where A_δ and B_δ are the matrices or partial derivatives evaluated on the nominal trajectory, which are

$$A_\delta = \frac{\partial f}{\partial x}(\tilde{x}, \tilde{u}) \tag{20}$$
$$B_\delta = \frac{\partial f}{\partial u}(\tilde{x}, \tilde{u}) \tag{21}$$

If there is a nonlinear output equation, we have

$$y(t) = h(x, u) \tag{22}$$

the fuction $h(x, u)$ can be expanded around the nominal trajectory, where the approximate description is

$$y_\delta = C_\delta x_\delta + D_\delta u_\delta \tag{23}$$

here the deviation output is given by

$$y_\delta = y - \tilde{y} \quad \tilde{y} = h(\tilde{x}, \tilde{u}) \tag{24}$$

where

$$C_\delta = \frac{\partial f}{\partial x}(\tilde{x}, \tilde{u}) \tag{25}$$

$$D_\delta = \frac{\partial f}{\partial u}(\tilde{x}, \tilde{u}) \tag{26}$$

In this development a nominal solution is assumed to exist for all $t \geq t_0$, so that the linearization makes sense as an approximation.

IV. Linearization by Bond Graph

Bond Graph represents a physical structure denoting power exchange in the physical system. Therefore, it is possible to code on the graph its mathematical structure, so, we can get a structure showing the causal relationships among the signals on the system.

The graphical information of the Bond Graph can be used to identify the nonlinear sections of a physical system. So, a direct graphical technique to obtain the linearized Bond Graph is presented. We consider the linearization by Bond Graph of a nonlinear system of states product (11), where the nonlinear part is formed by

$$x_i x_j, x_i u_k;\ i \neq j;\ i, j = 1, ..., n \text{ and } k = 1, ..., p \tag{27}$$

The general structure for linearization of (11) using Bond Graph, with the previous condition, is shown in figure 2.

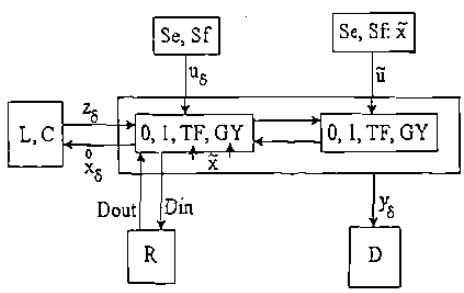

Figure 2. General structure of a system linearized.

The objetive to represent the linearization of the physical non-linear system in according of figure 2 is to get single relations on the modified junction structure matrix, $\tilde{S}$. This let us to know, the change of S due to the linerization. Next Lemma shows how to find the matrices of the linearized system from $\tilde{S}$.

Lemma

Consider the linearized scheme of figure 2. The structure of the system is given by

$$\begin{bmatrix} \dot{x}_\delta \\ D_{in} \\ y_\delta \end{bmatrix} = \tilde{S} \begin{bmatrix} z_\delta \\ D_{out} \\ u_\delta \\ \tilde{u} \end{bmatrix} \tag{28}$$

where

$$\tilde{S} = \begin{bmatrix} S_{11}^x + S_{11}^0 & S_{12} & S_{13}^x & S_{13}^0 \\ S_{21} & S_{22} & S_{23} & 0 \\ S_{31}^x + S_{31}^0 & S_{32} & S_{33}^x & S_{33}^0 \end{bmatrix} \tag{29}$$

The entries of S_{11}^x, S_{13}^x, S_{31}^x and S_{33}^x are the interconection of the elements that does not participate on the nominal trayectory of the system. The entries of S_{11}^0, S_{13}^0, S_{31}^0 and S_{33}^0 are on the nominal trajectory, u_δ is the input system and $\tilde{u}$ is the nominal input.

The representation of the system in state variables is given by

$$A_\delta = \left(S_{11}^x + S_{11}^0 + S_{12} M S_{21} + S_{13}^1\right) F \tag{30}$$

$$B_\delta = S_{13}^x + S_{12} M S_{23} \tag{31}$$

$$C_\delta = \left(S_{31}^x + S_{31}^0 + S_{32} M S_{21} + S_{33}^1\right) F \tag{32}$$

$$D_\delta = S_{33}^x + S_{32} M S_{23} \tag{33}$$

such that

$$S_{13}^0 \tilde{u} = S_{13}^1 x_\delta \tag{34}$$

$$S_{33}^0 \tilde{u} = S_{33}^1 x_\delta \tag{35}$$

where we select the entries of the matrices S_{13}^1 and S_{33}^1 to satisfy (34) and (35) respectively, being

$$M = (I - L S_{22})^{-1} L \tag{36}$$

Proof. For linearized system of the figure 2, substituting (1) into the first line of (28), we have

$$\dot{x}_\delta = \left(S_{11}^x + S_{11}^0\right) F x_\delta + S_{12} D_{out} + S_{13}^x u_\delta + S_{13}^0 u_0 \tag{37}$$

from (1) and (2) the second line of (28) gives

$$D_{in} = (I - S_{22} L)^{-1} \left(S_{21} F x_\delta + S_{23} u_\delta\right) \tag{38}$$

taking (10), (34) and (38) into (37):

$$\dot{x}_\delta = \left(S_{11}^x + S_{11}^0 + S_{12} M S_{21} + S_{13}^1\right) F x_\delta + \left(S_{13}^x + S_{12} M S_{23}\right) u_\delta \tag{39}$$

Comparing (19) with (39) we prove (30) and (31) using (34) and (36).

Otherwise, taking (1), (35) and (38) into the third line of (28) we have

$$y_\delta = \left(S_{31}^x + S_{31}^0 + S_{32}MS_{21} + S_{33}^1\right) Fx_\delta + \left(S_{33}^x + S_{32}MS_{23}\right) u_\delta \quad (40)$$

Comparing (23) with (40), we prove (32) and (33). ■

V. Procedure to obtain the Linearized Bond Graph

We present a graphical procedure to construct the linearized Bond Graph from a non-linear Bond graph of a physical system, considering that the system satisfies the conditions of the previous Lemma.

Procedure A

1.- Obtain the non-linear Bond Graph of the physical system.

2.- Identify the non-linear sections. They are in Transformers, TF and/or Gyrators, GY with states variables modules.

3.- Recognize the influence area of the TF and/or GY of step 2, following causal paths, from each state variable through TF and/or GY respectively, which is given by (27).

4.- The linearization is around of the nominal trajectory.

5.- The TF and/or GY modules of step 2 will be the nominal trajectory for the states variables respectively.

6.- Include bonds in according of step 3 where each causal path begins from the element of port-1 of the states variables of step 2 and this element is changed by an effort source if the element is C or by a flow source if the element is I.

7.- The value of the source of step 6 is the nominal trajectory of state variable.

8.- The TF or GY module additionals of the causal path of step 6 is the original of the Bond Graph of step 2.

VI. Example

Example 1.

Consider the d-q model of the synchronous machine. The model machine has salient poles, the exciting winding is placed on the direct axis. An amortisseur winding is represented by two short circuit winding, one on the d-axis and the other on the q-axis.

The assumptions of the model are: (1) the machine has a two pole character; (2) the armature windings a, b, c are sinusoidally distributed around the circunference of the rotor.

The Bond Graph model of the synchronous machine is shown in figure 3. This model is similar to [5], the difference is the exciting winding and the direction of some bonds.

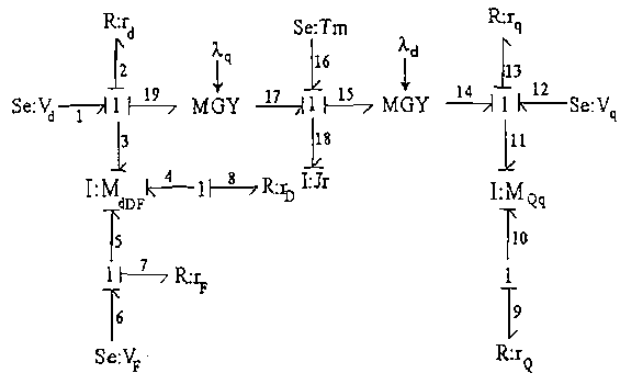

Figure 3. Bond Graph model of the synchronous machine.

The key vectors are

$$x^T = \left[\, e_{a_3} \quad e_{a_4} \quad e_{a_5} \quad e_{a_{10}} \quad e_{a_{11}} \quad e_{a_{18}} \,\right]$$
$$\dot{x}^T = \left[\, e_3 \quad e_4 \quad e_5 \quad e_{10} \quad e_{11} \quad e_{18} \,\right]$$
$$z^T = \left[\, f_3 \quad f_4 \quad f_5 \quad f_{10} \quad f_{11} \quad f_{18} \,\right]$$
$$D_{in}^T = \left[\, f_2 \quad f_7 \quad f_8 \quad f_9 \quad f_{13} \,\right]$$
$$D_{out}^T = \left[\, e_2 \quad e_7 \quad e_8 \quad e_9 \quad e_{13} \,\right]$$
$$u^T = \left[\, e_1 \quad e_6 \quad e_{12} \quad e_{16} \,\right]$$

where e_k, f_k, $k = 1, ..., 13$ denote voltages and currents respectively; e_{16} and e_{18} torques; f_{16} and f_{18} speeds in T_m and J_r respectively; e_{a_3}, e_{a_4} and e_{a_5} are the fluxes linkage in $I : M_{dDF}$ formed by mutuals and self inductances on d, D and F, respectively; $e_{a_{10}}$ and $e_{a_{11}}$ are the fluxes linkage in $I : M_{Qq}$ formed by mutuals and self inductances on Q and q, respectively; and $e_{a_{18}}$ is the rotational momentum in J_r. The damper winding is represented by D and Q on the d and q axis, respectively; the exciting winding is represented by F; and finally, d and q represent the conmutador winding on the the d and q axis, respectively.

In according with the procedure of section V, we can get the linearized Bond Graph represented in the figure 4.

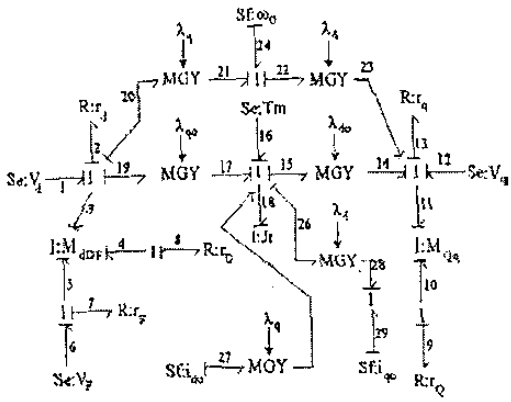

Figure 4. Linearized Bond graph of the synchronous machine.

The constitutive relations for the elements are defined by [4]

$$L = diag\{r_d, r_F, r_D, r_Q, r_q\} \quad (41)$$

$$F^{-1} = \begin{bmatrix} M_{dDF} & 0 & 0 \\ 0 & M_{Qq} & 0 \\ 0 & 0 & J_r \end{bmatrix} \quad (42)$$

where

$$M_{dDF} = \begin{bmatrix} L_d & M_{dD} & M_{dF} \\ M_{dD} & L_D & M_{DF} \\ M_{dF} & M_{DF} & L_F \end{bmatrix} \quad (43)$$

$$M_{Qq} = \begin{bmatrix} L_Q & M_{Qq} \\ M_{Qq} & L_q \end{bmatrix} \quad (44)$$

The junction structure for the system is given by (28) and (29) where

$$S_{11}^x = S_{22} = S_{23} = 0 \quad (45)$$

$$P = \begin{bmatrix} \lambda_{q_0} & 0 & 0 & 0 & -\lambda_{d_0} \end{bmatrix}$$

$$S_{11}^0 = \begin{bmatrix} 0_{5\times5} & -P^T \\ P & 0 \end{bmatrix} \quad S_{13}^x = \begin{bmatrix} \begin{bmatrix} 1 \\ 0 \end{bmatrix} & 0_{2\times3} \\ 0_{3\times1} & I_{3\times3} \end{bmatrix} \quad (46)$$

$$S_{12} = \begin{bmatrix} \begin{bmatrix} -1 & 0 & 0 \\ 0 & 0 & -1 \\ 0 & -1 & 0 \end{bmatrix} & 0_{2\times3} \\ 0_{3\times3} & \begin{bmatrix} -1 & 0 \\ 0 & -1 \\ 0 & 0 \end{bmatrix} \end{bmatrix} \quad (47)$$

$$S_{13}^0 = \begin{bmatrix} \begin{bmatrix} -\lambda_q & 0 & 0 \end{bmatrix} \\ 0_{3\times3} \\ \begin{bmatrix} \lambda_d & 0 & 0 \end{bmatrix} \\ \begin{bmatrix} 0 & \lambda_q & -\lambda_d \end{bmatrix} \end{bmatrix} \quad (48)$$

It is very common in electrical power systems to use the electrical current like state variable of this way, taking the derivative of (1) and (19), we have

$$\dot{z}_\delta = \left(FA_\delta F^{-1}\right) z_\delta + \left(FB_\delta\right) u_\delta \quad (49)$$

also, for electrical machines the folloowing form, is recomended

$$B_\delta u_\delta = -A_\delta F^{-1} z_\delta + F^{-1} \dot{z}_\delta \quad (50)$$

Using the lemma of section IV, from (34) and (42) to (45) we have

$$S_{13}^1 = \begin{bmatrix} \begin{bmatrix} 0_{4\times4} & \begin{bmatrix} \omega_0 \\ 0_{4\times1} \end{bmatrix} \end{bmatrix} & 0_{6\times1} \\ \begin{bmatrix} -\omega_0 & 0_{1\times4} \end{bmatrix} & \\ \begin{bmatrix} i_{q_0} & 0_{1\times3} & -i_{d_0} \end{bmatrix} & \end{bmatrix} \quad (51)$$

from (30), (41) to (48) we obtain

$$A_\delta F^{-1} = \begin{bmatrix} -R_{rDF} & \omega_0 N_{12} & N_{13} \\ -\omega_0 N_{21} & -R_{Qq} & -N_{23} \\ i_{q_0} N_{31} & -i_{d_0} N_{32} & 0 \end{bmatrix} \quad (52)$$

where

$$R_{dDF} = diag\{r_d, r_D, r_F\}; \quad R_{Qq} = diag\{r_Q, r_q\}$$

$$N_{12} = \begin{bmatrix} H_2 \\ 0_{2\times2} \end{bmatrix} \quad N_{13} = \begin{bmatrix} \lambda_{q_0} \\ 0_{2\times1} \end{bmatrix}$$

$$N_{21} = \begin{bmatrix} 0_{1\times3} \\ H_1 \end{bmatrix} \quad N_{23} = \begin{bmatrix} 0 \\ \lambda_{d_0} \end{bmatrix}$$

$$H_1 = \begin{bmatrix} L_d & M_{dD} & M_{dF} \end{bmatrix} \quad H_2 = \begin{bmatrix} M_{qQ} & L_q \end{bmatrix}$$

$$N_{31} = i_{q_0} H_1 - N_{13}^T \quad N_{32} = N_{23}^T - i_{d_0} H_2$$

and finally, from (31), (42) to (45) we obtain

$$B_\delta = \begin{bmatrix} \begin{bmatrix} \begin{bmatrix} 1 \\ 0 \end{bmatrix} & 0_{2\times3} \end{bmatrix} \\ \begin{bmatrix} 0_{2\times1} & \begin{bmatrix} 1 \\ 0 \end{bmatrix} & 0_{2\times2} \end{bmatrix} \\ \begin{bmatrix} 0_{1\times3} & 1 \end{bmatrix} \end{bmatrix} \quad (53)$$

Note that, from (50), (52) and (53) the linear model of the synchronous machine obtained by Bond Graph is the same that [4], being a simple methodology in this kind of systems.

Example 2.

Consider a Bond Graph representation of three-dimensional rigid body [8] shown in figure 5.

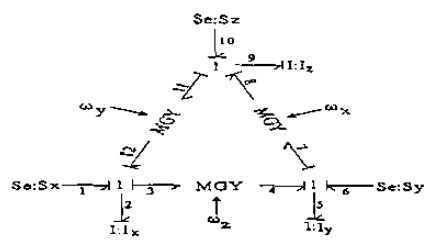

Figure 5. Bond Graph of a rigid body.

The key vectors are

$$\begin{aligned} x &= [\ e_{a_2} \quad e_{a_5} \quad e_{a_9}\ ] \\ \dot{x} &= [\ e_2 \quad e_5 \quad e_9\ ] \\ z &= [\ f_2 \quad f_5 \quad f_9\ ] \\ u &= [\ e_1 \quad e_6 \quad e_{10}\ ] \end{aligned}$$

where f_2, f_5 and f_9, e_2, e_5 and e_9 are the angular velocities and torques in a body-fixed coordinate system along the principal axes, respectively; e_{a_2}, e_{a_5} and e_{a_9} are rotationals momentums and e_1, e_6 and e_{10} are the applied torques.

Using the procedure of section V, we get the linearized Bond Graph represented in figure 6.

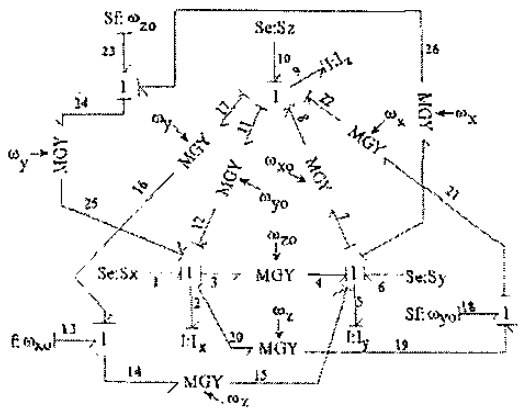

Figure 6. Bond Graph Linearized of three-dimensional rigid body.

The constitutive relation is

$$F = diag\left\{\frac{1}{I_x}, \frac{1}{I_y}, \frac{1}{I_z}\right\} \tag{54}$$

The junction structure for the system is given by (28) and (29) where

$$S_{11}^x = S_{12} = S_{22} = S_{23} = S_{21} = 0 \tag{55}$$

$$S_{11}^0 = \begin{bmatrix} 0 & -\frac{\omega_{z_0}}{I_z} & \frac{\omega_{y_0}}{I_y} \\ \frac{\omega_{z_0}}{I_z} & 0 & -\frac{\omega_{x_0}}{I_x} \\ -\frac{\omega_{y_0}}{I_y} & \frac{\omega_{x_0}}{I_x} & 0 \end{bmatrix} \tag{56}$$

$$S_{13}^0 = \begin{bmatrix} 0 & -\frac{\omega_z}{I_z} & \frac{\omega_y}{I_y} \\ \frac{\omega_z}{I_z} & 0 & -\frac{\omega_x}{I_x} \\ -\frac{\omega_y}{I_y} & \frac{\omega_x}{I_x} & 0 \end{bmatrix} \tag{57}$$

From (34),

$$S_{13}^1 = \begin{bmatrix} 0 & \frac{\omega_{z_0}}{I_y} & -\frac{\omega_{y_0}}{I_z} \\ -\frac{\omega_{z_0}}{I_x} & 0 & \frac{\omega_{x_0}}{I_z} \\ \frac{\omega_{y_0}}{I_x} & -\frac{\omega_{x_0}}{I_y} & 0 \end{bmatrix} \tag{58}$$

Obtaining the representation of the system of the form (50), from (30), we have

$$A_\delta F^{-1} = \begin{bmatrix} 0 & \omega_{x_0}\left(\frac{1}{I_y}-\frac{1}{I_z}\right) & \omega_{y_0}\left(\frac{1}{I_y}-\frac{1}{I_z}\right) \\ \omega_{z_0}\left(\frac{1}{I_y}-\frac{1}{I_z}\right) & 0 & \omega_{x_0}\left(\frac{1}{I_z}-\frac{1}{I_x}\right) \\ \omega_{y_0}\left(\frac{1}{I_x}-\frac{1}{I_y}\right) & \omega_{x_0}\left(\frac{1}{I_x}-\frac{1}{I_y}\right) & 0 \end{bmatrix} \tag{59}$$

and from (30),

$$B_\delta = [\ e_1 \quad e_6 \quad e_{10}\ ]^T \tag{60}$$

We observe that, a nonlinear system of states product represented in a Bond Graph model is linearized in a form graphical directly.

VII. Conclusions

A direct grahical procedure using Bond Graph for linearization of a nonlinear physical system of states product is presented. The system and linearization are determined in the physical domain. This methodology does not require to know nonlinear ordinary differential equations.

References

[1] Dean C. Karnopp, Ronald C. Rosenberg, "System Dynamics: A Unified Approach", Wiley, John & Sons, April (1975).

[2] Wilson J. Rugh, "Linear System Theory", Prentice-Hall, (1996).

[3] P.E. Wellstead, "Physical System Modelling", Academic Press, London, (1979).

[4] Anderson and Fouad, "Power System Control and Stability", Science Press, (1986).

[5] Dietrich Sahm, "A two-axis, Bond Graph Model of the Dynamics of Synchronous Electrical Machine", J. Flanklin Institute, Vol. 308, No.3 pp. 205-218, (1979).

[6] P. Kundur, "Power System Stability and Control", McGraw-Hill, (1994).

[7] C. Suer, G. Dauphin-Tanguy, "Bond graph approach for structural analysis of MIMO linear systems", J.Flanklin Inst., vol. 328, No.1 pp. 55-70, (1991).

[8] Peter Gawthrop, Lorcan Smith, "Metamodelling", Prentice-Hall, (1996).

C.6 Steady-State for a Physical System with Bond Graph Approach

Gonzalez-A. Gilberto, J. de Leon, R. Galindo

Sometido a Complex Systems, Intelligence and Modern Technology Applications (CSIMTA), September 19-22, Cherbourg, 2004.

Steady-State Error for a Physical System with Bond Graph Approach

González-A. Gilberto[1,2]*, J. De Leon[1]†, R. Galindo[1]‡
[1]University of Nuevo Leon, Department of Electrical Engineering
66451 San Nicolás de los Garza, N.L., Mexico.
[2] University of Michoacan, Faculty of Electrical Engineering
58030, Morelia, Michoacan, Mexico

Abstract. A graphical procedure to obtain the steady-state error in a closed loop system using a proportional control law in the physical domain is proposed. To get this objective a lemma and a procedure to calculate the difference in steady-state of a physical system using the Bond Graph in derivative causality is presented. Then, the proportional control law is applied in Bond Graph, therefore, a control in the physical domain is realized. We show that it is not necessary to find the inverse matrix A when the derivative causality is used.

Keywords.–Bond Graph, Steady-State, Proportional Control, Physical Control.

I. Introduction

The Bond Graph technique is an energy based modelling approach, unifying symbology for phenomena from different physical domains. Bond Graph is a directed graph whose nodes represent subsystems and its arrows, the transfer of energy between the subsystems. Bond Graph was established by [1]. The idea was developed by [2] and [3] how a powerful tool of modelling.

The dynamic of a physical system considers the elements that storage energy, when the dynamic period has finished, we have conditions of steady-state of the system. In a control system, it is common that the output can not reach the reference input of the system and it is very important to know this difference called steady-state error.

Nevertheless, the steady-state error require to calculate and to invert the matrix A, when the system is represented in a realization (A, B, C, D). As shown it is no necessary, if we obtain the Bond Graph in derivative causality of the system. So, we can get the response in steady-state directly [9, 10, 11].

Therefore, a graphical procedure to obtain the steady-state error of a system in the physical domain with a proportional control is presented.

In [11], we find some results about steady-state values using Bond Graph in derivative causality in a open loop system. Also, in [12], a control in Bond Graph using state estimated feedback is given.

Section II gives the Bond Graph model of a physical system. Section III resumes the steady-state in the physical domain. A lemma and a procedure to obtain the input-output difference of a open loop system is proposed in section IV. The steady-state error in a closed loop system using a proportional control in Bond Graph is presented in section V. The obtained results are applied in section VI. Finally, section VIII gives our conclusions.

II. Bond Graph Model [3, 5]

Consider the following scheme of a multiport LTI system which has the key vectors of figure 1.

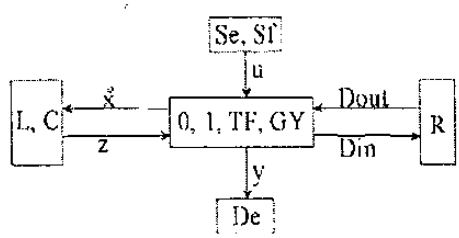

Figure 1. Key vectors of a Bond Graph

In figure 1, $(Se,\ Sf)$, $(L,\ C)$ and (R) denote the source, the storage and the dissipation fields, (De) the detector and $(0,\ 1,\ TF,\ GY)$ the junction structure with transformers, TF, and gyrators, GY.

*gilmichga@yahoo.com.mx
†drjleon@hotmail.com.mx
‡rgalindo@gama.fime.uanl.mx

The state $x \in \Re^n$ is composed of energy variables for effort, e, and flow, f, with integral causality, $u \in \Re^p$ denotes the plant input, $y \in \Re^q$ the plant output, $z \in \Re^n$ the co-energy, and $D_{in} \in \Re^r$ and $D_{out} \in \Re^r$ are a mixture of e and f showing the energy exchanges between the dissipation field and the junction structure.

The relations of the storage and the dissipation fields are:

$$z = Fx \quad (1)$$

$$D_{out} = LD_{in} \quad (2)$$

and the relations of the junction structure are given by:

$$\begin{bmatrix} \dot{x} \\ D_{in} \\ y \end{bmatrix} = S \begin{bmatrix} z \\ D_{out} \\ u \end{bmatrix} \quad (3)$$

where the junction structure of the system of the form:

$$S = \begin{bmatrix} S_{11} & S_{12} & S_{13} \\ S_{21} & S_{22} & S_{23} \\ S_{31} & S_{32} & S_{33} \end{bmatrix} \quad (4)$$

The entries of S take values inside the set $\{0, \pm 1, \pm m, \pm n\}$ where m and n are transformer and gyrator modules; S_{11} and S_{22} are square skew-symmetric matrices and S_{12} and S_{21} are matrices each other negative transpose. The state equation of the system is [8, 9]:

$$\begin{aligned} \dot{x} &= Ax + Bu \quad (5) \\ y &= Cx + Du \end{aligned}$$

where

$$A = (S_{11} + S_{12}MS_{21})F \quad (6)$$

$$B = (S_{13} + S_{12}MS_{23}) \quad (7)$$

$$C = (S_{31} + S_{32}MS_{21})F \quad (8)$$

$$D = S_{33} + S_{32}MS_{23} \quad (9)$$

being

$$M = (I - LS_{22})^{-1} L \quad (10)$$

Next section an analyses of the steady-state of the system using a Bond Graph in derivative causality will be given.

III. Steady-State [11]

The input-output difference in steady state can be calculated using (5), taking $\dot{x} = 0$, we have:

$$x_{ss} = -A^{-1}Bu_{ss} \quad (11)$$

$$y_{ss} = \left(D - CA^{-1}B\right) u_{ss} \quad (12)$$

from (11) and (12) we get

$$u_{ss} - y_{ss} = \left(I - D + CA^{-1}B\right) u_{ss} \quad (13)$$

The equation (13) gives the input-output in steady-state for an open loop system represented in space state, but we need A^{-1} and it is not easy to get for some high order systems.

We can use the Bond Graph in derivative causality to solve directly the problem to obtain A^{-1}.

Suppose that A is invertible and a derivative causality assignment is performed on the Bond Graph model [9, 10]. From (3) the junction structure is given by:

$$\begin{bmatrix} z \\ D_{ind} \\ y_d \end{bmatrix} = \begin{bmatrix} J_{11} & J_{12} & J_{13} \\ J_{21} & J_{22} & J_{23} \\ J_{31} & J_{32} & J_{33} \end{bmatrix} \begin{bmatrix} \dot{x} \\ D_{outd} \\ u \end{bmatrix}$$

$$D_{outd} = L_d D_{ind} \quad (14)$$

where the entries of J have the same properties as S. The storage elements in (14) have a derivative causality. So, D_{ind} and D_{outd} are defined of the same manner as D_{in} and D_{out}, they differs in which they depend on the causality assignment for the storage elements and that their junctions must have a correct causality assignment.

From (5) to (10) and (14), we obtain:

$$\begin{aligned} z &= A^*\dot{x} + B^*u \quad (15) \\ y_d &= C^*\dot{x} + D^*u \end{aligned}$$

where:

$$A^* = J_{11} + J_{12}NJ_{21} \quad (16)$$

$$B^* = J_{13} + J_{12}NJ_{23} \quad (17)$$

$$C^* = J_{31} + J_{32}NJ_{21} \quad (18)$$

$$D^* = J_{33} + J_{32}NJ_{23} \quad (19)$$

being,

$$N = (I - L_d J_{22})^{-1} L_d \quad (20)$$

The output state equations of this system in integral causality are given by (5). It follows, from (1), (5) and (15) that:

$$A^* = FA^{-1} \quad (21)$$

$$B^* = -FA^{-1}B \quad (22)$$

$$C^* = CA^{-1} \quad (23)$$

$$D^* = D - CA^{-1}B \quad (24)$$

From (19), (21), (11) and (12), we obtain the steady state:

$$\begin{aligned} x_{ss} &= F^{-1}B^*u_{ss} \quad (25) \\ y_{ss} &= D^*u_{ss} \end{aligned}$$

Next section, we propose a Lemma to get the input-output difference in steady-state of a system.

IV. Input-Output Difference in Steady-State

To get input-output difference in steady state of a system, we propose the following Lemma.

Lemma 1

Consider a LTI system represented in a Bond Graph in according of figure 1. Let a junction structure in derivative causality for steady-state conditions of the following form:

$$\begin{bmatrix} z \\ D_{ind} \\ \bar{y}_d \end{bmatrix} = \begin{bmatrix} J_{11} & J_{12} & J_{13} \\ J_{21} & J_{22} & J_{23} \\ J_{31} & J_{32} & J_{33}-I \end{bmatrix} \begin{bmatrix} \dot{x} \\ D_{outd} \\ u \end{bmatrix} \tag{26}$$

Then, the input-output difference in steady-state is

$$u_{ss} - y_{ss} = -\bar{D}^* u_{ss} \tag{27}$$

where

$$\bar{D}^* = D^* - I \tag{28}$$

Proof. Taking the second line of (28) and using (14), we have:

$$D_{ind} = (I - J_{22}L_d)^{-1}(J_{21}\dot{x} + J_{23}u) \tag{29}$$

from the third line of (25), (14) and (19),

$$\bar{y}_d = (J_{31} + J_{32}NJ_{21})\dot{x} + (J_{33} - I + J_{32}NJ_{23}) \tag{30}$$

so,

$$\bar{y}_d = C^*\dot{x} + \bar{D}^* u \tag{31}$$

where $C^* = J_{31} + J_{32}NJ_{21}$ and $\bar{D}^* = J_{33} + J_{32}NJ_{23}$ being $D^* = J_{33} + J_{32}NJ_{23}$.

The input-output difference in steady state is:

$$u_{ss} - y_{ss} = \left(I - D + CA^{-1}B\right) u_{ss} \tag{32}$$

using (24) in (32), we have:

$$u_{ss} - y_{ss} = -\left(D^* - I\right) u_{ss} \tag{33}$$

from (28) and (33) we prove (27). ■

Therefore, we present a simple and direct procedure to obtain the steady-state error from the Bond graph in derivative causality of the physical system, which is shown in figure 2.

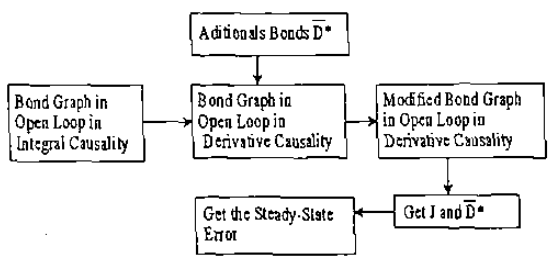

Figure 2 Scheme of procedure to get the steady state error.

Procedure 1

1.- Get the Bond Graph in open loop physical system in integral causality.

2.- Get the Bond Graph in derivative causality from the Bond Graph of step 1.

3.- Include the matrix J_{33}, the negative unit matrix, $-I$, of the following manner:

a) The negative unit matrix is a diagonal matrix, so, each output is connected with the respective input. If the input is an effort source, we use a 0-junction between the input and output, in other case, we use a 1-junction.

b) Is obtained an effort output using an active bond of the effort source, in other case a flow source is obtained a flow output.

c) The bond of the source from b) a connects to 1-junction if it is effort source, in other case, use a 0-junction.

d) From a) and c), the junctions are connected through a TF, if the input and output are the same kind of variable, in other case, use a GY. In both cases the module is -1.

e) The detector output signal is taked from the junction of a).

f) Using the modified Bond Graph, from (27) with (19), (20), (26) and (28), we obtain the input-output difference in steady-state.

Next, we introduce a procedure to obtain the steady-state error in a closed-loop system with a proportional control law in the physical domain.

V. Steady-State Error in a Closed Loop System using a Proportional Control

Consider the closed-loop system of figure 3.

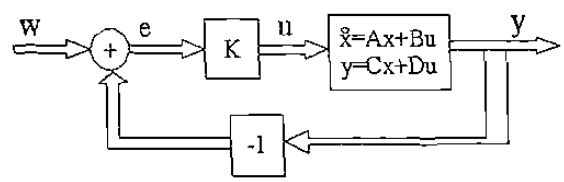

Figure 3 The closed-loop system.

In according with figure 3 and using (11) and (13), the steady-state error in closed-loop system, is given by:

$$e_{ss} = \left(I - D_c + C_c A_c^{-1} B_c\right) w_{ss} \tag{34}$$

where A_c, B_c, C_c and D_c denote the matrices A, B, C and D in closed loop of figure 3.

Using the previous procedure

$$e_{ss} = -\bar{D}_c^* w_{ss} \tag{35}$$

where:

$$\bar{D}_c^* = D_c^* - I \tag{36}$$

being,

$$D_c^* = D_c - C_c A_c^{-1} B_c \tag{37}$$

Using (26), (27) and (28) for the Bond Graph in closed loop system, (35) to (37) can be obtained directly.

So, we present a procedure to obtain directly the steady-state error in closed loop system using the Bond Graph model in derivative causality of the physical system, which is given on the scheme of the figure 4.

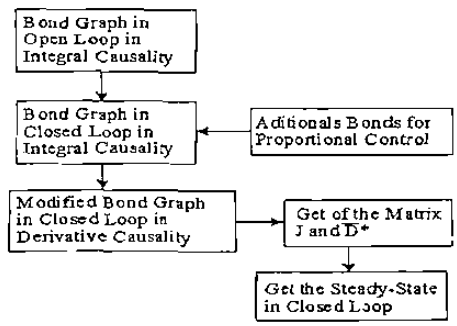

Figure 4 Scheme the steady-state error in closed loop using Bond Graph.

Procedure 2

1.- Get the Bond Graph of the open loop physical system in integral causality.

2.- Include the output feedback using an active bond between the flow output and a 1-junction, if the output of the system is effort uses a 0-junction.

3.- If the output and input are different kinds of variables the output after the junction of step 2 connects a GY with module of 1.

4.- The input of the system connects with the output of step 3 using a 1-junction, if the variables are flows in other case use a 0-junction.

5.- From steps 3 and 4, if the variable is the same kind to input of the system, connects the output of step 4 to TF, in other case use a GY; the module of TF or GY is the gain of the output feedback.

6.- The output of TF or GY from step 5, connects to input of the Bond Graph of step 1.

7.- The following steps consist to apply the procedure 1, to obtain first the Bond Graph in closed loop in derivative causality, to include bonds to have (36), then getting the matrix J, and finally, from (35) to calculate the steady-state error in closed loop system in the physical domain.

On the next section, an example is solved applying the procedures presented in this section.

VI. Example

Consider a CD motor and its Bond Graph shown in figure 5.

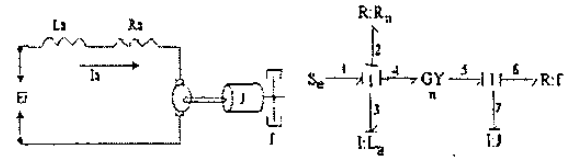

Figure 5. CD motor and its Bond Graph.

The key vectors are:

$$x = \begin{bmatrix} e_{a_3} \\ e_{a_7} \end{bmatrix}; \ \dot{x} = \begin{bmatrix} e_3 \\ e_7 \end{bmatrix}; \ z = \begin{bmatrix} f_3 \\ f_7 \end{bmatrix}$$

$$D_{in} = \begin{bmatrix} f_2 \\ f_6 \end{bmatrix}; \ D_{out} = \begin{bmatrix} e_2 \\ e_6 \end{bmatrix}; \quad \begin{matrix} y = f_6 \\ u = e_1 \end{matrix}$$

where e_2 and e_3 denote voltages; f_2 and f_3 currents in L_a and R_a respectively, e_6 and e_7 torques; f_6 and f_7 speeds in J and F respectively; e_{a_3} flux linkage in L_a; and e_{a_7} rotational momentum in J.

The constitutive relations for the elements are:

$$\begin{bmatrix} f_3 \\ f_7 \end{bmatrix} = \begin{bmatrix} \frac{1}{L_a} & 0 \\ 0 & \frac{1}{J} \end{bmatrix} \begin{bmatrix} e_{a_3} \\ e_{a_7} \end{bmatrix} \tag{38}$$

$$\begin{bmatrix} e_2 \\ e_6 \end{bmatrix} = \begin{bmatrix} R_a & 0 \\ 0 & f \end{bmatrix} \begin{bmatrix} f_2 \\ f_6 \end{bmatrix} \tag{39}$$

The input-output for the gyrator is:

$$\begin{bmatrix} e_4 \\ f_4 \end{bmatrix} = \begin{bmatrix} 0 & n \\ \frac{1}{n} & 0 \end{bmatrix} \begin{bmatrix} e_5 \\ f_5 \end{bmatrix} \tag{40}$$

The Bond Graph in derivative causality is shown in figure 6.

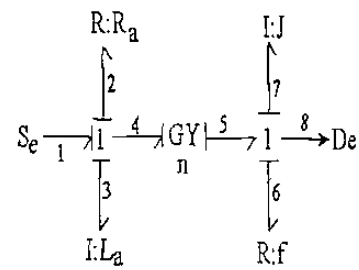

Figure 6. Bond Graph in derivative causality for the CD motor.

Applying the procedure given in the scheme of figure 2, we obtain the modified Bond Graph in derivative causality which is shown in figure 7.

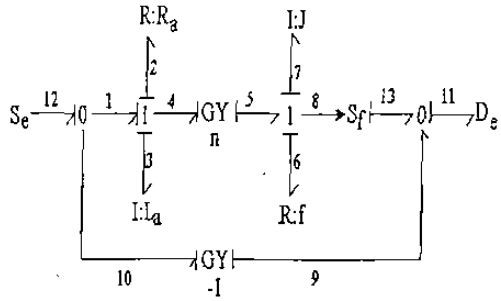

Figure 7. Modified Bond Graph in derivative causality of the DC motor.

Obtaining the input-output difference for the system, we require the junction structure matrix, J, from the Bond Graph of figure 7, we have:

$$\begin{aligned} J_{11} &= \begin{bmatrix} 0 & \frac{1}{n} \\ -\frac{1}{n} & 0 \end{bmatrix}; \; J_{13} = \begin{bmatrix} 0 \\ \frac{1}{n} \end{bmatrix} \\ J_{31} &= \begin{bmatrix} -\frac{1}{n} \\ 0 \end{bmatrix}^T; \quad \begin{matrix} J_{31} = J_{32} \\ J_{33} = \frac{1}{n} \end{matrix} \\ J_{11} &= J_{12} = J_{21} = J_{22}; \; J_{23} = J_{13} \end{aligned} \tag{41}$$

observe that from the figures 6 and 7, $L_d = L$, from (19), (20), (39) and (41) we obtain:

$$D^* = -\frac{n^2 + R_a f - n}{n^2 + R_a f} \tag{42}$$

from (27) and (28) the input-output difference is

$$u_{ss} - y_{ss} = \frac{n^2 + R_a f - n}{n^2 + R_a f} u_{ss} \tag{43}$$

Using the procedure of figure 4, the Bond Graph in closed loop with proportional control law shows in figure 8.

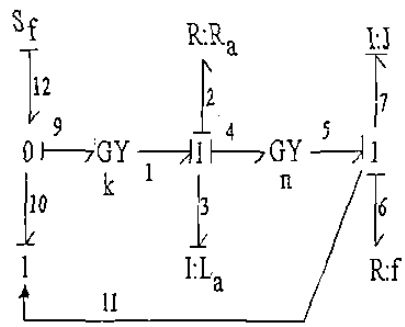

Figure 8 Bond Graph in closed loop in integral causality.

The Bond Graph in derivative causality with $D^* - I$ in closed loop is shown in figure 9.

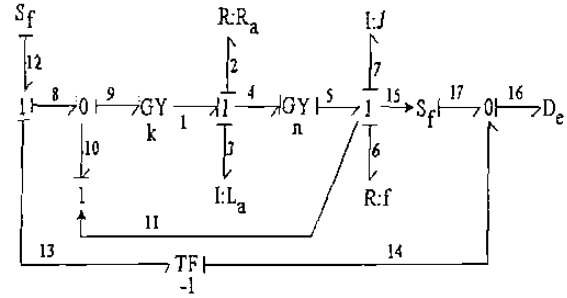

Figure 9. Modified Bond Graph in closed loop in derivative causality.

The junction structure matrix for the Bond Graph of figure 9 is:

$$\begin{aligned} J_{11} &= \begin{bmatrix} 0 & \frac{1}{n} \\ -\frac{1}{n+k} & 0 \end{bmatrix}; \; J_{13} = \begin{bmatrix} 0 \\ \frac{k}{n+k} \end{bmatrix} \\ J_{31} &= \begin{bmatrix} -\frac{1}{n+k} \\ 0 \end{bmatrix}^T; \quad \begin{matrix} J_{31} = J_{32} \\ J_{33} = \frac{k}{n+k} \end{matrix} \\ J_{11} &= J_{12} = J_{21} = J_{22}; \; J_{13} = J_{23}; \end{aligned} \tag{44}$$

From (19), (20), (27), (28), (34), and (36),

$$\bar{D}_k^* = -\frac{n^2 + R_a f}{n^2 + nk + R_a f} \tag{45}$$

the steady-state error is obtained from (35),

$$e_{ss} = \frac{n^2 + R_a f}{n^2 + nk + R_a f} \tag{46}$$

Note, that in (46) we know the behavior of the parameters of the system and the control gain in the steady-state error in the closed loop system.

Therefore, we present a graphical procedure to obtain the steady-state error in a closed loop system, which does not require to know the model of the system.

VII. Conclusions

A direct graphical procedure using Bond Graph to obtain the steady-state error for a closed loop physical system with a proportional control law is presented. This methodology does not require to know the transfer function or its realization (A, B, C, D) and lets to consider different kinds of energies.

REFERENCES

[1] Paynter, H. M., "Analysis and design og engineering", MIT press, Cambridge, Mass (1961).

[2] Dean C. Karnopp, Ronald C. Rosenberg, "System Dynamics: A Unified Approach", Wiley, John & Sons, April (1975).

[3] P.E. Wellstead, "Physical System Modelling", Academic Press, London, (1979).

[4] D. C. Karnopp, "Bond Graph in Control:Physical state variable and observers", J. Flanklin Institute 308(3) pp. 221-234, (1979).

[5] C. Suer, G. Dauphin-Tanguy, "Bond graph approach for structural analysis of MIMO linear systems", J.Flanklin Inst., vol. 328, No.1 pp. 55-70, (1991).

[6] Chi-Tsong Chen, "Linear System Theory and Design", Oxford University Press, (1999).

[7] P. J. Gawthrop, "Physical Model-Based Control: A Bond Graph Approach", J.Flanklin Institute, 332B(3), pp. 285-305, (1995).

[8] Peter Gawthrop, Lorcan Smith, "Metamodelling", Prentice-Hall, (1996).

[9] G. Duaphin- Tanguy y P. Borne, "Order Reduction of Multi-time Scale Systems Using Bond Graphs, the Reciprocal System and Sigular Perturbation Method", Journal of the Franklin Institute, Vol. 319, No. 1/2, pp. 157-171. Enero/Febrero 1985.

[10] C. Sueur y G. Dauphin- Tanguy, "Bond Graph Approach to Multi- Time Scale Systems Analysis", Journal of the Franklin Institute, Vol. 328, No. 5/6, pp. 1005-1026, 1991.

[11] Gonzalez-A. Gilberto, R. Galindo, "Steady-State Values for a Physical with Bond Graph Approach", 9th IEEE International Conference on Methods and Models in Automation and Robotics, Miedzyzdroje, Poland pp.1317-1322, 2003.

[12] Gonzalez-A. Gilberto, R. Galindo, "Direct Control in Bond Graph by State Estimated Feedback for MIMO LTI Systems", Proceedings of the 2002 IEEE International Conference on Control Applications, September 18-20, Glasgow, Scotland, U.K.